

UC San Diego

UC San Diego Electronic Theses and Dissertations

Title

Molecular mechanisms of HIV gp120-induced neurotoxicity

Permalink

<https://escholarship.org/uc/item/8zq2q0vx>

Author

Medders, Kathryn Elizabeth

Publication Date

2010

Peer reviewed|Thesis/dissertation

UNIVERSITY OF CALIFORNIA, SAN DIEGO

Molecular Mechanisms of HIV gp120-induced Neurotoxicity

A dissertation submitted in partial satisfaction of the
requirements for the degree Doctor of Philosophy

in

Molecular Pathology

by

Kathryn Elizabeth Medders

Committee in charge:

Professor Marcus Kaul, Chair
Professor Eliezer Masliah, Co-Chair
Professor Ian Everall
Professor Robert Rickert
Professor Bruce Torbett
Professor Dongxian Zhang

2010

Copyright

Kathryn Elizabeth Medders, 2010

All rights reserved.

The Dissertation of Kathryn Elizabeth Medders is approved, and it is acceptable in quality and form for publication on microfilm and electronically:

Co-Chair

Chair

University of California, San Diego

2010

DEDICATION

I would like to dedicate this body of work to my best friends: my mother Kathy, my father Darryl, and my brother Ryan. I love you all so very much, and I would not have made it this far without your unconditional love and support.

EPIGRAPH

Let me tell you the secret that has led me to my goal. My strength lies solely in my tenacity.

-- *Louis Pasteur*

TABLE OF CONTENTS

Signature Page	iii
Dedication.....	iv
Epigraph.....	v
Table of Contents	vi
List of Figures.....	ix
List of Tables.....	xii
Acknowledgements	xiii
Vita and Publications.....	xvii
Abstract of the Dissertation	xix
CHAPTER 1.....	1
INTRODUCTION.....	1
1.1. HIV-Associated Neurocognitive Disorders : Persistence Despite Combination Antiretroviral Therapies	1
1.2. Neurodegeneration in HAND : Role of Viral Envelope HIV-1 gp120	4
1.3. Contribution of Stress-Activated p38 MAPK Signaling in HAND and Other Neurodegenerative Diseases.....	8
1.4. Potential Mediators of Neuroprotection in HAND	12
MAIN OBJECTIVES AND SIGNIFICANCE	15
ACKNOWLEDGEMENTS	16
CHAPTER 2.....	17
MATERIALS AND METHODS.....	17
2.1. Reagents	17
2.2. Preparation of rodent cerebrocortical, mixed neuronal-glia cell cultures	18
2.3. Isolation and preparation of human monocyte-derived macrophages.....	19
2.4. Cell culture of human mononuclear THP-1 cells	20
2.5. Assessment of neuronal death	21
2.6. Mononuclear cell-mediated neurotoxicity.....	22

2.7.	siRNA nucleofection	22
2.8.	Immunofluorescent staining and deconvolution microscopy	23
2.9.	Cell lysates.....	24
2.10.	Immunocomplex kinase assay for p38 MAPK or SAPK/JNK activity... ..	25
2.11.	Immunoblotting	25
2.12.	RNA extraction, qRT-PCR and DNA microarray.....	26
2.13.	Chemokine, cytokine or growth factor ELISA and multiplex arrays.....	28
2.14.	Statistical analysis	29

CHAPTER 3..... 30

ACTIVATION OF P38 MAPK IS REQUIRED IN MONOCYTIC AND NEURONAL CELLS FOR HIV GP120-INDUCED NEUROTOXICITY..... 30

3.1.	Abstract.....	30
3.2.	Introduction	31
3.3.	Results	35
3.4.	Discussion.....	58
3.5.	Acknowledgements	67

CHAPTER 4..... 68

INHIBITION OF P38 MAPK ACTIVITY IN MONOCYTIC CELLS: A NOVEL, POTENTIAL ROLE OF LEUKOTRIENES IN GP120-INDUCED NEUROTOXICITY

4.1.	Abstract.....	68
4.2.	Introduction	70
4.3.	Results	73
4.4.	Discussion.....	95
4.5.	Acknowledgements	102

CHAPTER 5..... 104

CONCLUSIONS AND FUTURE DIRECTIONS..... 104

CHAPTER 6..... 113

APPENDIX	113
CHAPTER 7.....	135
REFERENCES.....	135

LIST OF FIGURES

CHAPTER 1

- Figure 1.1 Components of the HIV genome implicated in neuropathogenesis 5
- Figure 1.2 Schematic diagram of the role immune cells play in HIV-1 neuropathogenesis 6
- Figure 1.3 HIV-1 gp120 causes neuronal injury *in vivo* and *in vitro* 8
- Figure 1.4 The p38 MAPK signaling cascade primarily in monocytes is involved in cytokine production 11
- Figure 1.5 Schematic diagram of the involvement of p38 MAPK in HIV-1 gp120-induced activation of monocytes, production of neurotoxins and subsequent neuronal death... 12

CHAPTER 2

- Figure 2.1 Embryonic rat cerebrocortical, mixed neuronal-glia cells after 17 days *in vitro*. 19

CHAPTER 3

- Figure 3.1 Kinetics of p38 MAPK and JNK activation in mixed neuronal-glia cerebrocortical cell cultures upon exposure to neurotoxic HIV envelope protein gp120 36
- Figure 3.2 Inhibition of p38 MAPK prevents gp120-induced neuronal apoptosis in a dose-dependent fashion 39
- Figure 3.3 Presence of the neuroprotective chemokine CCL4 reduces the activation of p38 MAPK in the presence of neurotoxic gp120 in rat cerebrocortical cultures at 3 h and 24 h.. 41
- Figure 3.4 HIV-1 gp120 activates p38 MAPK in rat cerebrocortical neurons and microglia 43
- Figure 3.5 Depletion of microglia from mixed rat cerebrocortical cultures reduces the activation of p38 MAPK in the presence of neurotoxic gp120 at 3 h and 24 h 45

Figure 3.6	Inhibition of p38 MAPK in monocytic THP-1 cells abrogates the HIV-1 gp120-induced release of neurotoxic factors.....	47
Figure 3.7	HIV-1 gp120 stimulates secretion of neurotoxins from primary human macrophages	52
Figure 3.8	Reduction of endogenous p38 MAPK expression with siRNA in monocytic THP-1 cells prevents induction of neurotoxicity upon exposure to gp120.....	55
Figure 3.9	Inhibition of p38 MAPK in microglia-depleted rat cerebrocortical cultures rescues neurons from gp120-activated THP-1 neurotoxicity. ...	57

CHAPTER 4

Figure 4.1	LPS requires presence of microglia in rat cerebrocortical cultures to reduce neuronal survival.....	74
Figure 4.2	HIV-1 gp120 increases p38 MAPK activity, while LPS and Anisomycin increase p38 MAPK and SAPK/JNK activities in human monocytic THP-1 cells.....	76
Figure 4.3	Inhibition of p38 MAPK reduces the phosphorylation of HSP27 by HIV-1 gp120, LPS and Anisomycin in human monocytic THP-1 cells .	77
Figure 4.4	SB203580 increases neuronal survival after treatment with neurotoxic conditioned media from human monocytic THP-1 cells incubated with HIV-1 gp120, but not LPS.....	79
Figure 4.5	SB203580 alone increases release of several cytokines, chemokines and growth factors from human monocytic THP-1 cells after 24 h	82
Figure 4.6	LPS-stimulated production of cytokines, chemokines and growth factors after 24 h in human monocytic THP-1 cells.....	84
Figure 4.7	LPS or SB203580 alone, or combination of both (SB+LPS), may increase release of several cytokines, chemokines and growth factors from human monocytic THP-1 cells after 4 d.....	86
Figure 4.8	Heat map of genes differentially expressed by SB203580 versus control at 4 h in human monocytic THP-1 cells.....	89

Figure 4.9 Validation of microarray results with qRT-PCR assay of TNF, LTC4S and PLAUR at 4 h in human monocytic THP-1 cells.. 92

Figure 4.10 Inhibition of p38 MAPK activity reduces expression of LTC4S in human monocytic THP-1 cells at 24 h. 94

Figure 4.11 Cysteinyl leukotriene receptor antagonist, montelukast, prevents HIV-1 gp120-induced neurotoxicity..... 95

CHAPTER 5

Figure 5.1 Schematic diagram of the potential mechanism of HIV-1 gp120-induced neurotoxicity and the potential mechanism of p38 MAPK inhibition of HIV-1 gp120-induced neurotoxicity 112

LIST OF TABLES

CHAPTER 1

Table 1.1	Global Summary of the AIDS epidemic	2
Table 1.2	CSF penetration effectiveness (CPE) scores for FDA-approved antiretroviral drugs currently on the market.....	3

CHAPTER 4

Table 4.1	p38 MAPK-dependent genes differentially regulated by HIV-1 gp120 at 4 and 24 hours in human monocytic THP-1 cells	88
Table 4.2	Select genes differentially regulated by SB203580 alone at 24 hours in human monocytic THP-1 cells	89

CHAPTER 6

Table 6.1	Full list of genes differentially regulated by HIV-1 gp120-treated versus vehicle-treated human monocytic THP-1 cells	113
Table 6.2	Genes differentially regulated by SB203580 alone at 4 hours in human monocytic THP-1	116
Table 6.3	Full list of genes differentially regulated by SB203580 alone at 24 hours in human monocytic THP-1 cells	116
Table 6.4	Full list of genes differentially regulated by LPS versus SB+LPS at 4 and 24 hours in human monocytic THP-1 cells	123

ACKNOWLEDGEMENTS

First, I would like to thank my committee chair and thesis advisor, Professor Marcus Kaul, for his support throughout these past five plus years. He has helped me develop as a scientist and as a critical thinker. I am grateful for the opportunities I have had to learn from Dr. Kaul. As a researcher and a retired pharmacist, he inspired me to pursue my future career path as a pharmacist and researcher. I would also like to thank my committee for being supportive through my endeavors, whether in research or in pharmacy.

I would like to extend my gratitude to the past and present collaborators of the Kaul Lab. Thank you to Dr. Stuart A. Lipton for giving the Kaul Lab the foundation necessary for it to flourish. Thank you also to Dr. Cristian Achim and Dr. Ian Everall at UC San Diego for their support and enlightening conversations. To my lab mates, past and present, I very much appreciate your encouragement, your inspirational cubicle labeling, your counting skills and for listening to me even when I ramble.

Thank you to the great friends I have made while attending graduate school. Dr. Benjamin Sullivan, you are an amazing source of emotional, intellectual and financial (well, you were the first to graduate) support. Dr. Theresa Tiefenbrunn (Sample, 10-10-10), you have been a wonderful friend and roommate throughout these eventful six years. Thanks for sharing Lee, Lexi, Ringo, Micah and Ziggy (RIP or live happily with your new family) with me. To my fellow MolPath cohorts: Amanda, Anokhi, Cyndi, Erin, Heather, Jorge, Leslie, Matt, and Miki, you all have made it bearable. Survival through graduate school requires friends like you. Congrats to those

that have received their doctorates and to those that will soon. Thanks to Karen Wei for spending many days and nights talking through everything. Dr. Leslie Crews: I heart you and know that without you this would have been even more daunting.

Thank you to Kathleen Kazules, the greatest Graduate Coordinator to ever exist.

I would also like to thank my new family at Skaggs School of Pharmacy and Pharmaceutical Sciences. To the class of 2013: I have immensely enjoyed our first year together and cannot wait to grow more with you in the years to come.

And last but definitely not least, I give all my love and gratitude to my family, who are my emotional anchors and intellectual catapults. To my dad, Darryl Medders, you are the rock I hold onto through every storm. You are my voice of reason, but you give me the strength to dream big. To my mom, Kathryn Joan Medders, you showed me how to be a hard worker and care for others purely through example. You are my laughter and my whimsy, but you keep me grounded when necessary. To my brother, Ryan Medders, you amaze me with your gift of gab and your endless enthusiasm. We will always have each other to depend upon. I am so proud of you and cannot wait to see what the future has in store for us both. Here's to our transition from "daigakuinsei" to "sensei"! I would like to give a special mention to my baby Kia for choosing me to take her home 11 years ago and blessing my life with purrs, snores and unconditional love. To Grandma Medders: Thank you for your love and support. I hope that after perusing through my dissertation, you realize why my middle name is "tired." And in loving memory of my Grandpa Medders, Grandma Sally and Grandpa

Carl: I miss you terribly and I wish you had been able to see the day I became Dr. Medders, but I know you were always proud of me.

Chapter 1, in part, contains modified figures that appear in Nature Reviews Neuroscience 2007; with kind permission from Nature Publishing Group: Ellis RJ, Langford D, Masliah E (2007) HIV and antiretroviral therapy in the brain: neuronal injury and repair. Chapter 1, in part, also contains a modified figure that appears in Drug Discovery Today: Therapeutic Strategies 2006; with kind permission from Elsevier Limited: Mayer RJ and Callahan JF. 2006. p38 MAP kinase inhibitors: A future therapy for inflammatory diseases. Chapter 1, in part, also contains a modified figure that appears in Nature 2001; with kind permission from Nature Publishing Group: Kaul M, Garden GA, Lipton SA (2001) Pathways to neuronal injury and apoptosis in HIV-associated dementia.

Chapter 2, in part, contains excerpts of the material as it will appear in The Journal of Immunology 2010, volume 185. With kind permission from The American Association of Immunologists, Inc: Medders KE; Sejbuk, Natalia; Maung, Ricky; Desai, Maya K; Kaul, Marcus (2010) Activation of p38 MAPK is required in monocytic and neuronal cells for HIV gp120-induced neurotoxicity. The dissertation author was the primary investigator and author of this paper.

Chapter 3, in full, has been accepted for publication as it will appear in The Journal of Immunology 2010, volume 185. With kind permission from The American Association of Immunologists, Inc: Medders KE; Sejbuk, Natalia; Maung, Ricky; Desai, Maya K; Kaul, Marcus (2010) Activation of p38 MAPK is required in

monocytic and neuronal cells for HIV gp120-induced neurotoxicity. The dissertation author was the primary investigator and author of this paper.

Chapter 4, in full, is currently being prepared for submission for publication; Medders KE and Kaul M (2010). The dissertation author is the primary investigator and author of this material.

VITA

EDUCATION

- 2001 Bachelor of Science, University of California, San Diego
- 2004 Master of Science, University of California, Davis
- 2009-2013 Doctor of Pharmacy Candidate, University of California, San Diego
Skaggs School of Pharmacy and Pharmaceutical Sciences
- 2010 Doctor of Philosophy, University of California, San Diego

RESEARCH EXPERIENCE

- 2000-2001 Laboratory Assistant, Developmental Biology Laboratory, University of California, San Diego
- 2001-2003 Research Technician, Sanford-Burnham Medical Research Institute
- 2004-2005 Research Assistant, Sanford-Burnham Medical Research Institute
- 2005-2010 Graduate Student Researcher, University of California, San Diego;
Sanford-Burnham Medical Research Institute

PUBLICATIONS

1. Medders KE and Kaul M. Inhibition of p38 MAPK activity in monocytic cells: potential protective regulators of gp120-induced neurotoxicity. In preparation 2010.

2. Maung R, Kerr S, Medders KE, Desai MK, Alirezaei M, Chiu S, Staton M, Hult B, Everall IP, Lipton SA, and Kaul M. Inhibition of NMDA receptor-gated ion channels and L-type Ca²⁺ channels both prevent CXCR4-mediated neurotoxicity of SDF-1/CXCL12. In preparation 2010.
3. Medders KE, Sejbuk N, Maung R, Desai MK, and Kaul M (2010) Activation of p38 MAPK is required in monocytic and neuronal cells for HIV gp120-induced neurotoxicity. *J Immun.* Vol. 185. In press August 2010.
4. Kaul M, Ma Q, Medders KE, Desai MK, and Lipton SA (2007) HIV-1 coreceptors CCR5 and CXCR4 both mediate neuronal cell death but CCR5 paradoxically can also contribute to protection. *Cell Death Differ.* Feb; 14(2):296-305.

ABSTRACT OF THE DISSERTATION

Molecular Mechanisms of HIV gp120-induced Neurotoxicity

by

Kathryn Elizabeth Medders

Doctor of Philosophy in Molecular Pathology

University of California, San Diego, 2010

Professor Marcus Kaul, Chair

Professor Eliezer Masliah, Co-Chair

Human immunodeficiency virus (HIV)-1 associated neurocognitive disorders (HAND) are characterized by cognitive impairment, motor dysfunction and progressive neurodegeneration. These neuropathological features are accompanied by infiltration of monocytic cells into the central nervous system (CNS); increases in

inflammatory mediators in the cerebral spinal fluid (CSF); and activation of stress-activated signaling cascades such as the p38 Mitogen-Activated Protein Kinase (MAPK) pathway. Several neurotoxic substances have been implicated in the etiology of HAND, including HIV-1 encoded protein Tat and HIV-1 envelope glycoprotein 120 (gp120). Soluble gp120 can activate macrophages and microglia to produce neurotoxins. Therefore, the objectives of this dissertation were: 1) to investigate the cellular mechanisms of neuronal injury in *in vitro* models of HAND; 2) to examine the role of HIV-1 gp120 in neurotoxicity within different brain cell populations; and 3) to analyze the activation of stress-activated kinase p38 MAPK and its downstream targets in the mechanisms of HIV-1 gp120-mediated neurotoxicity.

To address these aims, *in vitro* studies using pharmacological compounds, heterologous expression and messenger RNA (mRNA) silencing were performed to inhibit p38 MAPK activity. These studies demonstrated that p38 MAPK signaling within both neurons and monocytic cells is critical for gp120-induced neurotoxicity. Using gene microarray and protein multiplex arrays, several genes were identified that are regulated by p38 MAPK and affect the neurotoxic phenotype of monocytes exposed to gp120. After pharmacological inhibition of p38 MAPK activity, neuroprotective beta chemokines and growth factors were found to be upregulated in addition to proinflammatory cytokines, while the arachidonate metabolism gene LTC₄ synthase was down-regulated. These modulations possibly contribute to the reduction in gp120-induced macrophage-mediated neurotoxicity after inhibition of p38 MAPK activity. In fact, blocking the cysteinyl leukotriene receptor on microglia-depleted

cerebrocortical cells increased neuronal survival after exposure to neurotoxic THP-1 supernatants.

Taken together, the studies presented in this thesis establish that the p38 MAPK signaling cascade plays a vital role in HIV-1 neuropathogenesis by stimulating neuronal apoptosis and by possibly increasing the release of inflammatory mediators, such as cysteinyl leukotrienes, from monocytic cells. Future therapeutic approaches could target these molecular pathways to prevent or rescue neuronal populations from injury in patients with HAND.

CHAPTER 1

INTRODUCTION

1.1. HIV-ASSOCIATED NEUROCOGNITIVE DISORDERS : PERSISTENCE DESPITE COMBINATION ANTIRETROVIRAL THERAPIES (cART)

Human immunodeficiency virus (HIV)-1 is a lentivirus of the retroviral family that targets and infects CD4-positive (CD4+) cells, including T lymphocytes and cells of the monocytic lineage (dendritic cells, macrophages, microglia, and monocytes). Depletion of CD4+ T cells below 200/ μ l by the virus is seen as a diagnostic marker for the development of acquired immunodeficiency syndrome (AIDS), causing immune dysfunction and subsequent susceptibility to opportunistic infections and death. In 2008, roughly 33 million people worldwide (1.4 million in the United States) are estimated to be living with HIV; 2 million died (25,000 in the US) from AIDS-related deaths and 2.7 million (55,000 in the US) were newly infected (UNAIDS 2009 report, Table 1-1). However, what was once considered an immediate death sentence is now largely considered to be a chronic, yet manageable disease due to the advent of antiretroviral drugs and introduction of combination antiretroviral therapies (cART), especially within the United States (Naggie et al., 2010).

Despite pharmaceutical management of the systemic, life-threatening effects of HIV, several conditions that lower the quality of life for HIV-positive patients have emerged, particularly in patients living with HIV for decades. Treating signs and



symptoms normally observed in an aged population, such as osteoporosis and memory loss, have become the greater challenge for physicians and their patients. In fact of those living with HIV, approximately 50% have some form of HIV-associated neurocognitive disorders (HAND) regardless of cART treatment (Woods et al., 2009). These neurological abnormalities range in intensity from asymptomatic neurocognitive impairment (ANI) to mild neurocognitive disorders (MND) to the more severe HIV-1-associated dementia (HAD) (Ellis et al., 2007). The less severe forms of HAND (ANI and MND) are more prevalent among HIV patients in the post-cART era and symptoms include behavioral alterations; slowed motor skills and information processing; and memory and learning impairment (Woods et al., 2009).

Table 1.1 Global Summary of the AIDS epidemic. UNAIDS 2009 report on the prevalence and incidence of HIV and AIDS from around the world.

Global summary of the AIDS epidemic	
<i>December 2008</i>	
Number of people living with HIV in 2008	
Total	33.4 million [31.1 – 35.8 million]
Adults	31.3 million [29.2 – 33.7 million]
Women	15.7 million [14.2 – 17.2 million]
Children under 15 years	2.1 million [1.2 – 2.9 million]
People newly infected with HIV in 2008	
Total	2.7 million [2.4 – 3.0 million]
Adults	2.3 million [2.0 – 2.5 million]
Children under 15 years	430 000 [240 000 – 610 000]
AIDS-related deaths in 2008	
Total	2.0 million [1.7 – 2.4 million]
Adults	1.7 million [1.4 – 2.1 million]
Children under 15 years	280 000 [150 000 – 410 000]

The ranges around the estimates in this table define the boundaries within which the actual numbers lie, based on the best available information.

2009 AIDS epidemic update

UNAIDS  World Health Organization 

Several theories exist as to how HIV-1 can disrupt central nervous system (CNS) performance. Shortly after initial infection, HIV-1 is thought to cross the blood brain barrier (BBB) and enter the brain via infected macrophages. CNS invasion may provide a stable reservoir for latent infection and development of HAND (Gras et al., 2010). In addition, CNS penetration effectiveness (CPE) scores have been assigned to currently available antiretroviral drugs for BBB penetration and correlated to CSF viral loads, with zidovudine, nevirapine and indinavir/ritonavir being among the best (Letendre et al., 2010; Table 1-2). Of note, therapeutics may not be able to sufficiently target and suppress HIV in the brain as a majority of the recommended regimens of antiretroviral drugs are poor to moderate penetrators into the CNS (Letendre et al., 2010; bolded in Table 1-2).

Table 1.2 CSF penetration effectiveness (CPE) scores for FDA-approved antiretroviral drugs currently on the market

BBB Penetration	CPE Score	Antiretroviral Drugs (ARV)
Best	4	zidovudine, nevirapine, indinavir/ritonavir
Moderately Good	3	abacavir, emtricitabine , delavirdine, efavirenz , darunavir/ritonavir , fosamprenavir/ritonavir, indinavir, lopinavir/ritonavir, maraviroc, raltegravir
Moderately Poor	2	didanosine, lamivudine, stavudine, etravirine, atazanavir/ritonavir , atazanavir, fosamprenavir
Poor	1	tenofovir , zalcitabine, nelfinavir, ritonavir, saquinavir/ritonavir, saquinavir, tipranavir/ritonavir, enfuvirtide

**Adapted from Letendre SL, et al, 2010 Top HIV Med.; BBB; Blood Brain Barrier; Bolded ARV are those recommended by the US Department of Health and Human Services.

The CNS generally has been considered immunologically privileged, with relatively little inflammatory response. However, recent evidence suggests that inflammation is actively involved in the progression of CNS disorders, such as HAND (Gras et al., 2010). Importantly, neuroinflammation in the post-cART era seems to be similar to or escalated from the pre-CART era (Anthony et al., 2008). Examinations of HIV encephalitis (HIVE), the neuropathological correlate of HIV-1 infection in the CNS, revealed the presence of multinucleated giant cells, activated resident microglia, infiltration of peripheral monocytic cells, widespread reactive astrogliosis, myelin pallor, and decreased synaptic and dendritic densities or neurodegeneration (Adle-Biassette et al., 1998; Masliah et al., 1997; Petito et al., 1986). The severity of HIVE correlates with the presence of activated microglial or macrophage-like cells and CSF viral loads. Therefore, the current favored theory for HIV-associated neuropathogenesis is that CNS injury is mainly caused by the release of neurotoxic factors from activated or invading immune cells (Kraft-Terry et al., 2009; McArthur et al., 2010).

1.2. NEURODEGENERATION IN HAD: ROLE OF VIRAL ENVELOPE gp120

HIV-1, the most common and pathogenic strain of the virus, consists of several components that may be responsible by different mechanisms for the neuropathogenesis of HAD, the most severe form of HAND (Figure 1.1). The HIV genome consists of genes which encode for specific viral proteins: *gag*, encodes viral nucleocapsid proteins such as p24; *pol*, encodes the viral protease, reverse

transcriptase and integrase; *env*, encodes the viral envelope glycoproteins gp120 (extracellular glycoprotein) and gp41 (transmembrane glycoprotein); *tat*, encodes transactivator of transcription; *rev*, encodes a regulator of expression of viral protein; *vif*, encodes viral infectivity factor; *vpu*, encodes viral protein U; *vpr*, encodes viral protein R; and *nef*, encodes negative regulatory factor.

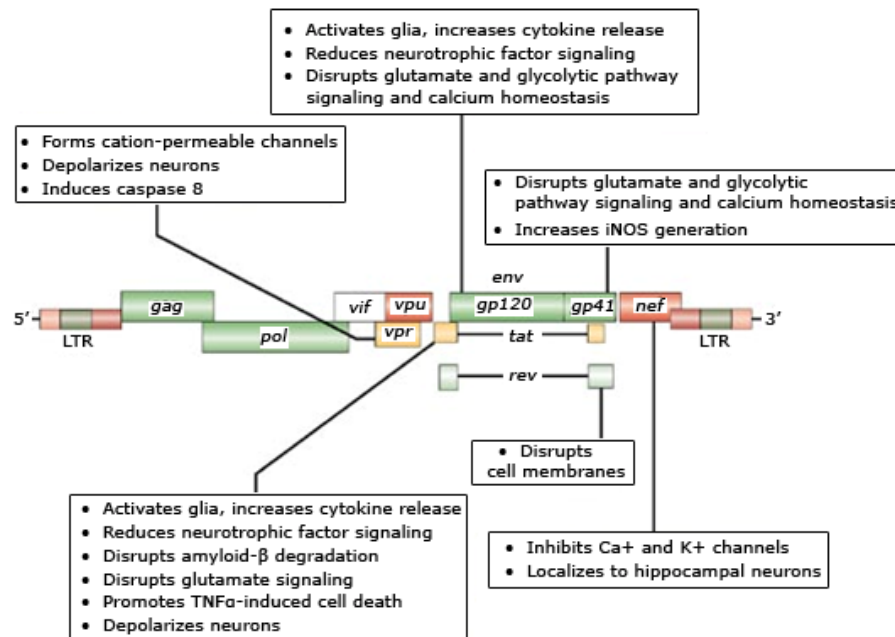


Figure 1.1 Components of the HIV genome implicated in neuropathogenesis. HIV encodes for nine viral proteins from; the structural (*gag*, *pol*, *env* (envelope/gp120, gp41)), regulatory (*tat* (transactivator of transcription), *rev* (regulatory for expression of viral proteins)), and accessory (*vpu*, *vpr* (viral protein r), *vif*, *nef* (negative factor)) proteins. Five of these can be released from the virus or infected cells and are thought to be involved in CNS injury (*Env* (*gp120* and *gp41*), *Nef*, *Rev*, *Vpr*, and *Tat*). Schematic diagram adapted from Ellis et al., 2007.

For the purpose of this dissertation, I will be primarily focusing on the viral envelope glycoprotein 120 (gp120) as it is the most reported component of HIV-1 thought to be neurotoxic and play a vital role in HIV-associated neurodegeneration (Ellis et al., 2007). The current model for HIV-1 gp120 neuropathogenesis indicates

that HIV-infected monocytes/macrophages infiltrate into the CNS and are able to release soluble gp120 and/or activate astrocytes, microglia, macrophages, monocytes or other resident immune cells within the brain. These activated cells are thought to then produce chemokines, cytokines and neurotoxins that cause neuronal injury and subsequent neuronal death (Figure 1.2) (Kaul et al., 2001). Although some groups have reported a potential direct neurotoxic effect of HIV-1 gp120 on neurons (Nguyen et al., 2009; Singh et al., 2005), release of neurotoxins from HIV infected monocytes (Giulian et al., 1990) or HIV-1 gp120-treated monocytes (Giulian et al., 1993; Medders et al., 2010) have proven to be most relevant to the development of neurodegeneration of HAD and HIVE.

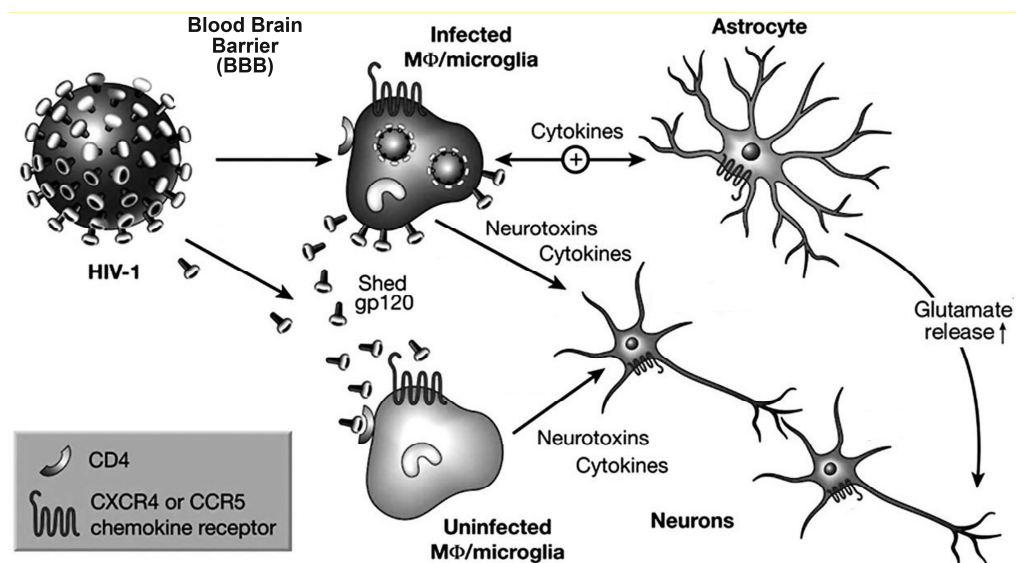


Figure 1.2 Schematic diagram of the role immune cells play in HIV-1 neuropathogenesis. HIV is able to hijack the immune system to enter into the CNS where it is able to cause injury to neurons via potential proinflammatory cytokines or other neurotoxin production. Diagram is adapted from Kaul et al., 2001.

Although rodents are not infected by HIV, they are sensitive to the neurotoxic action of its viral envelope protein gp120 (Toggas et al., 1994). An *in vivo* model of HAD has been used to investigate the neuropathogenesis of HAD. Transgenic mice overexpressing HIV-1 gp120 (gp120tg) in astrocytes present with considerable neuronal loss, astrogliosis, and an increased number of activated microglia cells in the brain at 6 months of age or greater (Ellis et al., 2007; Toggas et al., 1994). Additionally, these mice at around one year of age exhibit similar behavioral impairments similar to those seen in HAD patients (D'hooge et al., 1999).

Alternative *in vitro* approaches have provided abundant information about HIV-1 gp120-induced neurodegeneration, similar to that observed in gp120tg mice (Figure 1.3). Importantly, HIV-1 gp120 produces injury and apoptosis in both primary rodent and human mixed neuronal-glia cultures (Kaul et al., 2001). HIV-1 gp120-induced neuronal death requires the activation of apoptotic signaling pathways including caspases 3, 8 and 9 and p53 (Garden et al., 2004). Neuronal injury and death stimulated by HIV-1 gp120 is thought to be mostly via NMDA excitotoxicity, which can be rescued by specific antagonists of NMDA receptors *in vivo* and *in vitro* (Dreyer et al., 1990; Toggas et al., 1996).

In vitro models of HIV-1 gp120-induced neurotoxicity have also provided useful insight into the signaling pathways and potential identification of neurotoxins released by activated monocytes. HIV-1 gp120 has been reported to activate glia, primarily astrocytes and microglia (Lee et al., 2003; Ronaldson et al., 2009). In addition, previous studies have shown that HIV-1 gp120 may induce the release of glutamate, L-cysteine, quinolinic acid, arachidonic acid, PAF, free radicals, TNF, and

other inflammatory mediators from macrophages/microglia/monocytes, which may sensitize neurons to excitotoxicity (Cheung et al., 2008; Fantuzzi et al., 2008; Giulian et al., 1993; Giulian et al., 2005; Kaul et al., 2001; Lee et al., 2005). However, the exact mechanisms of HIV-1 gp120-induced release of inflammatory or excitotoxic mediators from monocytic cells remains to be fully understood.

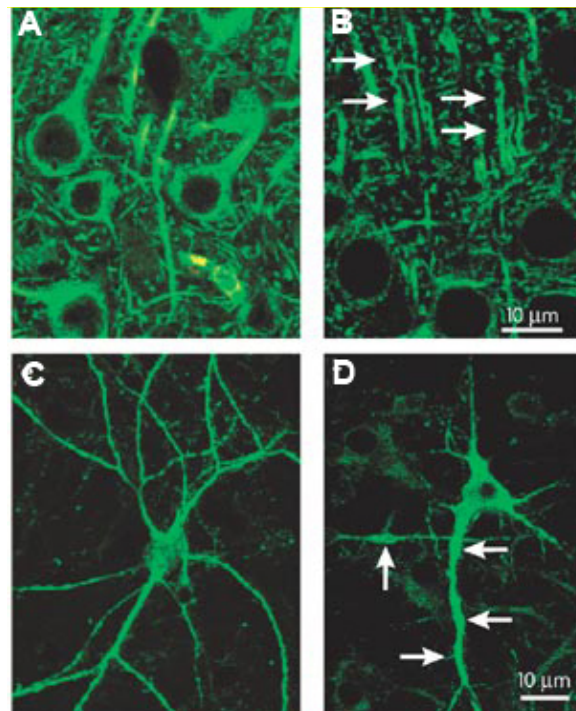


Figure 1.3 HIV-1 gp120 causes neuronal injury *in vivo* and *in vitro*. (A) Wild type mouse prefrontal cortex section stained for MAP-2 (mature neuron marker) showing normal neuronal structures. (B) HIV-1 gp120 transgenic mouse (gp120tg) prefrontal cortex stained for MAP-2 showing disrupted neuronal structures (arrows) and reduction in MAP-2 staining. (C) Human neuronal culture without HIV-1 gp120 treatment and (D) with gp120 showing neuronal injury (arrows). Figure adapted from Ellis et al., 2007.

1.3. CONTRIBUTION OF STRESS-ACTIVATED p38 MAPK SIGNALING IN HAND AND OTHER NEURODEGENERATIVE DISEASES

Mitogen-activated protein kinases are intracellular enzymes that are activated in response to stimuli from the extracellular environment. Several stimuli are known to activate these kinases, including osmotic stress or pro-inflammatory cytokines. The stress-activated protein kinase/mitogen-activated protein kinase or p38 MAPK and cJun N-terminal kinase (JNK) are among the most studied in pathological or disease conditions, including neurodegeneration. Most importantly, p38 MAPK has been implicated in HIV-gp120-induced neuronal death or injury (Kaul et al., 1999; Medders et al., 2010) and plays an important role in the activation of the monocytic cell lineage (Kaul et al., 2001).

There are two well-studied signaling pathways that regulate the activation of p38 MAPK. The canonical activation pathway of p38 MAPK includes the serine/threonine kinases (MKKKs), which phosphorylate and activate the dual specificity MAPK kinases (MKKs such as MKK3, MKK4, and MKK6) which in turn phosphorylate p38 MAPK. Alternatively, recent studies have shown that the non-canonical activation pathway of p38 MAPK involves auto-phosphorylation aided by the association of p38 MAPK with TGF β -activated protein kinase 1-binding protein 1 (TAB1) (Kang et al., 2006). Both pathways lead to dual phosphorylation of the kinase at Thr 180 and Tyr 182 residues which is required for activation of p38 MAPK (Ono et al., 2000). The canonical activation pathway can be triggered by many stimuli and is involved in many responses, including inflammation (Lee et al., 1999). However, the role of TAB1 triggered auto-phosphorylation still remains elusive (Ono et al., 2000).

The activation of p38 MAPK results in diverse responses via phosphorylation of its substrates, mostly kinases and transcription factors. The kinase substrates of p38

MAPK include MAPK-activated protein kinase 2 (MK2), MK3, and MK5. Activation of p38 MAPK has been shown to increase cytokine production by direct phosphorylation of downstream factors either by transcriptional regulation or by messenger RNA (mRNA) stabilization, especially in monocytic cells (Figure 1.4) (Dean et al., 1999; Ono et al., 2000). There are four isoforms of p38 MAPK (α , β , γ , and δ). Of these, the α -isoform (MAPK14) and β - isoform (MAPK11) have been identified as the main targets of potent anti-inflammatory imidazoles, such as the compound SB203580 (Lee et al., 1999). Past studies have identified p38 α MAPK as the principal isoform responsible for the inflammatory response (Kang et al., 2008). In fact, several inhibitors of p38 α MAPK have been developed for the treatment of inflammatory disorders, such as psoriasis, arthritis or chronic obstructive pulmonary disease with mixed success in clinical trials due to possible side effects (Mayer et al., 2006).

There is substantial amount of evidence associating elevated p38 MAPK activation to inflammation of the brain, as that seen in HIVE patients and Alzheimer's disease (AD) (Kaminska et al., 2009). HIV-1 gp120 has been shown to stimulate production of proinflammatory cytokines from monocytic cells, which could be prevented by p38 MAPK inhibition (Cheung et al., 2001; Fantuzzi et al., 2008; Lee et al., 2005). Similarly, the well-studied inflammatory stimulus bacterial endotoxin lipopolysaccharide (LPS) was able to induce production of NO and TNF in a p38 MAPK-dependent manner in primary rat and human microglia (Lee et al., 2000; Xing et al., 2008). In addition, Culbert et al. provided evidence that MK2 deficient mice no longer produced TNF and reduced neurotoxicity after stimulation with LPS or the AD

neurotoxin β -amyloid ($A\beta$) when compared to wild-type microglia (Culbert et al., 2006).

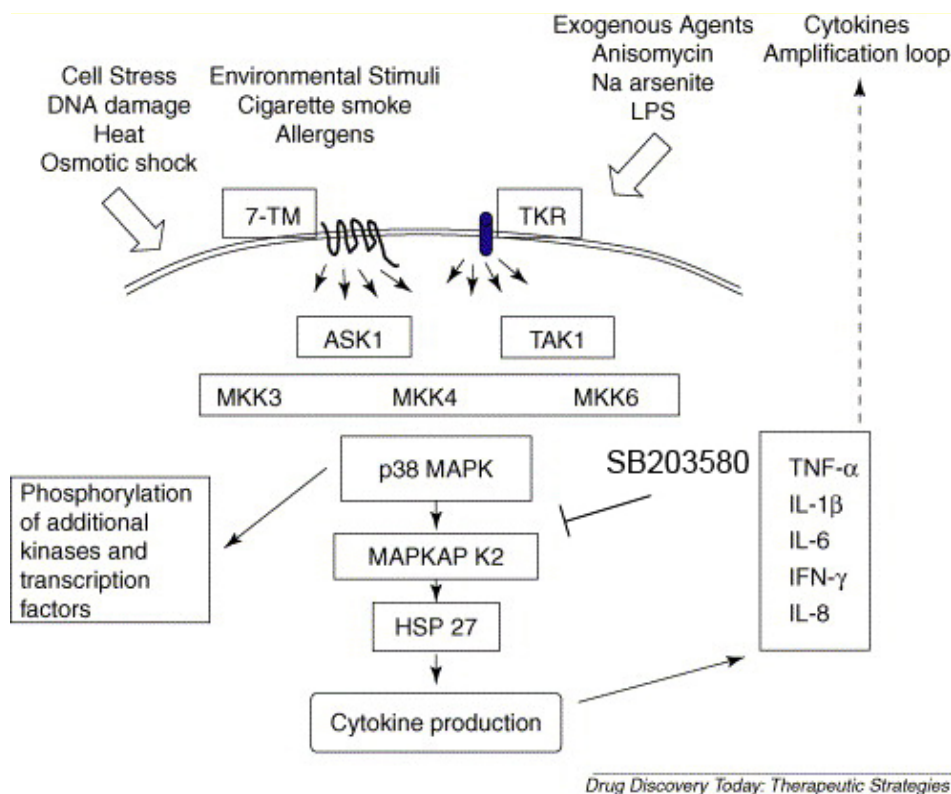


Figure 1.4 The p38 MAPK signaling cascade primarily in monocytes is involved in cytokine production. Cytokines regulated by p38 MAPK have been implicated in neuroinflammation and HIV-gp120 neurotoxicity. Upstream activators include apoptosis signal-regulated kinase (ASK1) and the mitogen-activated protein kinase (MKKs or MEKs); downstream effectors include mitogen-activated protein kinase-activated protein kinase-2 (MK2) and other MKs. Pharmacological inhibitor SB203580 blocks the ATP-binding site of p38 MAPK and prevents it from activating its downstream substrates. Schematic diagram adapted from Mayer et al., 2006.

Activation of p38 MAPK signaling also occurred in neurons that were co-cultured with LPS-activated microglia and this signaling was vital to induction of neuronal death (Xie et al., 2004). $A\beta$ -induced activation of p38 MAPK resulted in up-regulation of pro-inflammatory cytokines TNF α , iNOS, and IL-1 β , and subsequent neuronal death (Delgado et al., 2008). Our and other groups have shown that inhibition of p38 MAPK activity *in vitro* with pharmacological inhibitor SB203580 or dominant

negative p38 α AF (TGY substituted with AGF) prevented neuronal apoptosis induced by HIV-1 gp120 or glutamate (Chaparro-Huerta et al., 2008; Choi et al., 2007; Kaul et al., 1999; Kaul et al., 2007). Taken together, p38 MAPK signaling is a likely candidate for both the activation of monocytic cells, like microglia, and neuronal injury in response to soluble, monocytic-derived neurotoxic molecules in HIV-1 gp120-associated neurodegeneration (Figure 1.5). However, the mechanism of p38 MAPK-mediated HIV-1 gp120-induced neuronal death and possible neurotoxin production; and in which cell-type p38 MAPK mediates neurotoxicity still remain largely unknown.

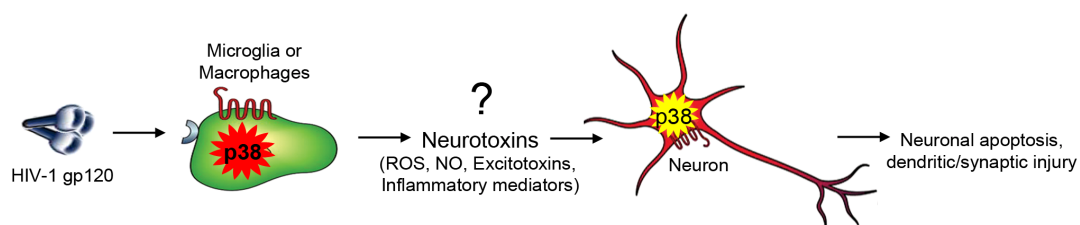


Figure 1.5 Schematic diagram of the involvement of p38 MAPK in HIV-1 gp120-induced activation of monocytes, production of neurotoxins and subsequent neuronal death. The identity of neurotoxins produced from HIV-1 gp120-activated monocytes still remain to be completely identified (?).

1.4. POTENTIAL MEDIATORS OF NEUROPROTECTION IN HAND

Many factors have been investigated for their potential in preventing neurodegeneration caused by HIV-1 and its viral envelope protein gp120. Current approaches include preventing neurotoxic signaling (such as p38 MAPK) with small molecules, increasing the amount of beta chemokines in the CNS and finally by

strengthening the ability of neurons to overcome neurotoxicity caused by HIV-1 infection or HIV-1 gp120.

Small molecules such as lithium have been implicated in prevention of HIV-1 gp120-induced neurotoxicity (Everall et al., 2002; Nguyen et al., 2009). Lithium prevents neuronal death by inhibiting the kinase GSK-3 β (Everall et al., 2002; Nguyen et al., 2009). Interestingly, GSK-3 β has been shown to be a possible downstream substrate of p38 MAPK (Thornton et al., 2008). Furthermore, recent studies have shown that lithium prevents pro-inflammatory cytokine production by inhibiting p38 MAPK activity (Hui et al., 2010). Further studies are needed to associate administration of the neuroprotective lithium in HIV-1 gp120 neurotoxicity to potential inhibition of p38 MAPK. Highly specific inhibitors of p38 MAPK may also be a protective therapeutic for HIV-1 gp120-induced neurotoxicity, although many inhibitors have been pulled from clinical trials due to adverse side effects, such as liver damage (Mayer et al., 2006). Interestingly, NDMA receptor antagonists such as memantine (on the market) or MK801, which inhibit excitotoxicity in neurons, have also been shown to reduce the activation of p38 MAPK after brain injury (Anh et al., 2000).

Beta chemokines (CCL3, CCL4, and CCL5), as natural ligands for HIV coreceptors, are known to suppress HIV-1 infection and disease progression (Cocchi et al., 1995). These reports suggested that suppression occurs through steric hindrance, receptor internalization, and/or via CCR5-mediated protective signaling against HIV. In support of this, our group and others have found that the CCL4 and CCL5 block neuronal death caused by HIV-1 gp120 *in vitro* (Kaul et al., 1999; Kaul et al., 2007;

Meucci et al., 1998). Beta chemokines also stimulate p38 MAPK in monocytes, but this differs from HIV-1 gp120 stimulation of p38 MAPK by potentially different mechanisms. As shown in previous studies, HIV-1 gp120 was able to stimulate p38 MAPK activation and inflammatory monocyte chemotactic protein-1 (MCP-1/CCL2) from monocytic cells, while CCL4 stimulated p38 MAPK without CCL2 production.

Neurotrophic factors promote the survival of neurons, primarily by reducing dendritic injury and promoting growth (Nosheny et al., 2007; Peng et al., 2008). As mentioned previously, neurodegeneration observed in HAD patients is linked to neuronal apoptosis and injury to synaptic or dendritic processes similar to other neurodegenerative disease. Therefore, neurotrophic factors are good candidates for the treatment of these disorders. In addition, previous studies have shown that HIV-1 gp120 was able to reduce the amounts of brain derived neurotrophic factor (BDNF) (Peng et al., 2008) and platelet derived growth factor (PDGF) (Nosheny et al., 2007) in neurons and addition of exogenous BDNF or PDGF were able to ameliorate the neurotoxic effects of HIV-1 gp120 by promoting neuronal survival. The regulation of neurotrophic factors such as PDGF in monocytes by HIV-1 gp120 or p38 MAPK activation remains to be further explored in the future.

MAIN OBJECTIVES AND SIGNIFICANCE

The main objectives of this dissertation are to 1) investigate the cellular mechanisms of neuronal injury in *in vitro* models of HAND; 2) examine the role of HIV-1 gp120 in neurotoxicity within different brain cell populations; and 3) analyze the activation of stress-activated kinase p38 MAPK and its downstream targets in the mechanisms of HIV-1 gp120-mediated neurotoxicity.

My hypothesis is that HIV-1 gp120-mediated alterations in signaling cascades such as the p38 MAPK are centrally involved in both the initiation of neuronal apoptosis and activation of the neurotoxic phenotype of mononuclear phagocytic cells in HIV-1 gp120-induced neurodegeneration implicated in syndromes such as HAND. I propose that activation of these pathways by HIV-1 gp120 dysregulates homeostatic conditions essential for the maintenance of neuronal survival.

Identification of signaling pathways and potential downstream factors responsible for the neurotoxic phenotype of mononuclear cells exposed to HIV-1 envelope protein may provide therapeutic targets for the reduction of HAND symptoms, which prevail regardless of current combination antiretroviral therapies. Preventing neurotoxicity by regulating these pathways with selective agents could prove useful as an additive treatment to current antiretroviral therapies which significantly curtail the virus in the periphery. The quality of life for the thousands of patients living with HIV could be greatly improved with these potential future therapies.

ACKNOWLEDGEMENTS

Chapter 1, in part, contains modified figures that appear in Nature Reviews Neuroscience 2007; with kind permission from Nature Publishing Group: Ellis RJ, Langford D, Masliah E (2007) HIV and antiretroviral therapy in the brain: neuronal injury and repair. Chapter 1, in part, also contains a modified figure that appears in Drug Discovery Today: Therapeutic Strategies 2006; with kind permission from Elsevier Limited: Mayer RJ and Callahan JF. 2006. p38 MAP kinase inhibitors: A future therapy for inflammatory diseases. Chapter 1, in part, also contains a modified figure that appears in Nature 2001; with kind permission from Nature Publishing Group: Kaul M, Garden GA, Lipton SA (2001) Pathways to neuronal injury and apoptosis in HIV-associated dementia.

CHAPTER 2

MATERIALS AND METHODS

2.1. REAGENTS

Recombinant gp120 from different HIV-1 strains, SF2 (dual-tropic) or SF162 (CCR5-preferring), were obtained from NIH AIDS Research and Reference Reagent Program. Recombinant human chemokines were purchased from R&D Systems (Minneapolis, MN). A specific p38 MAPK inhibitor, SB203580, was obtained from Calbiochem (San Diego, CA). Bacterial endotoxin lipopolysaccharide (LPS) was purchased from Sigma (St. Louis, MO). Chemokines and HIV gp120 were reconstituted in 0.1% bovine serum albumin (BSA) at 100 X the final concentration and controls received BSA vehicle alone (0.001% final concentration). Kinase inhibitor was dissolved in DMSO at 1,000 X the final concentration (0.1-10 μ M) and was added to the cultures for 15 min prior to treatment with 200 pM or 1 nM HIV-1 gp120 strains or neurotoxic supernatants from THP-1 cells for different incubation times. Montelukast (specific cysteinyl leukotriene 1 receptor (CysLT1) antagonist) was purchased from Cayman Chemical (Ann Arbor, MI) and dissolved in DMSO and diluted to 1,000 X the final concentration (1 μ M) before pre-incubation in cerebrocortical cultures for 30 min prior to treatment with THP-1 neurotoxic supernatants. Protein synthesis inhibitor/antibiotic and potent activator of p38 MAPK,

anisomycin, was purchased from Calbiochem (San Diego, CA). Anisomycin was dissolved in DMSO at 1,000 X the final concentration (10 µg/ml).

2.2. PREPARATION OF CEREBROCORTICAL, MIXED NEURONAL-GLIAL CELL CULTURES

Rat mixed neuronal/glial cerebrocortical cultures were prepared from embryos of Sprague-Dawley rats at day 15 to 17 of gestation, as previously described by our group (Kaul et al., 1999; Kaul et al., 2007). In brief, cells were cultured in 35 mm dishes with poly-L-lysine-coated glass coverslips (1.87×10^6 cells per dish) or poly-L-lysine-coated clear bottom 96 well plates for imaging (BD Falcon; 0.087×10^6 cells per well) and D10C medium containing 80% DMEM with high glucose (Invitrogen), 10% FBS (Hyclone), 10% F12 (Hyclone), 3% 1 M HEPES (Omega), 200 mM L-glutamine (Invitrogen), and 100 U/ml penicillin with 100 µg/ml streptomycin (Invitrogen). Cell populations consisted of ~30% neurons, ~70% astrocytes and ~0.1 to 1% microglia (Kaul et al., 2007) and, generally, were used after 17 days in vitro (DIV) when the majority of neurons were considered to be fully differentiated and susceptible to NMDA toxicity. For most experiments, rat cultures were transferred into pre-warmed Earle's balanced salt solution (EBSS) containing 1.8 mM Ca^{2+} and 5 µM glycine without Mg^{2+} . For some experiments in which the contribution of microglia to neurotoxicity was investigated, microglia were depleted by pre-treatment of the cultures overnight with 7.5 mM L-leucine methyl ester (Kaul et al., 1999). Importantly, rodents express CXCR4 and CCR5 homologues, which are capable of

interacting with HIV-1 via gp120 binding (Kaul et al., 1999; Kaul et al., 2007). Murine cerebrocortical cell cultures from CCR5/CXCR4 double knockout embryos were prepared as previously published by our group (Kaul et al., 2007) and are similar to their above described counterpart derived from rat embryos with the exception that they comprise ~ 4-5% microglia. All experiments involving animals have been approved by the Institutional Animal Care & Use Committee of the Sanford-Burnham Medical Research Institute.

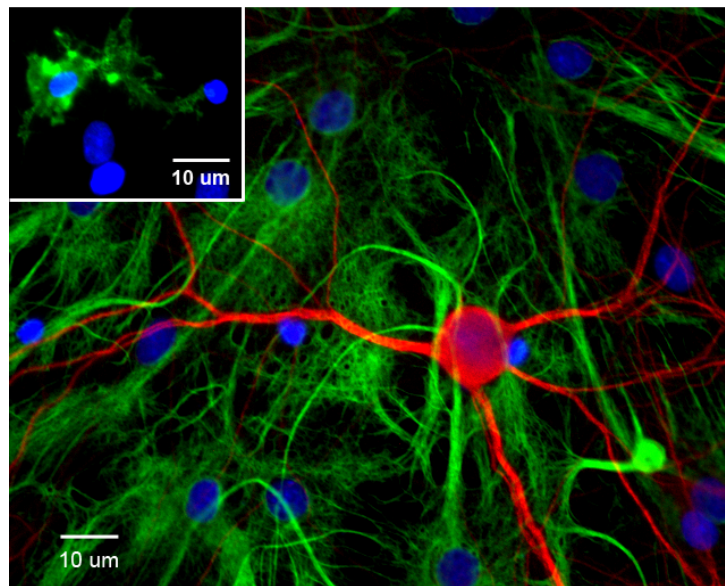


Figure 2.1 Embryonic rat cerebrocortical, mixed neuronal-glia cells after 17 days *in vitro* (DIV). Microtubule-Associate Protein 2 (MAP-2) is a marker for mature neurons as seen in red; Glial Fibrillary Acidic Protein (GFAP) is a marker for astrocytes as seen in green (main image, not inset); CD11b is marker for microglia and macrophages as seen in green (inset) above. Microglia were depleted from cultures as an experimental model by incubation of cerebrocortical cultures with 7.5 mM leucine methyl ester (LME) 4 h to overnight without injury to astrocytes or neurons (as described above and in previous studies (Kaul M et al., 1999)).

2.3. ISOLATION AND PREPARATION OF MONOCYTE-DERIVED MACROPHAGES

The preparation of human primary monocyte-derived macrophages (MDM) using a Ficoll gradient was performed as previously described (Kaul et al., 1995; Terheyden et al., 2005). In brief, whole blood from consenting healthy donors was obtained through the Normal Blood Donor Service of The Scripps Research Institute's (TSRI) at Scripps Health Green Hospital, La Jolla, CA (P.I.: Daniel R. Salomon, M.D., TSRI, La Jolla CA; IRB Protocol: # 09-5252). Following an initial centrifugation step of the heparinized blood at 200 x g for 20 min, buffy coat cells were isolated using density gradients of Ficoll-paque (ρ 1.073; GE Health Life Sciences, Piscataway, NJ) and transferred into 75 cm² cell culture flasks (Kaplan et al., 1982). After allowing adherence in RPMI 1640 containing 2 mM glutamine, antibiotics (Penicillin/Streptomycin) and 10% human AB serum (RPMI-ABS) at 37°C, 6% CO₂, in humidified atmosphere, non-adherent cells were removed by rigorous washing with warm RPMI 1640 (37°C) without supplements. Adherent monocytes were then cultured for 7 days in the above serum-containing medium to allow for differentiation into MDM (Kaplan et al., 1982). For harvest and further experimentation the cells were detached by treatment with phosphate buffered saline (PBS) containing EDTA (Sigma, 0.2 g/l) for 5 to 10 min at 37°C and scraping with a rubber policeman. After washing three times in PBS cells were reseeded at 0.25×10^6 cells / 0.5 ml medium per well in 24 well plates. Cell viability was monitored with Trypan Blue exclusion and usually exceeded 95%.

2.4. CELL CULTURE OF HUMAN MONONUCLEAR THP-1 CELLS

Human mononuclear THP-1 cells, a model for monocyte lineage cells, including microglia and macrophages (Giulian et al., 1993; Giulian et al., 1990), were maintained in medium containing 90% RPMI (Gibco), 10% FBS (Hyclone), 2 mM L-glutamine (Sigma), and a combination of 100 U/ml penicillin with 100 µg/ml streptomycin (P/S, Sigma) at 37°C with 5% CO₂ and are usually split 1:3 to 1:4 once to twice a week after reaching approximately 1×10^6 cells per milliliter. For siRNA experiments, THP-1 cells were plated at 0.2×10^6 cells/ml after reaching a density of $0.3\text{-}0.4 \times 10^6$ cells/ml. Upon reaching a density of $0.6\text{-}0.7 \times 10^6$ cells/ml, cells were collected for nucleofection of siRNA duplexes using the Amaxa nucleofector system (Walkersville, MD) and the supplier's protocol.

2.5. ASSESSMENT OF NEURONAL DEATH

Neuronal apoptotic death and loss was analyzed as previously described (Kaul et al., 2007). In brief, the number of neurons were quantified by immunostaining for the neuron-specific marker microtubule-associated protein 2 (MAP-2), and apoptotic nuclei were identified morphologically after staining nuclei with the DNA dye Hoechst 33342. Alternatively, apoptosis was quantified by terminal deoxynucleotidyl transferase dUTP nick end labeling (TUNEL; Apoptosis Detection System/Fluorescein, Promega, Madison, WI) to detect fragmented nuclear DNA in apoptotic nuclei as seen in Figure 3.8. Neuronal survival was calculated from the percentage of neurons remaining after subtraction of those that had undergone apoptosis. Three to eight independent experiments were performed for each treatment.

2.6. MONONUCLEAR CELL-MEDIATED NEUROTOXICITY

In order to obtain conditioned cell culture supernatants, human mononuclear THP-1 cells or primary MDM were incubated for 24 h or 4 days in the presence or absence of recombinant viral envelope gp120 of HIV strains SF2 and SF162 or LPS in the same media used to culture rat cerebrocortical cells (THP-1 cells) or RPMI-ABS (MDM). The controls without gp120 or LPS received 0.001% BSA (vehicle) only, or CCL4/MIP-1 β or CCL5/RANTES (both at 20 nM). For some experiments, THP-1 cells were transduced using adenoviral expression vectors (AdV) encoding a dominant-negatively interfering mutant of p38 MAPK or GFP as control 2 days before the exposure to HIV-1 gp120 or BSA control in THP-1 culture media or RPMI-ABS in the case of MDM (Kaul et al, 2007). All AdV were kindly provided by Dr. J. Han, The Scripps Research Institute, La Jolla, CA (Zhao et al., 1999), and amplified and titrated using standard procedures. Following a 1 or 4 day stimulation period, cell-free supernatants were transferred at a final 10% concentration to the mixed rat neuronal-glial cultures depleted of microglia (as described in the *Tissue culture* section above) maintained in D10C medium as readout for neurotoxicity (Giulian et al., 1993; Giulian et al. 1990). If not stated otherwise, neuronal survival was assessed after 72 h of incubation, neuronal survival as described above. In addition, THP-1 cell lysates were collected as described below for immunoblotting.

2.7. siRNA NUCLEOFECTION

MAPK14 (p38 α MAPK) siRNA or non-targeting siRNA duplexes were obtained from Dharmacon/Thermo Fisher Scientific (Lafayette, CO) and Ambion/Applied Biosystems (Austin, TX). Silencer MAPK14 siRNA (ID# 1217 and 1312) duplexes from Ambion are referred to as “sip38 α -1” and “sip38 α -2,” respectively, in this manuscript. ON-TARGETplus MAPK14 siRNA (J-003512-21) from Dharmacon is referred to as “sip38 α -3” in this manuscript. The siRNA duplexes were transfected into THP-1 cells at a density of 1×10^6 cells/ml using Amaxa (Walkersville, MD) nucleofector kits according to the manufacturer’s instructions. Briefly, 48 h after nucleofection with 2 μ g siRNA, THP-1 cells were treated for 24 h with 200 pM HIV-1 gp120_{SF2} or gp120_{SF162}. Supernatants or conditioned media from these treatments were then collected and used at 10% final concentration on microglia-depleted rat cerebrocortical cultures as previously described for neurotoxicity analysis. The mononuclear THP-1 cells were collected and analyzed for p38 MAPK via Western blot.

2.8. IMMUNOFLUORESCENT STAINING AND DECONVOLUTION MICROSCOPY

After treatment and washing with PBS, rat cerebrocortical cultures were fixed for 25 min with 4% PFA at 4°C and subsequently permeabilized with either 0.2% Triton X-100 for 5 min at room temperature (for staining of MAP-2 or TUNEL alone) or 100% methanol for 10 min at -20°C (for staining of phosphorylated p38 with or

without MAP-2). Primary antibodies included mouse anti-MAP-2 (1:500, Sigma M4403; St. Louis, MO), chicken anti-MAP-2 (1:5000, Abcam ab5392; Cambridge, MA), rabbit anti-ACTIVE p38 (1:1000, Promega V1211; Madison, WI), and mouse anti-CD11b (1:150, Serotec MCA275; Raleigh, NC). Secondary antibodies included goat anti-rabbit or anti-mouse or anti-chicken IgGs Alexa 594/488/647 (1:2000, Invitrogen; Carlsbad, CA) and horse anti-mouse IgG Texas Red (1:150, Vector Labs; Burlingame, CA). Controls were included in which primary antibodies were either omitted or replaced with irrelevant IgG of the same subclass. Nuclear DNA was stained with Hoechst H33342. Deconvolution microscopy was performed as described earlier with filters for DAPI, FITC, CY3 and CY5 with the only modification that a constraint iterative algorithm was used for deconvolution (Slidebook software, Intelligent Imaging Innovations; Denver, CO) (Kaul M et al., 2007).

2.9. CELL LYSATES

After washing with PBS, cerebrocortical cells or mononuclear THP-1 cells were harvested by adding 1 X Cell Lysis Buffer (20 mM Tris-HCl (pH 7.5), 150 mM NaCl, 1 mM Na₂EDTA, 1 mM EGTA, 1% Triton, 2.5 mM sodium pyrophosphate, 1 mM beta-glycerophosphate, 1 mM Na₃VO₄, 1 µg/ml leupeptin; Cell Signaling; Beverly, MA) supplemented with 5 mM NaF (Serine/Threonine protein phosphatase inhibitor) and Complete Protease Inhibitor Cocktail (Roche; Indianapolis, IN) on ice for 10 min. The lysed samples were transferred to microcentrifuge tubes, sonicated 4 times 5 seconds, and then cleared by centrifugation (13,200 rpm, 10 min) at 4°C.

Lysate total protein concentrations were determined using the BCA protein assay kit (Pierce/Thermo Fisher Scientific; Rockford, IL). Alternatively, in some experiments THP-1 cells or MDM were directly dissolved at 0.25×10^6 cells / 150 μ l of SDS-containing gel loading-buffer (187.5 mM Tris-HCl (pH 6.8 at 25°C), 6% (w/v) SDS, 30% glycerol and 0.03% (w/v) bromophenol blue; Cell Signaling Technology, Beverly, MA).

2.10. IMMUNOCOMPLEX KINASE ASSAY FOR p38 MAPK OR SAPK/JNK ACTIVITY

The kinase assays for phosphorylated p38 MAPK and JNK were performed using the kinase assay kits from Cell Signaling Technology following the supplier's instructions. In brief, immobilized anti-phospho-p38 MAPK monoclonal antibody was used to immunoprecipitate active p38 MAPK from cell lysate (200-400 μ g total protein), followed by an in vitro kinase assay using ATF-2 as a substrate. ATF-2 phosphorylation was detected by western blotting using phospho-ATF-2 antibody (1:1000; Cell Signaling). For SAPK/JNK kinase activity, c-Jun fusion protein linked to agarose beads was used to pull down JNK enzyme from cell extracts (200-400 μ g total protein); and phospho-c-Jun antibody was measured via western blotting (1:1000; Cell Signaling). All protein kinase assays were standardized for total cellular protein amount and lysate volume used in the initial immunoprecipitation step.

2.11. IMMUNOBLOTTING

For Western blotting analysis of whole cell lysates or substrates of kinase assays, 4 X LDS sample buffer and 10 X reducing agent (Invitrogen; Carlsbad, CA) were added to samples containing equal amounts of total protein (10, 30 or 50 μ g for lysates; 2 μ g kinase substrate) and heated for 5 min at 100°C. Alternatively, cell lysates in SDS-containing gel loading-buffer were made 41 mM in dithiothreitol and heated. Samples were then electrophoretically separated on SDS-PAGE gels (NUPAGE; Invitrogen) under reducing conditions and subsequently electro-transferred to PVDF membranes (Bio-Rad; Hercules, CA). After blocking, membranes were incubated with gentle agitation overnight at 4°C with specific primary antibodies against ACTIVE p38 or ACTIVE JNK (1:100 (for cerebrocortical cells) – 1:1000 (for THP-1 cells and MDM); Promega), total p38 or JNK (1:1000, Cell Signaling), phospho-HSP27 (Ser 82) (1:1000, Millipore), total HSP27 (1:40000, Sigma), LTC4S (1:500, Cayman Chemicals) and β -actin or GAPDH (1:20,000; Ambion). The membranes were then incubated with secondary antibodies conjugated with horseradish-peroxidase for 30 min and exposed to SuperSignal Pico chemoluminescent detection kit (Pierce). Western blotting results were analyzed using Adobe Photoshop or ImageJ (NIH) and densitometric measurements normalized against housekeeping β -actin or GAPDH expression levels.

2.12. RNA EXTRACTION, QRT-PCR AND DNA MICROARRAY

RNA was isolated from THP-1 cells after 15 min pretreatment with 10 μ M SB203580 and subsequent treatment for 4 h to 24 h with 200 pM HIV gp120 or 1 μ g/ml LPS using RNeasy kits commercially available from Qiagen (Valencia, CA). Roughly 2×10^6 cells were collected to obtain 500 ng – 2 μ g RNA. RNA quality (A260/A280 ratio \sim 1.8-2.0) was tested using the NanoDrop system from Thermo Scientific (Rockford, IL). High quality RNA was then provided to the Microarray/QPCR Facility Core at Sanford-Burnham Medical Research Institute and DNA microarray was performed using the whole genome gene-expression analysis HumanHT-12 v4 Expression BeadChip kit from Illumina (San Diego, CA). Microarray results were further analyzed using the GeneSpring GX platform, provided kindly by Dr. Roy Williams (Bioinformatics Core, Sanford-Burnham Medical Research Institute). RNA was also reverse-transcribed into cDNA using the QuantiTect kit from Qiagen. Quantitative real-time polymerase chain reaction (qRT-PCR) was then performed on the cDNA to confirm TNF mRNA microarray results using Power SYBR Green Mastermix from Applied Biosystems (Carlsbad, CA) and the qRT-PCR machine from Agilent Technologies (Santa Clara, CA). The following primers were used for qRT-PCR: human TNF α forward: 5'- ATG AGCA CTG AAA GCA TGA TCC-3' and reverse: 5'-GAG GGC TGA TTA GAG AGA GGT C-3' (Harvard PrimerBank ID 25952111a1); human LTC4S forward: 5'-CTG TGC GGC CTG GTC TAC CTG-3' and reverse: 5'-GGG AGG AAG TGG GCG AGC AG-3' (James et al., 2006); human PLAUR forward: 5'-TAT TCC CGA AGC CGT TAC CTC and reverse: 5'-TCG TTG CAT TTG GTG GTG TTG-3' (Harvard PrimerBank ID 4505865a2); human β -actin forward: 5'- CAT GTA CGT TGC TAT CCA GGC-3'

and reverse: 5'- CTC CTT AAT GTC ACG CAC GAT-3' (Harvard PrimerBank ID 4501885a1). The following thermal cycle protocol was utilized for the reactions: 95°C 10 min; 95°C 30 sec, 60°C 1 min, 72°C 30 sec for 40 cycles; 55°C 5 min. Relative differences in gene expression among groups were expressed using the threshold cycle (Ct) values. The delta Ct (Δ Ct) values of the genes of interest were first normalized with values obtained from housekeeping β -actin of the same samples, and then the relative differences between control and each treatment group were calculated and expressed as relative to control, in triplicate.

2.13. CHEMOKINE, CYTOKINE OR GROWTH FACTOR ELISA AND MULTIPLEX BEAD ARRAYS

Culture supernatants were harvested from human THP-1 cells or MDM in culture media after 24 hours to 4 days post-treatment with silencing RNA, SB203580, HIV gp120, and/or LPS. These samples were analyzed in biological and technical triplicate for IL-1 β , TNF α , CCL5/RANTES, and CCL2/MCP-1 by enzyme-linked immunosorbent assays (ELISA) using commercially available kits from R&D Systems (Minneapolis, MN). Alternatively, the culture supernatants were analyzed for 13 different human analytes (IL-1 β , TNF α , PDGFA/A and B/B, CCL2, CCL5, CCL3, CCL4, CXCL1, VEGF, CCL20, IP-10, and CXCL8/IL8) using commercially available custom-made LEGENDplex bead array assays from BioLegend (San Diego, CA) with data acquired on a Bio-Plex instrument from Bio-Rad (Hercules, CA).

2.14. DATA AND STATISTICAL ANALYSIS

The data are expressed as mean values \pm SEM for three-nine independent experiments. Statistical analysis was performed applying one-way ANOVA followed by Fisher's PLSD post hoc test or student's t-test using the StatView software package (version 5.0.1, SAS Institute Inc.). The significance level was set at $p < 0.05$. The immunoblotting and immunofluorescence images are representative samples of the at least three independent experiments performed.

CHAPTER 3

ACTIVATION OF P38 MAPK IS REQUIRED IN MONOCYTIC AND NEURONAL CELLS FOR HIV GP120-INDUCED NEUROTOXICITY

Copyright 2010. The American Association of Immunologists, Inc.

3.1. ABSTRACT

HIV-1 envelope protein gp120 has been implicated in neurotoxin production by monocytic cells, namely macrophages and microglia, and the pathogenesis of HIV-1 associated neurocognitive disorders (HAND). We previously showed in rodent cerebrocortical cell cultures containing microglia, astrocytes and neurons, that overall inhibition of p38 MAPK signaling abrogated the neurotoxic effect of HIV-1 gp120. However, the time course of p38 MAPK activation and the contribution of this kinase in the various cell types remained unknown. In this study, we found that for HIV gp120-induced neurotoxicity to occur, active p38 MAPK is required in monocytic lineage cells, namely macrophages and microglia, and neuronal cells. In cerebrocortical cell cultures HIV-1 gp120 stimulated a time-dependent overall increase of active p38 MAPK and the activated kinase was primarily detected in microglia and neurons. Interestingly, both increased activation of p38 MAPK and neuronal death in response to gp120 were prevented by prior depletion of microglia, or in the presence of CCR5 ligand CCL4 or of p38 MAPK inhibitors. In human monocytic THP-1 cells and primary monocyte-derived macrophages (MDM), HIV

gp120 stimulated production of neurotoxins was abrogated by prior introduction into the cells of a dominant-negative p38 MAPK mutant or p38 MAPK siRNA. In addition, the neurotoxic effects of cell-free supernatants from gp120-stimulated monocytic THP-1 cells were prevented in microglia-depleted cerebrocortical cells pretreated with a pharmacological inhibitor of p38 MAPK. Thus, p38 MAPK signaling was critical upon exposure to HIV gp120 for both the neurotoxic phenotype of monocytic cells and subsequent toxin-initiated neuronal apoptosis.

3.2. INTRODUCTION

Patients infected with HIV-1 can develop neurological complications in addition to AIDS, including motor and cognitive dysfunctions termed HIV-1-associated neurocognitive disorders (HAND) (Antinori et al., 2007). In the central nervous system (CNS), invading infected mononuclear phagocytes, namely monocytes and macrophages, and resident microglia may be acting as a reservoir for HIV-1 (Gonzalez-Scarano et al., 2005; Koenig et al., 1986; Porcheray et al., 2006). By secreting viral proteins that are thought to also stimulate uninfected microglia and macrophages to release neurotoxins, those infected immune cells are presumed to be ultimately responsible for the development of HAND (Gonzalez-Scarano et al., 2005; Kaul et al., 2001). Development of HAND has been correlated to the neuropathological diagnoses of HIV encephalitis (HIVE) characterized by widespread reactive astrogliosis, myelin pallor, decreased synaptic and dendritic density, selective neuronal loss, and the infiltration and accumulation of monocytic cells, including

blood-derived macrophages and resident microglia (Masliah et al., 1992; Masliah et al., 1997). In fact, loss of neuronal processes and synapses and activation of both uninfected and infected microglia appears to constitute the best correlate to CNS impairment after HIV-1 infection (Adle-Biassette et al., 1999; Glass et al., 1995). However, the molecular mechanism of how HIV-1 triggers macrophage/microglial activation and neurotoxicity are not completely understood.

Several *in vitro* and *in vivo* studies have shown that the envelope glycoprotein gp120 of various HIV-1 strains produce injury and apoptosis in both primary human and rodent neurons (Giulian et al., 1993; Hesselgesser et al., 1998; Kaul et al., 1999; Kaul et al., 2007; Meucci et al., 1998; Shi et al., 1996; Singh et al., 2005; Toggas et al., 1994). HIV-1 gp120 coreceptors, in particular chemokine receptors CXCR4 and CCR5, are besides CD4 the first sites of host-virus interaction. Although CCR5 and CXCR4 are present not only on macrophages and microglia but also on neurons and astrocytes (Kaul et al., 2007), HIV-1 gp120 requires CD4 receptors, which are only located on cells of immune lineage, to efficiently engage coreceptors and infect target cells (Gonzalez-Scarano et al., 2005; Kaul et al., 2001). However, interaction between gp120 and CXCR4/CCR5, independent of CD4, has been shown to cause activation of the G protein-coupled receptor and contribute to intracellular Ca^{2+} accumulation and signaling (Hesselgesser et al., 1997). Thus, direct interaction of gp120 with neuronal chemokine receptors (Hesselgesser et al., 1997; Hesselgesser et al., 1998) may contribute to neuronal injury, while activation of macrophage HIV co-receptors and subsequent release of neurotoxins, such as excitotoxins, chemokines and/or pro-inflammatory cytokines, presumably provide the predominant trigger for neuronal

injury and death, as previously suggested (Cheung et al., 2008; Giulian et al., 1993; Kaul M et al., 1999; O'Donnell et al., 2006; Porcheray et al., 2006). In support to the latter, depletion or inactivation of microglia in mixed neuronal-glial cell cultures completely abrogates HIV-1 gp120-induced neuronal death (Garden et al., 2004; Kaul M et al., 1999). Furthermore, we have previously shown that both CCR5 and CXCR4 can mediate the neurotoxic effect of gp120 depending on the co-receptor usage of the virus strain from which the envelope protein originated (Kaul et al., 2007).

In addition, β -chemokines and natural CCR5 ligands CCL3 (MIP-1 α), CCL4 (MIP-1 β), and CCL5 (RANTES) have been reported to be major suppressors of HIV-1 infection and disease progression (Cocchi et al., 1995). These reports suggested that suppression occurs through steric hindrance, receptor internalization, and/or via CCR5-mediated protective signaling against HIV. In support of this, our group and others have found that the CCR5 ligands CCL4 and CCL5 block neuronal death caused by HIV-1 gp120 *in vitro* (Kaul et al., 1999; Meucci et al., 1998).

Macrophages or microglia are principal targets for both β -chemokines and gp120 variants, but the mechanism in which gp120-induced chemokine receptor signaling in macrophages/microglia results in a neurotoxic phenotype is not well-defined. However, previous studies have shown that possible mechanisms of HIV-1 neuropathogenesis involve the perturbation of intracellular signaling by HIV-1 gp120 and subsequent release of neurotoxic factors from activated macrophages and microglia (Del Corno et al., 2001; Giulian et al., 1993; Kaul et al., 1999; Kerr et al., 1997; O'Donnell et al., 2006; Porcheray et al., 2006; Zheng et al., 1997). Intracellular signaling pathways such as those of Src family kinase Lyn (Cheung et al., 2008),

PI3K²⁰, Akt (Kaul et al., 2007), the focal adhesion-related proline-rich tyrosine kinase Pyk2 (Del Corno et al., 2001; Cheung et al., 2008), phosphatidylcholine phospholipase C (PC-PLC) (Fantuzzi et al., 2008), proteins of the MAPK family (Del Corno et al., 2001; Kaul et al., 1999; Kaul et al., 2007; Perfettini et al., 2005) and the transcription factor p53 (Garden et al., 2004; Perfettini et al., 2005) have been implicated as potential pathways responsible for gp120-induced macrophage activation and neurotoxicity. Of these, MAPKs are involved in several diverse biological activities including differentiation, proliferation, apoptosis and inflammation (Ono et al., 2000). The stress-activated p38 MAPK has been shown to be responsible for neuronal death, microglial/macrophage activation and proinflammatory cytokine production in several CNS disorders (Barber et al., 2004; Barone et al., 2001; Choi et al., 2007; Kaul et al., 1999; Kaul et al., 2007; Johnson et al., 2003). In fact, we previously showed that inactivating p38 MAPK with p38-specific pharmacological inhibitor SB203580 or dominant negative p38 α (p38 α AF) in mixed neuronal-glia cultures prevented neuronal death triggered by HIV-1 gp120 while others reported that blocking p38 MAPK activity also ameliorated glutamate toxicity in neuron-rich cell cultures (Choi et al., 2007; Kaul et al., 1999; Kaul et al., 2007). However, the molecular mechanism of p38 MAPK activation and its cell-specific responses downstream of chemokine receptor signaling in gp120-mediated neurotoxicity is still unknown.

For this purpose, we investigated the neurotoxic effects of HIV-1 gp120 on cell type-specific p38 MAPK signaling pathways using both primary mixed neuronal-glia cerebrocortical cultures from rodents and human mononuclear/monocytic THP-1 cells or primary human monocyte-derived macrophages (MDM) as models for

macrophages and microglia. We found that HIV-1 gp120 activated p38 MAPK primarily in neurons and microglia, but not in astrocytes. We also found that depletion of microglia from mixed cultures and pretreatment with neuroprotective CCL4 reduced the activation of neuronal p38 MAPK after gp120 exposure. In addition, monocyte/macrophage-like THP-1 cells and MDM also required p38 MAPK for gp120-induced neurotoxin production. However, inhibiting p38 MAPK activation in neurons prevented death induced by neurotoxic media derived from gp120-stimulated THP-1 cells, whereas absence of HIV coreceptors in cerebrocortical neurons and astrocytes failed to protect the cell cultures from gp120-induced neurotoxicity of the monocytic cells. Our results suggested that p38 MAPK signaling is responsible for both the neurotoxic phenotype of macrophages/microglia and the initiation of neuronal apoptosis upon exposure to HIV gp120.

3.3. RESULTS

3.3.1. HIV-1 gp120-induced neuronal death requires p38 MAPK activation

We have previously shown that envelope protein gp120 derived from CCR5-preferring, CXCR4-preferring as well as dual-tropic HIV-1 strains can induce neurotoxicity and that this toxicity is equally mediated by the respective HIV coreceptors (Kaul et al., 2007). In order to extend the analysis of the HIV-1 coreceptor signaling pathways responsible for mediating neuronal death we investigated the kinetics and involvement of different MAPK pathways in induction of neuronal death

by gp120. We used in vitro non-radioactive immunocomplex kinase assays for the stress-activated kinases (SAPK) p38 MAPK and, for comparison, SAPK/c-Jun N-terminal kinase (JNK) with p-ATF2 and p-cJun as substrate readouts, respectively.

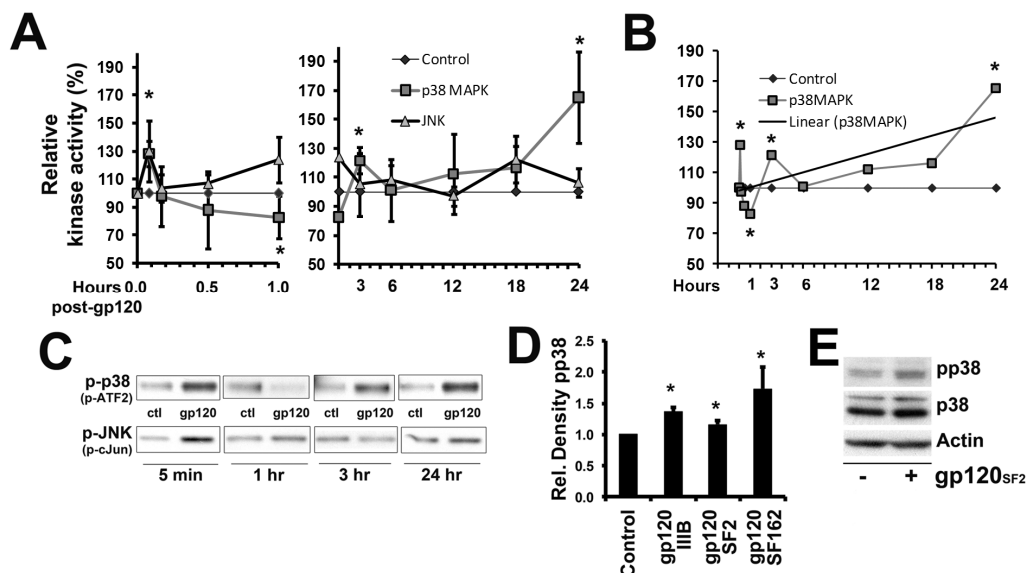


Figure 3.1 Kinetics of p38 MAPK and JNK activation in mixed neuronal-glia cerebrocortical cell cultures upon exposure to neurotoxic HIV envelope protein gp120. HIV-1 gp120_{SF2} causes significant deviation of p38 MAPK activity from baseline control condition at 5 min, 1 h, 3 h, and 24 h with an overall increase (A, and B for trend line for p38 MAPK activity). In contrast, activity of JNK is only significantly elevated at 5 min (A and C). Cerebrocortical cultures were incubated with dual-tropic gp120_{SF2} (200 pM) for the indicated time periods prior to immunoprecipitation and kinase assay analysis. The kinase activity of p38 MAPK and JNK using ATF-2 and c-Jun as substrates, respectively, were each detected by immunoblotting following the supplier's protocol as mentioned in the Materials and Methods section. The kinase activity in untreated controls was measured for each time point and defined as the 100% baseline value (A). Error bars represent the S.E.M. of four to nine independent experiments (A and B). Representative western blots of p-ATF2 (p-p38) and p-cJun (p-JNK) kinase assay results were shown after exposure to gp120 at 5 min, 1 h, 3 h and 24 h (C). In addition, recombinant gp120 of CXCR4-preferring (IIIIB), dual-tropic (SF2) and CCR5-preferring (SF162) HIV-1 all activate p38 MAPK in cerebrocortical cells at 24 h (D). Examples of active pp38 MAPK, p38 MAPK and actin western blots used for densitometry analysis 24 h after gp120_{SF2} treatment are shown in (E). Equal amounts of cellular protein (10 µg per lane) were analyzed by SDS PAGE and Western blotting (D and E). The two bands detected as total p38 MAPK represent the α - (lower) and β - (upper) isoform of the kinase while the p-p38 MAPK is mostly of the α -isoform (E). Error bars represent the S.E.M. of three independent experiments. * = $p < 0.05$ compared with control (A, B and D).

Cerebrocortical cell cultures were incubated for various time periods with HIV gp120 or vehicle as control as described for neurotoxicity assays (Kaul et al., 1999;

Kaul et al., 2007). Subsequently, the cells were transferred onto ice, quickly washed once with ice-cold PBS and lysed. The active kinases were precipitated from the cell lysate and exposed to assay substrates in the presence of ATP. Phosphorylated substrates were then visualized by Western blotting and quantified by densitometry. Baseline and HIV-1 gp120-induced activities of the protein kinases were assessed for each time point. In response to HIV-1 gp120SF2 exposure activation of p38 MAPK occurred early, in a short-lived peak at 5 min, followed by a temporary drop below baseline at 1 h. After the lowered kinase activity at 1 h, p38 kinase activity showed a sustained increase that was most pronounced above baseline at 3 h and 24 h (Figure 3.1A). Thus, despite some variability between different batches of primary cerebrocortical cell cultures, which is to be expected, we observed a consistent pattern at early and late time-points of initial, temporary up- and down-regulation with an overall increase in p38 MAPK activity after exposure to gp120 (Figure 3.1A). Altogether, the data indicated an overall trend towards increased kinase activity for p38 MAPK after gp120 exposure over a 24 h period (Figure 3.1B, trend line).

For comparison, the activity of JNK, which was monitored in the same way, showed a less pronounced deviation from the baseline over 24 h, except for the 5 min time point. Figure 3.1C shows representative Western blot data for p38 MAPK (p-ATF2) and JNK (p-cJun) kinase assays at the significant time points of 5 min, 1 h, 3 h, and 24 h. In addition, direct immunoblotting for phospho-p38 MAPK was also used to detect the active kinase within rat cerebrocortical cultures (Figure 3.1D and 3.1E). Increased phosphorylation of p38 MAPK occurred in response to gp120 from CXCR4-, CCR5- and CCR5/CXCR4-preferring (dual-tropic) HIV-1 strains (IIIB,

SF162 and SF2, respectively; Figure 3.1D). Representative Western blot data showing increased phosphorylated p38 MAPK after 200 pM gp120SF2 treatment for 24 h is shown in Figure 3.1E. Based on the finding that the activity of p38 MAPK deviated from baseline upon exposure to HIV gp120 most consistently at 5 min and 1 h and at 3 h and 24 h, we focused in subsequent experiments primarily on p38 MAPK activity at those time periods.

3.3.2. Active p38 MAPK is required for HIV-1 gp120-induced neuronal death in mixed neuronal-glial cerebrocortical cell cultures in a dose-dependent fashion.

After observing that activation of p38 MAPK to less than twice the baseline activity sufficed to mediate neuronal death, we assessed the dose-dependence of the neuroprotective effect that pharmacological inhibition of p38 MAPK showed in earlier studies. Therefore, we exposed primary rat cerebrocortical cultures to increasing doses of the p38 MAPK-specific pharmacological inhibitor, SB203580, prior to HIV-1 gp120 exposure. SB203580 acts as a competitive ATP-binding inhibitor which interrupts the kinase activity of p38 MAPK (Davies et al., 2000; Lee et al., 1999). We treated the cultures with the compound at 0.1, 1.0 and 10 μ M concentrations 15 min prior to treatment with 200 pM dual-tropic viral envelope protein gp120 from HIV-1 SF2 strain for 24 h. Controls received the vehicles for SB203580 (DMSO) and gp120 (PBS/BSA, 0.001% final concentration) (Kaul et al., 1999; Kaul et al., 2007). Subsequently, we assessed neuronal survival as readout for neurotoxicity by fluorescence microscopy using a combination of immunolabeling of neurons for

MAP-2 in combination with nuclear DNA staining by H33342 as described in the Materials and Methods section. As expected, HIV gp120 reduced neuronal survival by about $23 \pm 3.3\%$ in the absence of any p38 MAPK inhibitor whereas all the tested SB203580 concentrations lacked neurotoxicity (Figure 3.2).

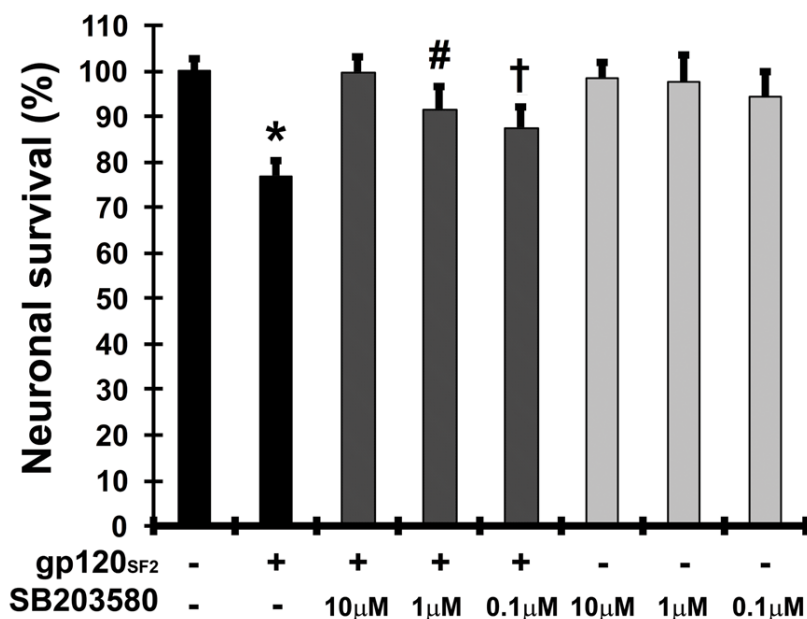


Figure 3.2 Inhibition of p38 MAPK prevents gp120-induced neuronal apoptosis in a dose-dependent fashion. Rat cerebrocortical cultures were incubated for 24 h with or without gp120_{SF2} (200 pM) in the presence or absence of 0.1, 1 or 10 μM of p38 MAPK inhibitor SB203580. Neuronal survival was assessed using fluorescence microscopy after fixation, permeabilization and immunolabeling of neurons for MAP-2 in combination with nuclear DNA staining by H33342. Error bars represent the S.E.M. of three to six independent experiments. * = $p < 0.001$ compared to control value; # = $p < 0.02$ compared to value for gp120; and † = $p < 0.01$ compared to value for control and gp120 (ANOVA with Fisher's PLSD post hoc test).

Pretreatment of cultures with 10 μM SB203580 completely abrogated reduction in neuronal survival after gp120 treatment ($p < 0.0001$ compared to gp120; Figure 3.2), confirming our previous studies (Kaul et al., 1999; Kaul et al., 2007). Using 1.0 μM SB203580 to inhibit p38 MAPK activity, significantly increased

neuronal survival after gp120 treatment to a slightly lesser extent than 10 μ M ($p < 0.02$, compared to gp120; Figure 3.2). Pretreatment of cultures with 0.1 μ M SB203580 was found to result in neuronal survival that was significantly lower than in the control ($p < 0.02$) but significantly higher than in gp120 without kinase inhibitor ($p < 0.05$; Figure 3.2). These results indicated only a partial protection against gp120 toxicity at concentrations lower than 1.0 μ M and thus a causal, dose-dependent contribution of active p38 MAPK to gp120-induced neuronal injury and death.

3.3.3. Neuroprotective β -chemokine CCL4 reduces HIV-1 gp120-induced p38 MAPK activation

Previously, we found that the presence of CCL4, the natural ligand for CCR5, abrogated the neurotoxicity of gp120 in cerebrocortical cells (Kaul et al., 2007; Choi et al., 2007). Using the same experimental approach as in the previously reported neurotoxicity studies and the above discussed kinase assay, we found that treatment with CCL4 during exposure to the viral envelope protein suppressed the increase of p38 MAPK activity at 3 h and 24 h but not at 5 min (Figure 3.3). This finding suggested that an increased activity of p38 MAPK at 3 and 24 h, but not 5 min, reflected a neurotoxic process. Whereas under protective conditions, such as the presence of the CCR5 ligand, p38 kinase activity remained close to background levels except for the early 5 min time point. Compared to the 1, 3 and 24 h time points, the activity of p38 MAPK at 7 h and 15 h was more variable and on average closer to baseline. That finding was in line with the observations for the same time period made

during the experiments shown in Figure 3.1A. Since CCR5 is present in neuronal and glial cells, the protective ligand CCL4 could possibly have prevented an increase of p38 MAPK activity by interaction with neurons and/or glia (Kaul et al., 2007).

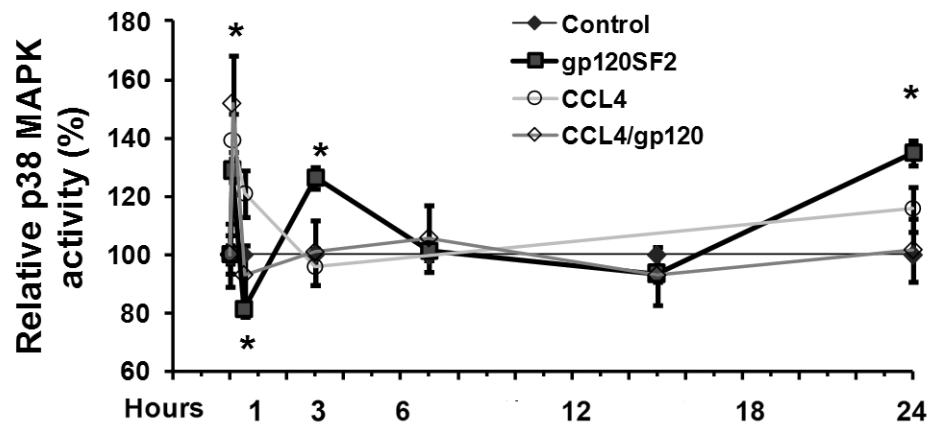


Figure 3.3 Presence of the neuroprotective chemokine CCL4 reduces the activation of p38 MAPK in the presence of neurotoxic gp120 in rat cerebrocortical cultures at 3 h and 24 h. Note that the activity of p38 MAPK at 7 h and 15 h was more variable and on average closer to baseline as it was expected for this time period from the experiments shown in Figure 3.1A. Neuroprotective CCL4 (20 nM) was added immediately prior to HIV-1 gp120 (200 pM) incubation (Kaul et al., 1999; Kaul et al., 2007). p38 MAPK activity was detected by immunoblotting and evaluated using densitometry of p-ATF-2 as described in Materials and Methods section. The kinase activity in BSA vehicle-treated controls was measured for each time point and defined as the 100% baseline value. As a separate control, activity of p38 MAPK for treatment with CCL4 alone was assessed at 5 min, 1 h, 3 h and 24 h only. Error bars represent the S.E.M. of four independent experiments. * = $p < 0.05$ compared with control.

3.3.4. HIV-1 gp120 activates p38 MAPK predominantly in neurons and microglia, but not in astrocytes

While all cells within the rat cerebrocortical cultures express p38 MAPK protein (Figure 3.4), the spatial distribution of p38 MAPK activity induced by exposure to HIV-1 gp120 had not been defined. In order to localize activated p38

MAPK, we performed immunostaining on cultures treated for 24 h with 200 pM HIV-1 gp120 or vehicle control. These cultures were co-stained for active p38 MAPK, the neuronal marker (MAP-2), microglia marker (CD11b), and/or DNA dye Hoechst H33342. Phosphorylated or activated p38 MAPK was primarily found within neurons and microglia at 24 h post-gp120 stimulation within rat cerebrocortical cell cultures (Figure 3.4A). As previously shown, these cultures consisted of about 70-75% astrocytes, 25-30 % neurons and less than 1% microglia (Kaul et al., 2007). Therefore, most of the active p38 MAPK within our rat cerebrocortical cultures appeared to reside in neurons. In fact, about 20% of the cerebrocortical cell cultures consisted of neurons positive for active/phosphorylated p38 MAPK (pp38) with or without gp120 treatment at 5 min ($21.3 \pm 1.7\%$ vs. $21.1 \pm 2.0\%$), 1 h ($21.1 \pm 1.6\%$ vs. $20.3 \pm 1.8\%$), 3 h ($22.9 \pm 2.0\%$ vs. $23.0 \pm 1.8\%$) and 24 h ($21.8 \pm 2.1\%$ vs. $17.2 \pm 1.7\%$), (Figure 3.4B). A reduction in the number of pp38-positive neurons at 24 h compared to control was observed (Figure 3.4B), correlating to a loss of neurons after 24 h post-gp120 as seen in Figure 3.2. Overall, immunofluorescent staining suggested that at any time between 71-85% of neurons were pp38-positive regardless of gp120 treatment whereas pp38-positive microglia were detected as early as 10 min into exposure to gp120 but not vehicle control (data not shown).

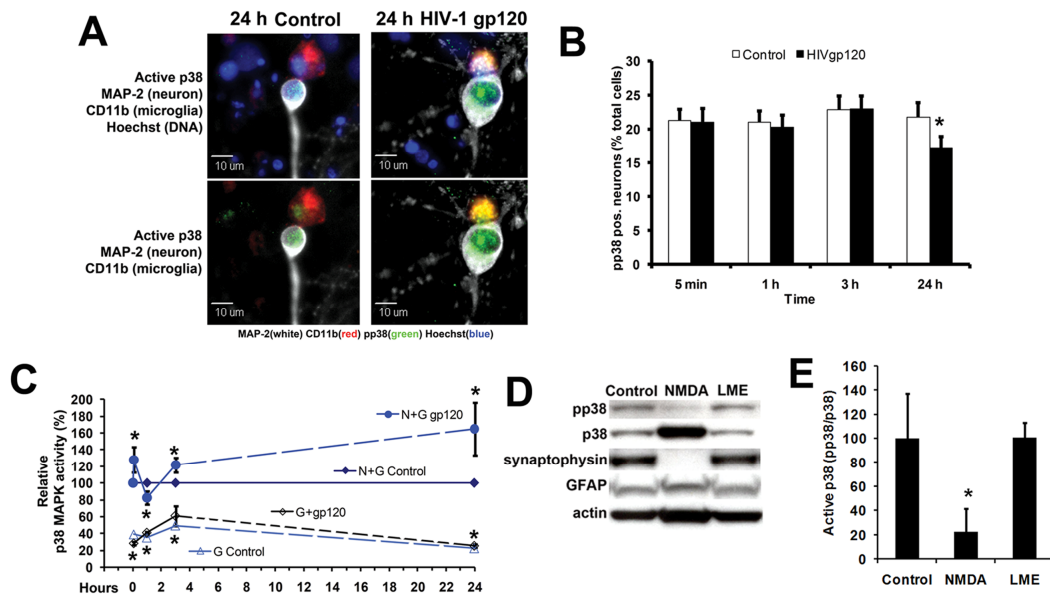


Figure 3.4 HIV-1 gp120 activates p38 MAPK in rat cerebrocortical neurons and microglia. Activated p38 MAPK primarily localizes to rat neurons and microglia after treatment with HIV-1 gp120_{SF162}; (A) immunofluorescence staining for p38 MAPK, neuronal MAP-2 and microglial CD11b after 24 h treatment. Rat cerebrocortical cultures were treated with 0.001% BSA (Control) or 200 pM HIV-1 gp120_{SF162} (HIV-1 gp120), fixed with 100% methanol, and then immunolabeled with p-p38 (green), neuronal marker MAP-2 (white), microglia marker CD11b (red) and DNA stain Hoechst H33342 (blue). Virtually the same results were obtained when cerebrocortical cells were treated with gp120_{SF2} (not shown). Neurons showing activated p38 MAPK (pp38) immunostaining were quantified after 5 min, 1 h, 3 h, and 24 h after treatment with gp120 via microscopy (B). The number of neurons positive for activated p38 MAPK were reduced at 24 h post-gp120 treatment. Cell lysates were analyzed for p38 MAPK activation after removal of neurons from culture with 300 μ M NMDA treatment for 20 min two days prior to incubation with 200 pM gp120_{SF2} for 24 h (G Control or G gp120) using p38 MAPK kinase assay (C). Without neurons, baseline p38 MAPK activity is significantly lower than that from complete cultures; and gp120 treatment does not deviate from control treatment without neurons (C). Cell lysates were also analyzed by immunoblotting after 20 min 300 μ M NMDA pre-treatment two days earlier to deplete cultures of neurons or following overnight pre-treatment with 7.5 mM LME to ablate microglia or without pretreatment (control) using anti-active p38 MAPK (pp38), anti-p38 MAPK, anti-synaptophysin, anti-GFAP and anti-actin antibodies (D). Densitometry of basal expression levels of active p38 MAPK/total p38 MAPK in culture after NMDA pre-treatment (Glia Only) or LME pre-treatment (No Microglia) or Control (Neurons + Glia) from Western blot data is shown in (E). Note that equal amounts of total protein were loaded for each sample and thus the Glia-Only sample contains relatively more glial proteins than the other samples. Error bars represent the S.E.M of three independent experiments (C and E). Scale bar in images, 10 μ m. For all significance analysis, * = $p < 0.05$ compared to control.

We also performed p38 MAPK kinase assays on rat cerebrocortical cultures depleted of neurons after 20 min pretreatment with 300 μ M N-methyl-D-aspartic acid

(NMDA) 2 days prior to exposure to HIV gp120. These experiments showed that neurons contributed $47.6 \pm 1.1\%$ of total protein found within the cerebrocortical cell lysates ($n = 30$; data not shown). Cultures consisting of neurons and glia (N + G) or neuron-depleted glia-only cultures (G) were assayed for p38 MAPK kinase activity after 5 min, 1 h, 3 h, and 24 h treatments with gp120 (Figure 3.4C). Glia-only cultures had a significantly reduced basal p38 MAPK activity (* $p < 0.05$ compared to N+G Control values) and no difference in p38 MAPK activity between control and gp120-treated cultures was witnessed after depletion of neurons (Figure 3.4C).

In fact, immunoblotting experiments indicated that removal of neurons reduced the basal levels of activated p38 MAPK by $77.8 \pm 4.5\%$ compared to control cerebrocortical culture (Neurons + Glia) (Figure 3.4D and 3.4E). Depletion of microglia (LME), on the other hand, did not detectably change the amount of active or total p38 MAPK at basal levels (Figure 3.4D and 3.4E).

3.3.5. Microglial depletion reduces HIV-1 gp120-induced p38 MAPK activation in cerebrocortical neurons

In previous studies, depletion of microglia from cerebrocortical cultures with L-leucine methyl ester (LME) was found to abrogate the neurotoxicity of gp120 (Kaul et al., 1999; Kaul et al., 2007). Using the same experimental approach as in the previously reported neurotoxicity studies, we found that prior depletion of microglia before exposure to the viral envelope protein also suppressed the increase of p38 MAPK activity at 3 h and 24 h but not at 5 min (Figure 3.5). Hence, the increased

activity of p38 MAPK in response to HIV-1 gp120 from 3 h onward is dependent on the presence of microglia. Our observation also suggested that the early peak of p38 MAPK activity at 5 min occurred independently of microglia, and thus through a direct interaction of gp120 with astrocytes and/or neurons. Moreover, and similar to the findings in the experiments with CCL4, this peak at 5 min was apparently not associated with neurotoxicity.

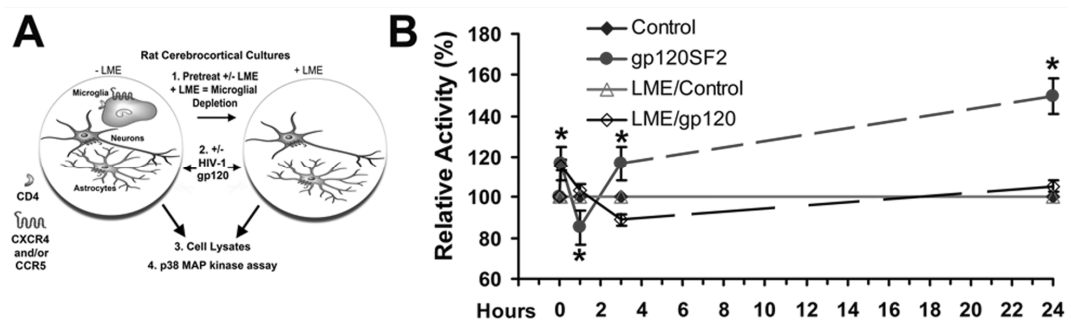


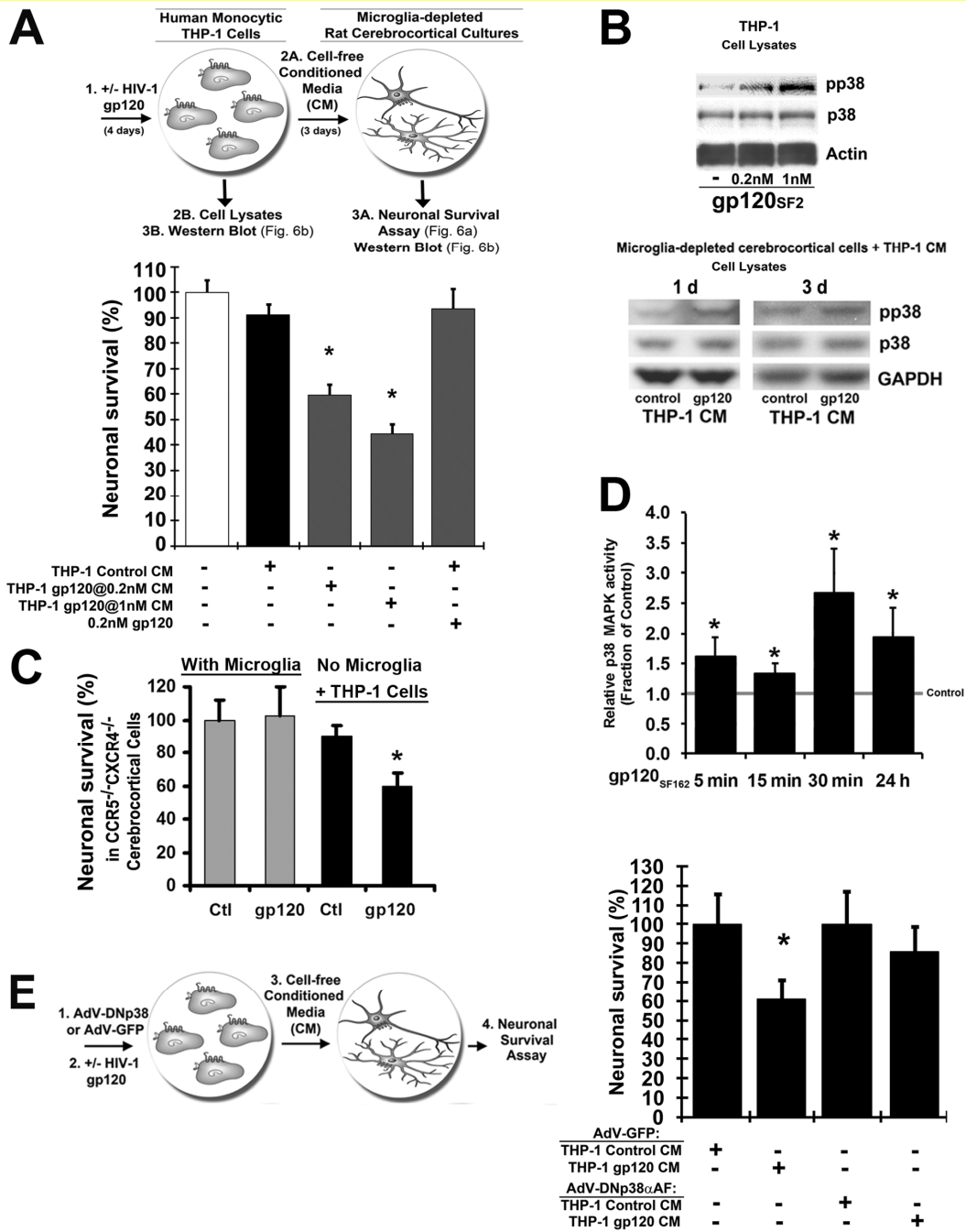
Figure 3.5 Depletion of microglia from mixed rat cerebrocortical cultures reduces the activation of p38 MAPK in the presence of neurotoxic gp120 at 3 h and 24 h. Depletion of microglia was accomplished by overnight pre-treatment with 7.5 mM L-leucine methyl-ester (LME) and was followed by treatment with gp120_{SF2} for 5 min, 1 h, 3 h, and 24 h and collection of cell lysates for p38 MAPK kinase assay as shown in schematic diagram (A). Kinase assay results were detected by immunoblotting and evaluated using densitometry of p-ATF-2 (B) as described in the legend to Figure 3.1. The kinase activity in BSA vehicle-treated controls (with or without LME pre-treatment) was measured for each time point and defined as the 100% baseline value. Error bars represent the S.E.M. of three to nine independent experiments. * = $p < 0.05$ compared with control.

3.3.6. Mononuclear cells require p38 MAPK activation for gp120-induced neurotoxin production

In an alternative approach to assess the role of monocytic lineage cells and of HIV-1 coreceptors in the neurotoxicity of gp120, we used human mononuclear THP-1 cells and primary MDM as models for macrophages and microglia. Like primary

human MDM, monocytic THP-1 cells express besides CD4, CXCR4 and CCR5, are permissive to HIV infection, and produce neurotoxins in response to HIV-1 virus and gp120 (Giulian et al., 1990; Giulian et al., 1993; He et al., 1997). In the present study both THP-1 cells and MDM were incubated with 200 pM or 1 nM HIV-1 gp120SF2 for 4 d and then the cell-free supernatant/conditioned media (CM) was transferred into microglia-depleted rat cerebrocortical cultures (at 10% cerebrocortical culture media volume) for 3 d. HIV-1 gp120 induced neurotoxin production in both THP-1 cells (Figure 3.6) and MDM (Figure 3.7). THP-1+gp120 CM reduced neuronal survival in an envelope-dose dependent fashion by approximately 40-60% of rat cerebrocortical cultures exposed to control CM or not treated with CM (Figure 3.6A). Control CM did not significantly affect neuronal survival. In contrast, control supernatants from BSA/vehicle-exposed THP-1 cells or control THP-1 CM spiked with HIV gp120 did not significantly increase neuronal death in microglia-depleted cerebrocortical cell cultures.

Figure 3.6 Inhibition of p38 MAPK in monocytic THP-1 cells abrogates the HIV-1 gp120-induced release of neurotoxic factors. Cell-free conditioned media (CM) from THP-1 cells was collected after treatment for 4 d with 200 pM or 1 nM gp120_{SF2} or 0.001 % BSA. Microglia-depleted rat cerebrocortical cultures were then treated with control (THP-1 Control) CM or neurotoxic (THP-1 gp120 @ 0.2, or 1 nM) CM for 3 d and analyzed for neuronal survival as shown in (A). Neuronal survival was assessed using fluorescence microscopy of neuronal MAP-2 and nuclear DNA as described in the legend to Figure 3.2. After incubation with gp120_{SF2} or BSA vehicle control for 4 d to generate conditioned media, THP-1 cells were lysed and 25 µg protein of each sample was analyzed by immunoblotting using antibodies against the active and total form of p38 MAPK, respectively, and an antibody against loading control protein actin as indicated (B, upper panel). Following depletion of microglia and exposure to THP-1CM for 1 and 3 d rat cerebrocortical cells were lysed and analyzed by Western blotting in the same way as the THP-1 cells except that GAPDH was used as loading control (B, lower panel). Note the increase of activated, phospho-p38 MAPK in both THP-1 cells after gp120 stimulation and microglia-deficient cerebrocortical cells after exposure to cell-free CM from gp120-exposed THP-1 cells. Introduction of human monocytic THP-1 cells into CCR5^{-/-}/CXCR4^{-/-} mouse cerebrocortical cell cultures confers susceptibility to gp120 neurotoxicity (C). The viral envelope protein fails to induce neurotoxicity in cerebrocortical cells comprising neurons, astrocytes and microglia that lack the chemokine receptors (Kaul et al., 2007). THP-1 cells were added to the mixed neuronal-glial cell cultures following prior treatment with LME and washes to remove endogenous microglia. Cultures with and without THP-1 cells were incubated for 24 hrs with 200 pM of gp120 from HIV-1SF162 or BSA vehicle as control. Neuronal survival was assessed by fluorescence microscopic quantification of MAP-2+ neurons and nuclear DNA as described above for panel (A). Kinetic of p38 MAPK activation in THP-1 cells exposed to gp120 (D). The monocytic cells were incubated with gp120 (200 pM) for the indicated time periods prior to immunoprecipitation and kinase assay analysis as described in the legend to Fig. 1. (E) THP-1 cells were transduced with a dominant negative inactive p38 MAPK mutant (AdV DNp38 α AF) or a GFP control construct (AdV GFP), at a MOI of 10, 2 d prior to inoculation for 4 d with or without 200 pM gp120SF2. Rat cerebrocortical cultures were then exposed for 3 d to a 10% concentration of THP-1 CM as shown in schematic diagram and assessed for neuronal survival (E). Error bars represent the S.E.M. of three to six independent experiments, * = $p < 0.001$ (A and E), < 0.04 (C), < 0.05 (D) compared to values for control (ANOVA with Fisher's post hoc test).



Interestingly, THP-1 cells exposed to gp120_{SF2} also showed increased levels of phosphorylated p38 MAPK in a dose-dependent manner after 4 d, suggesting that activation of the kinase in mononuclear cells correlated with neurotoxin production (Figure 3.6B, upper panel). Furthermore, we found that cell-free neurotoxic THP-1 media generated by incubation of the cells with 200 pM gp120 caused in comparison with control CM an increase of active p38 MAPK in microglia-depleted cerebrocortical neuronal cells after 1 and 3 days exposure (Figure 3.6B, lower panel).

Since the media conditioned by THP-1 cells and MDM in the presence of gp120 must be expected to carry over viral envelope protein onto microglia-free cerebrocortical cells, it could be possible that gp120 acted directly on neuron and astrocytes contributing to neurotoxicity in synergy with a factor secreted by gp120-stimulated but not control-treated mononuclear cells. In order to assess a potential role for HIV coreceptors in such a hypothetical scenario, we introduced 15,000 monocytic THP-1 cells into 300,000 murine cerebrocortical cells deficient in both HIV coreceptors ($CCR5^{-}/CXCR4^{-}$) that were previously pretreated with L-leucine methyl-ester (LME) to deplete endogenous microglia (5% final concentration of THP-1 cells as replacement for microglia). For introduction into murine microglia-free cerebrocortical cultures, THP-1 cells were first suspended in conditioned media of the same mouse cell culture at 1.5×10^6 cells/ml. This cell suspension was then distributed at 10 μ l/well into the cerebrocortical cells that were previously treated with LME and washed to remove potentially remaining microglia cell debris and excess LME. THP-1 cells, however, did not adhere to cerebrocortical cultures even in the presence of HIV gp120 (data not shown). Of note, cerebrocortical cells comprising

neurons, astrocytes and microglia but lacking both major HIV co-receptors are themselves resistant to induction of gp120 neurotoxicity (Kaul et al., 2007). The chemokine receptor-deficient cerebrocortical cultures with and without THP-1 cells were then exposed for 24 h to gp120 or BSA as a control. Neuronal survival was determined after fixation, permeabilization and immunolabeling of neurons with MAP-2 in combination with nuclear staining using H33342 by fluorescence microscopy (Figure 3.6C).

Exposure of cerebrocortical cultures to gp120 in the absence of THP-1 cells, or to THP-1 cells alone (after pretreatment with LME) did not significantly change neuronal survival. However, addition of gp120 in the presence of THP-1 cells caused a significant demise of neurons (Figure 3.6C). This finding suggested that the presence of mononuclear cells expressing CXCR4 and CCR5 (besides CD4) sufficed to restore susceptibility to gp120 toxicity in combined CCR5-CXCR4-deficient cerebrocortical cells and further supported a critical role of monocyte-lineage cells and their HIV coreceptors in gp120-induced neurotoxicity. On the other hand, the findings also showed that an interaction with neuronal or astrocytic HIV coreceptors of any potentially carried-over gp120 in the CM of mononuclear cells is dispensable for neurotoxicity to occur. Finally, this experimental approach revealed that a 24 h incubation of THP-1 cells with HIV gp120 sufficed to produce significant neurotoxicity.

Therefore, we next analyzed whether gp120 triggered activation of p38 MAPK in THP-1 cells during a 24 h exposure. The monocytic cells were exposed for 5, 10, 15, and 30 min, and 24 h to gp120 or BSA vehicle as control and p38 MAPK activity

was subsequently assessed in cell lysates using an immunocomplex kinase assay as described above for rat cerebrocortical cells. The kinase assay showed that exposure of monocytic cells to gp120 resulted in a significant increase of active p38 MAPK at all four time points (Figure 3.6D).

Similar to THP-1 cells, MDM+gp120 CM reduced neuronal survival to between 70 and 80% of rat cerebrocortical cultures treated with control MDM CM (Figure 3.7A). Of note, MDM+gp120 CM retrieved after 4 days was not significantly more toxic than CM of the same sample collected earlier, after only 24 h incubation. Control MDM CM collected at 24 h and 4 d, or spiked with gp120 before addition to microglia-depleted cerebrocortical cells, and CM from MDM incubated with CCL4 or CCL5 all lacked neurotoxicity thus confirming the specificity of the toxic effect triggered by HIV gp120.

Comparable to THP-1 cells, although less pronounced, MDM exposed to 200 pM gp120 of HIV-1 SF2 and SF162 showed increased levels of phosphorylated p38 MAPK after 4 d, again suggesting that activity of the kinase in mononuclear cells correlated with neurotoxin production (Figure 3.7B).

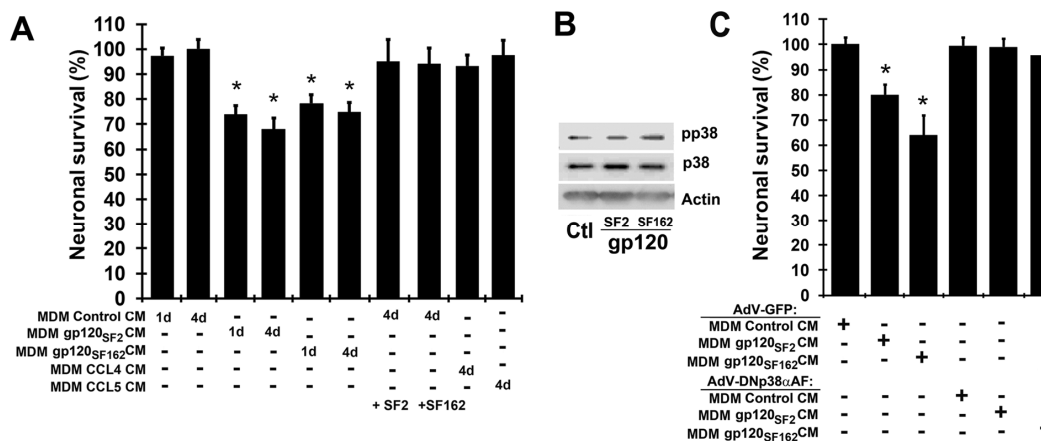


Figure 3.7 HIV-1 gp120 stimulates secretion of neurotoxins from primary human macrophages. Cell-free conditioned media (CM) from human monocyte-derived macrophages (MDM) was collected after treatment for 1 d ('1d') and 4 d ('4d') with 200 pM HIV-1 gp120_{SF2} or gp120_{SF162} or with 0.001% BSA. Microglia-depleted rat cerebrocortical cultures were then treated with a 10% concentration of control (MDM Control) CM or neurotoxic (MDM gp120_{SF2} or gp120_{SF162}) CM for 3 d and analyzed for neuronal survival (A). Neuronal survival was assessed using fluorescence microscopy of neuronal MAP-2 and nuclear DNA as described in the legend to Figure 3.2. (B) Equal numbers of MDM in each sample were lysed in SDS-containing gel-loading buffer and protein was analyzed by immunoblotting using antibodies against the active and total form of p38 MAPK, respectively, and an antibody against loading control protein actin as indicated. (C) Inhibition of p38 MAPK activity in primary human MDM abrogates the HIV-1 gp120-induced release of neurotoxic factors. MDM were transduced with dominant negative inactive p38 MAPK mutant (AdV DNp38αAF) or a GFP control construct (AdV GFP), at a MOI of 10, 2 d prior to inoculation for 4 d with or without 200 pM gp120_{SF2} or gp120_{SF162}. Rat cerebrocortical cultures depleted of microglia were then exposed for 3 d to a 10% concentration of MDM CM and assessed for neuronal survival. Error bars represent the S.E.M. of three independent experiments, * = $p < 0.001$ compared to values for control (ANOVA with Fisher's post hoc test).

Next, we assessed the importance of p38 MAPK signaling in monocyte lineage cells after gp120 treatment. To analyze whether or not p38 MAPK in mononuclear cells contributes to gp120-induced neurotoxicity, we successfully infected THP-1 cells and MDM each at a multiplicity of infection (MOI) of 10 with adenoviruses expressing GFP (AdV-GFP) or dominant-negative p38αAF MAPK (AdV-DNp38α) (Zhao et al., 1999) 2 d prior to HIV-1 gp120_{SF2} exposure. The dominant-interfering p38αAF MAPK, but not AdV-GFP, strongly reduced the release of neurotoxins by both THP-1 cells and MDM due to HIV-1 gp120_{SF2} treatment increasing neuronal

survival (Figure 3.6E and Figure 3.7C, respectively). Reduction of neurotoxin release was due to the presence of the DNp38 α kinase mutant and not the result of decreased mononuclear cell viability, as the viability of both the control (AdV-GFP)- and AdV-DNp38 α - infected cells, in THP-1 and MDM, respectively, were equivalent (data not shown).

Altogether, the experiments showed equally in THP-1 cells and MDM that HIV gp120 triggered neurotoxin production which in turn could be prevented by inhibiting active p38 MAPK and thus supported the suitability of THP-1 cells as a model for macrophage-mediate neurotoxicity of the viral envelope protein. Hence, in order to further investigate the role of endogenous p38 MAPK in gp120-induced neurotoxicity, we utilized small interfering RNA (siRNA) technology to knockdown expression of p38 α MAPK in THP-1 cells prior to incubation with HIV-1 gp120_{SF162}. We were able to efficiently reduce expression of endogenous p38 MAPK protein by 50-75% compared to non-targeting (NT) siRNA (* $p < 0.001$) using three different and separate p38 α MAPK siRNA duplexes, sip38 α -1, α -2, and α -3, with or without gp120_{SF162} treatment (Figure 3.8A and 3.8B). Conditioned media collected from THP-1 cells nucleofected with p38 α MAPK siRNA for 48 h (efficient knockdown between 48-72 h, data not shown) and treated with gp120_{SF162} for an additional 24 h (p38 α siRNA:THP-1 gp120_{SF162} CM) was significantly less neurotoxic than CM from THP-1 cells nucleofected with NT siRNA and treated with gp120_{SF162} (NT siRNA:THP-1 gp120_{SF162} CM) (Figure 3.8C). The incubation with gp120 was limited to 24 h in order to stay within the time frame of maximal reduction of p38 MAPK protein expression in the presence of the specific siRNAs. Importantly, these

experiments also showed that incubation with gp120 for 24 h was sufficient to obtain significantly neurotoxic conditioned media. Direct neuronal interaction with gp120 did not appear to cause significant amounts of neuronal death in the absence of microglia, as observed after addition of gp120 to microglia-depleted cultures. In contrast, as a control 20 min exposure to 300 μ M NMDA prior to 24 hr incubation in control CM was still able to induce excitotoxic neuronal death (Figure 3.8C).

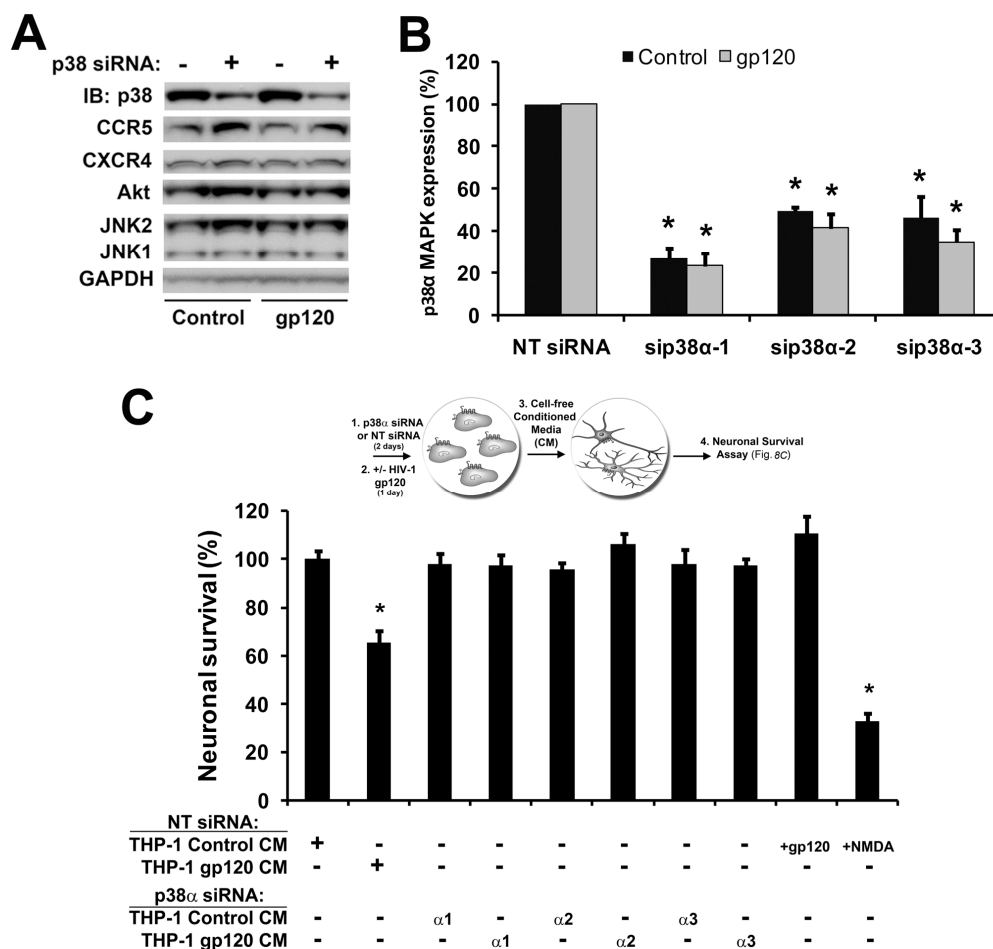


Figure 3.8 Reduction of endogenous p38 MAPK expression with siRNA in monocytic THP-1 cells prevents induction of neurotoxicity upon exposure to gp120. Three separate small interfering RNAs (siRNA) sequences of p38 α MAPK (MAPK14) (sip38 α -1, α -2, α -3) were utilized to knockdown expression of p38 MAPK by 50-75% compared to non-targeting (NT) siRNA in THP-1 cells after 48 h via Amaxa nucleofection techniques, followed by subsequent 200 pM gp120_{SF162} 24 h treatment (A and B). Representative western blots of THP-1 cell lysates treated 24 h with or without 200 pM gp120_{SF162} beginning 48 h after siRNA nucleofection (-, NT or non-targeting; or +, sip38 α -1); p38 MAPK, CCR5, CXCR4, Akt, JNK1/2, and GAPDH protein levels are shown (A). Densitometric analysis of cell lysates from three independent siRNA experiments showed a significant reduction in protein amount only for p38 MAPK (B) but no significant change for CCR5 or any other tested protein. Cell-free conditioned media (CM) from THP-1 cells was collected 2 d after nucleofection of siRNA (NT or sip38 α -1, α -2, α -3) followed by treatment for 24 h with 200 pM gp120_{SF162} or 0.001% BSA (vehicle control). Microglia-depleted rat cerebrocortical cultures then received the THP-1 CM for 3 d and subsequently were analyzed for neuronal survival (C). Neuronal survival was assessed via microscopic quantification of neuronal MAP-2 and nuclear DNA and compared using NTsiRNA: THP-1 Control CM-treated cultures as overall control condition (C). Direct treatment of microglia-depleted cerebrocortical cultures with gp120 did not produce significant neuronal death (NT siRNA: THP-1 Control CM + gp120), however direct NMDA treatment (NT siRNA: THP-1 Control CM + NMDA; 300 μ M, 20 min) showed unimpaired neuronal response to excitotoxic insult (C). Error bars represent the S.E.M. of three independent experiments, * = $p < 0.001$ compared to values for NT siRNA controls (ANOVA with Fisher's post hoc test).

3.3.7. Inhibition of p38 MAPK activation in cerebrocortical neurons suffices to prevent neuronal death stimulated by gp120-induced neurotoxic media from mononuclear THP-1 cells

We next tested whether inhibition of p38 MAPK activity in neurons would suffice to prevent neuronal death upon neurotoxic stimuli from THP-1 cells treated with HIV-1 gp120. Therefore, prior to treatment of microglia-depleted rat cerebrocortical cultures with gp120-induced neurotoxic THP-1 conditioned media, we pretreated the cerebrocortical cultures with 10 μ M SB203580 or DMSO as vehicle control for 15 min (Kaul et al., 1999; Kaul et al., 2007). As before, THP-1 cells were separately incubated with HIV-1 gp120_{SF2} or gp120_{SF162} for 4 d in order to obtain neurotoxic and non-toxic control supernatants. The THP-1 conditioned media (CM) was then transferred onto SB203580-pretreated microglia-depleted rat cerebrocortical cultures (at 10% cerebrocortical culture media volume) for 3 d. Interestingly, inhibition of p38 MAPK by 10 μ M SB203580 in microglia-depleted rat cerebrocortical cultures prior to the addition of gp120-induced neurotoxic THP-1 CM prevented neuronal apoptotic death (Figure 3.9) indicating that p38 MAPK is a crucial mediator not only in toxin-producing macrophages/microglia but also in toxin-sensitive neurons. Again, spiking non-toxic THP-1 CM with additional 200 pM gp120_{SF2} or gp120_{SF162} before application to microglia-depleted rat cerebrocortical cultures failed to produce neurotoxicity; confirming the requirement of microglia for gp120-induced neuronal death (Figure 3.9A, THP-1CM control + SF2 or SF162).

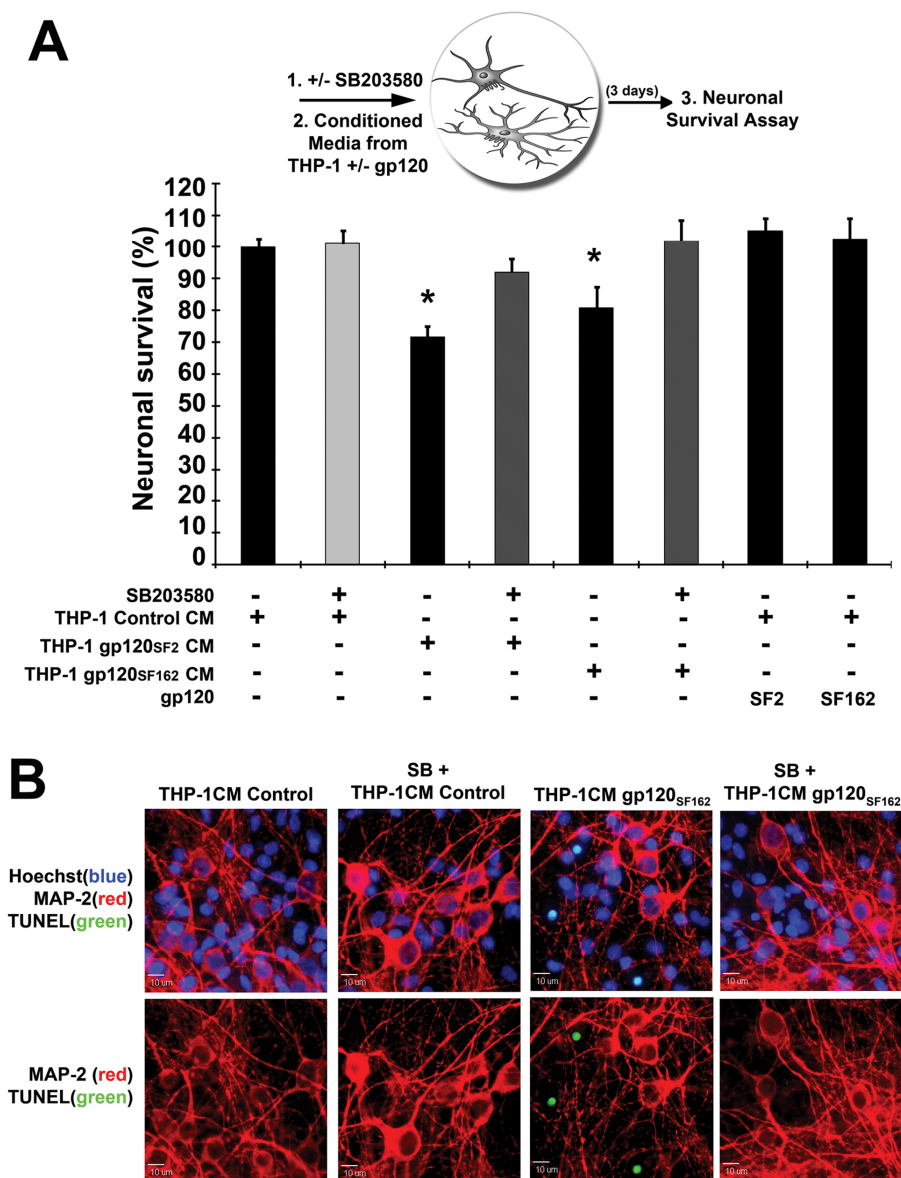


Figure 3.9 Inhibition of p38 MAPK in microglia-depleted rat cerebrocortical cultures rescues neurons from gp120-activated THP-1 neurotoxicity. Cell-free conditioned media (CM) from THP-1 was collected after treatment for 4 d with gp120_{SF2}, gp120_{SF162} or 0.001% BSA. Microglia-depleted rat cerebrocortical cultures were then pre-treated with 10 μ M SB203580 for 15 min prior to treatment with control or neurotoxic THP-1 CM and either analyzed for p38 MAPK activation via western blot after 24 h or for neuronal survival after 3 d as shown in schematic diagram (A). Neuronal survival was assessed using quantification of apoptotic, TUNEL+ nuclei (green), neuronal MAP-2 immunostaining (red), and nuclear DNA (blue); representative examples of images used for quantification are shown (B). Direct treatment of microglia-depleted cerebrocortical cultures with gp120 did not produce significant neuronal death (THP-1Control CM + SF2 or SF162) (A). Error bars represent the S.E.M. of three independent experiments, * = $p < 0.05$ (ANOVA with Fisher's post hoc test).

3.4. DISCUSSION

The interaction of HIV gp120 with CD4 and the viral coreceptors, CCR5 and/or CXCR4, has been shown to be vital to productive infection and to stimulation of intracellular signaling cascades presumably responsible for most pathological effects of viral-host interactions (Cheung et al., 2008; Choi et al., 2007; Del Corno et al., 2001; Fantuzzi et al., 2008; Hesselgesser et al., 1998; Kaul et al., 1999; Kaul et al., 2007; Kitai et al., 2000; Meucci et al., 1998; O'Donnell et al., 2006; Ohagen et al., 1999; Porcheray et al., 2006; Singh et al., 2005; Zheng et al., 1999). Previously, we and others showed that the stress-related p38 MAPK can apparently mediate gp120-induced neuronal death (Kaul et al., 1999; Kaul et al., 2007; Singh et al., 2005). Furthermore, activation of p38 MAPK has been observed following gp120 treatment in macrophages and thus implicated in HIV pathogenesis and the development of AIDS (Del Corno et al., 2001; Lee et al., 2003). However, the present study supplies evidence that p38 MAPK and its activity are essential to not only the reduction of neuronal survival by HIV-1 gp120, but also the neurotoxic phenotype of gp120-exposed microglia and macrophages. In addition, both consequences of exposure to HIV-1 gp120, the overall increased activation of p38 MAPK in neurons and neuronal death, are dependent on the presence of microglia. Therefore, this is the first study to show that p38 MAPK in two different cell types may be culpable and necessary for gp120-induced neurotoxicity in a mixed glial-neuronal environment.

Activation of p38 MAPK above baseline by HIV envelope protein gp120 has previously been reported for striatal neurons for a time frame of up to 4 h of exposure (Singh et al., 2005). However, our results presented here show that p38 MAPK activity fluctuates at earlier time points after a short-lived initial rise, and after a decrease at 1 h displays an overall increasing trend over a 24 h time course. This difference may be due to the fact that Singh et al. used striatal neuron-rich cultures as their experimental model and treated with more than twice the amount of gp120 (500 pM) than applied in our study (200 pM) (Choi et al., 2007; Kaul et al., 1999; Kaul et al., 2007). On the other hand, the early increase of p38 MAPK activation at 5 min gp120 exposure was represented in both studies. This early peak in p38 MAPK activity does not correlate with neuronal death in our study as it was not abolished by pre-treatment with CCL4 or by microglial depletion from mixed cultures, which has been shown in our studies to inhibit gp120-induced reduction in neuronal survival (Kaul et al., 1999; Kaul et al., 2007).

The initial peak of p38 MAPK activity at 5 min due to CCL4 alone or gp120 alone or CCL4+gp120 is most likely due to neuronal activation since it is not abolished after microglial depletion but absent in neuron-deficient cultures exposed to gp120. The question of why the temporary rise of p38 MAPK activity at 5 min is apparently not associated with neurotoxicity and the underlying question of how the rise in kinase activity at 5 min is different from the rise between 1 and 3 h and up to 24 h remains unknown at this time and is subject of ongoing studies. One possible explanation for the gradual up and down of p38 MAPK activity in surviving neurons may be a yet to be defined mechanism leading to a disturbance of the regulatory

balance between phosphorylation and de-phosphorylation by phosphatases. However, CCL4 has previously been shown to immediately activate p38 MAPK in C6 glioblastoma cell lines (Misse et al., 2001) and this was also the case in our neuronal cultures (Figure 3.3). We were also able to show that CCL4-stimulated p38 MAPK activity diminished to basal levels within 1 h exposure and stayed similar to control up to 24 h. Thus, our study is the first to show CCL4-induced p38 MAPK activity in neuronal cultures over a 24 h time period and how it is different from gp120-induced p38 MAPK activity. The question of why CCL4 was unable to block gp120-induced p38 MAPK at 5 min when incubated together also remains to be investigated, although we have previously shown that CCL4 can prevent neuronal death caused by the viral envelope (Kaul et al., 2007). That finding could be explained by direct competition at the receptor level and, in the case of CXCR4-prefering gp120, via heterologous desensitization, which we demonstrated in the same study. Both mechanisms may occur at the level of macrophage chemokine receptors, which is further supported by our present study.

Other related questions for future investigations are first why CCL4, in contrast to gp120, fails to produce a lasting increase in active p38 MAPK, and second, how a CCR5-binding viral envelope, but not the β -chemokine, can cause neurotoxicity. While our present study cannot provide the answers to those two questions, CCL4 and gp120 represent different ligands for the same receptor, and as such may elicit different or even opposing effects. Importantly, gp120 binds with greater affinity to chemokine receptors if CD4 is also present (as in macrophages/microglia and lymphocytes) and previous studies by other groups have

shown that even different natural ligands for the same receptor, such as CCR5 and its ligands CCL3, -4, -5, -8 and -14, can have different activities and trigger diverse signaling within the same cell population (Mueller et al., 2002; Oppermann et al., 2004).

Although p38 MAPK activation is known to be important for gp120-induced neuronal death (Kaul et al., 1999; Kaul et al., 2007; Singh et al, 2005), the distribution of phosphorylated p38 MAPK had not been investigated. Our report shows that phosphorylated p38 MAPK is localized in both neurons and microglia in mixed cerebrocortical cell cultures. Importantly, based on detection by immunofluorescence, active p38 MAPK in microglia occurs at early time points upon treatment with gp120 and may be sustained over 24 h, while neuronal p38 MAPK activation appears to occur downstream of microglial kinase activation after longer exposure to gp120 or possible neurotoxins from activated microglia. The number of neurons counted positive for phosphorylated p38 MAPK staining does not appear to be different from control at 5 min, 1 h and 3 h, but is significantly reduced at 24 h, in line with reduction in neuronal survival at 24 h. However, besides counting of cells positive for phosphorylated p38 MAPK a quantitative readout for p38 MAPK activity between control and gp120 treatments is provided by our kinase assay results. Baseline activity of p38 MAPK appeared to mostly reside within neurons as shown by the low remaining activity in glial cells after deletion of the neuronal population, which made up about 30% of the total cell population in the rat cerebrocortical cultures. Furthermore, our results suggest that the majority of the gp120-induced p38 MAPK activity originates in the neuronal cell population. In addition, the combination of

immunofluorescent detection and immunocomplex kinase assay indicated that the increase or decrease of p38 MAPK activity during the first 3 h was not based on a significant change in the number of cells positive for active kinase but rather reflected a change of p38 MAPK activity within a given number of cells. Therefore, neurons surviving 24 h after gp120 exposure appear to represent a smaller cell population that either is still in the process of dying or tolerates a higher p38 MAPK activity than that occurring under the respective control conditions. Given the fact that inhibition of p38 MAPK activity was protective, the variable measurements of kinase activity between 3 h and 24 h presumably reflect a temporary deactivation of the active kinase by phosphatases as well as the death and consequent drop-out of neurons that previously contributed to an overall increasing kinase activity in the cell culture as a whole. An additional and not mutually exclusive explanation is that primary, mixed neuronal-glial cell cultures do not grow in a synchronized fashion as for example cell lines do, and therefore different neurons in a given culture may respond to neurotoxins and eventually enter into a cell death pathway (apoptosis) at different times. Thus, the fluctuations of p38 MAPK activity may result from the dynamic interplay of activation and inactivation of the kinase as well as the gradual demise of neurons.

We also performed Western blotting experiments to address the question of active p38 MAPK in cerebrocortical neurons exposed to conditioned media from THP-1 cells (Figure 3.6). We detected increased p38 MAPK activity in the microglia-depleted cerebrocortical cultures at 24 h and 3 d after treatment with neurotoxic THP-1 conditioned media. Of note, the results shown in Figures 3.6 and 3.8 indicated that at 24 h the demise of a significant part of neurons has already occurred. Thus, our

findings suggested that the remaining, surviving neurons (and astrocytes) may indeed have adapted, at least for the time of the experiment, to an increased p38 MAPK activity. The possibility of such an adaptation in surviving neurons is a novel hypothesis that warrants future investigations.

Other groups have shown that gp120 triggers p38 MAPK activation in macrophages and monocytes, which can enter in the brain soon after HIV infection and presumably contribute to the development of HAND (Del Corno et al., 2001; Lee et al., 2008). In concurrence with these previous studies, gp120 elicited p38 MAPK activation in rat microglia and in our model for microglia, human monocytic THP-1 cells and primary MDM. These mononuclear cells produced significant neurotoxicity upon treatment with gp120 for 24 h to 4 d. Activation of p38 MAPK by HIV-1 gp120 in these phagocytic cells must occur before the activation of the same kinase increases in neurons as evidenced by the kinetic of p38 MAPK in gp120-treated monocytic THP-1 cells and the reduction of neuronal death (Kaul et al., 1999; Kaul et al., 2007) and decrease in kinase activity signal in cerebrocortical cells after microglial depletion. In addition, suppressing p38 MAPK activity in monocytic THP-1 cells and primary MDM via the dominant-negative inactive p38 MAPK mutant caused a significant reduction in neurotoxicity. Thus, the dominant-negative inactive p38 α MAPK mutant suggests a critical role of p38 MAPK signaling in macrophages and microglia for gp120-induced neurotoxicity. Furthermore, this finding was consistent with our observation of p38 MAPK-dependent gp120 neurotoxicity in the mixed rat cerebrocortical cultures that were obtained using the same adenoviral constructs (Kaul

et al., 1999; Kaul et al., 2007) and various dosages of the pharmacological inhibitor SB203580 (Figure 3.2).

In addition, the similarity of the results obtained in this study with primary human MDM and THP-1 cells, strongly supports the notion that the latter cell type is a very suitable model of microglia and macrophages. Therefore, additional experiments were performed using monocytic THP-1 cells. In particular, knockdown of endogenous p38 α MAPK via three separate siRNA duplexes all derived from exon 2, similar to studies using a macrophage-specific deletion of p38 α MAPK in vivo (Kim et al., 2008), significantly and specifically reduced expression of the protein by 50-75% in mononuclear THP-1 cells. The α isoform of p38 MAPK is thought to be the most important isoform involved in inflammatory regulation (Kim et al., 2008; Kang et al., 2008) and a possible therapeutic target for CNS disorders beyond HAND and HIV-associated dementia, such as Alzheimer's disease (Munoz et al., 2007). Importantly, in our hands knockdown of p38 α MAPK by 50-75% sufficed to abrogate gp120-induced neurotoxicity similar to the significant reduction seen with over-expression of the dominant-negative mutant of the kinase; supporting the theory that p38 MAPK is vital for macrophage-mediated neurotoxicity of HIV gp120, but does not necessarily involve all p38 MAPK molecules available in the cell. This interpretation is in line with our observation that besides partial depletion of p38 MAPK protein, lower concentrations of the p38 MAPK pharmacological inhibitor SB203580 than what we previously assessed (Choi et al., 2007; Kaul et al., 1999; Kaul et al., 2007) can both sufficiently and specifically suppress HIV-1 gp120-induced neurotoxicity.

In our studies using mixed neuronal-glia cell cultures, direct neuronal interaction with gp120, did not appear to cause significant amounts of neuronal death in the absence of microglia, as observed when gp120 was added to microglia-deficient cultures directly or via spiking of control THP-1 supernatants. However, it could potentially be possible that gp120 acted directly on neuron and astrocytes contributing to neurotoxicity in synergy with a factor secreted by gp120-stimulated but not control-treated mononuclear cells. Therefore, we performed neurotoxicity assays in mouse cerebrocortical cultures deficient in both HIV coreceptors (double CCR5/CXCR4 knockouts) which are even in the presence of endogenous microglia themselves resistant to gp120-induced neurotoxicity (Kaul et al., 2007). Therefore, we replaced endogenous microglia with monocytic THP-1 cells in order to selectively provide monocytic cells possessing HIV-coreceptors. The results showed that without HIVgp120 co-receptors present in neurons and astrocytes, gp120-treated THP-1 cells (and their supernatants) remained neurotoxic. Hence, the presence of mononuclear cells expressing CXCR4 and CCR5 (besides CD4) sufficed to restore susceptibility to gp120 toxicity in combined CCR5-CXCR4-deficient cerebrocortical cells, and a direct interaction of gp120 with neurons or astrocytes, at least via chemokine receptors, was dispensable for induction of neuronal death.

On the other hand, inhibition of p38 MAPK in rat cerebrocortical neurons and astrocytes prior to the addition of gp120-induced mononuclear cell-derived neurotoxins prevented neuronal apoptosis as shown in Figure 3.9. This data suggests that inhibition of stress-related signaling via p38 MAPK, at the level of neurons (and possibly astrocytes) also succeeded in protecting against gp120-induced

macrophage/microglia neurotoxicity and thus revealed a potential mechanism to rescue mature neurons from HIV gp120-induced injury and death even if neurotoxins are present. However, our findings also emphasize the potential of limiting or abrogating the upstream involvement of macrophages/microglia in HIV-1 gp120 neurotoxicity. Therefore, further investigation into the mechanism of macrophage/microglia-mediated gp120 neurotoxicity is warranted.

Importantly, our results revealed that p38 MAPK provides a causal link in the neurotoxic mechanism triggered by HIV-1 gp120 in two disparate cell types similar to the behavior of the transcription factor p53 as previously shown (Garden et al., 2004). This comparable requirement for p38 MAPK and p53 warrants further investigation since it has been reported that direct phosphorylation of p53 by p38 MAPK is a critical step in the induction of apoptosis in HIV-1/gp120 induced syncytia (Perfettini et al., 2005).

Although p38 MAPK activity in both cell types is important for the overall neurotoxic effect of HIV-1 gp120 and β -chemokines and pharmacological inhibitors of p38 MAPK affect neurons and glial cells, the blockade of p38 MAPK activity in microglia or neurons, respectively, suffices to ameliorate toxicity of gp120. Thus our finding that blockade of the kinase in macrophages/microglia, the primarily productively HIV-infected cell type in the brain, suffices to prevent the indirect neurotoxicity of the viral envelope protein may offer new cell-type specific therapeutic strategies for protection of the CNS against HIV-associated injury and functional impairment.

3.5. ACKNOWLEDGEMENTS

We thank Dr. Jiahuai Han (The Scripps Research Institute, La Jolla, CA) for adenoviral vectors, Dr. Stuart Lipton (Sanford-Burnham Medical Research Institute, La Jolla, CA) for support during the initial phase of the project, and Dr. Pedro Aza-Blanc (Sanford-Burnham Medical Research Institute) for advice on the selection of siRNAs. We also thank Rebecca Ruf and Cyrus De Rozieres for technical assistance in Western blotting and tissue culture, and Cari Cox and Irene Catalan for help with tissue culture and image analysis.

Chapter 3 contains figures and text of the material accepted into *The Journal of Immunology* 2010. Medders K, Sejbuk N, Maung R, Desai MK, and Kaul M (2010) Activation of p38 MAPK is required in monocytic and neuronal cells for HIV gp120-induced neurotoxicity. *J Immun.* Vol. 185. The dissertation author was lead author and investigator of this paper.

The work in Chapter 3 was supported by National Institutes of Health R01 Grants NS050621 and MH087332.

CHAPTER 4

INHIBITION OF MACROPHAGE-MEDIATED P38 MAPK ACTIVITY: A NOVEL, POTENTIAL ROLE OF LEUKOTRIENES IN GP120-INDUCED NEUROTOXICITY

4.1. ABSTRACT

Several studies have suggested that the neuropathology observed in HIV-associated neurocognitive disorders (HAND) is due to the neurotoxic HIV-1 envelope protein gp120, which is correlated with increased activation of monocytic cells and signaling through stress-activated pathways, such as p38 MAPK. Activation of macrophages and p38 MAPK have also been implicated in inflammation, for instance after bacterial endotoxin lipopolysaccharide (LPS) exposure. Therefore, we hypothesized that p38 MAPK signaling might play an important role in the HIV-1 gp120-induced neurotoxic phenotype of macrophages possibly through its up-regulation of inflammatory mediators, similar to LPS. To support this hypothesis, LPS induced macrophage-mediated neurotoxicity, similar to HIV-1 gp120. Immunocomplex kinase assay and immunoblot studies demonstrated that p38 MAPK activation was increased from basal levels in gp120- and LPS-treated THP-1 cells whereas active SAPK/JNK was only observed after LPS exposure. In addition, upstream p38 MAPK activator TAB1 and downstream p38 MAPK substrate heat shock protein 27 (HSP27) were found in complex with basal and gp120-induced

phosphorylated p38 MAPK, via co-immunoprecipitation. Furthermore, phosphorylation of HSP27 stimulated by gp120 and LPS was reduced by p38 MAPK inhibitor SB203580. Our previous studies indicated p38 MAPK activity as vital for the neurotoxic phenotype of gp120-activated macrophages and subsequent neuronal death. Therefore, to further investigate downstream mediators of neurotoxic p38 MAPK in human monocytic THP-1 cells we inhibited p38 MAPK activity utilizing pharmacological and siRNA knockdown. Pharmacological inhibition of p38 MAPK activity reduced the neurotoxic phenotype of THP-1 cells stimulated by gp120, but not LPS. Surprisingly, using multiplex arrays (gene and protein) we found that non-neurotoxic p38 MAPK-specific inhibitor, SB203580, alone triggered the expression of potential protective factors while reducing expression of potential neurotoxic pathways, and paradoxically increased the expression and release of pro-inflammatory mediators. For instance, SB203580 reduced the expression of leukotriene C₄ synthase (LTC₄S), an enzyme responsible for production of neurotoxic cysteinyl leukotrienes. Moreover, pre-treatment of microglia-depleted cerebrocortical cultures with the cysteinyl leukotriene receptor (CYSLT1) antagonist montelukast prevented reduction in neuronal survival caused by gp120-conditioned THP-1 cells, implicating leukotriene biosynthesis in gp120 neurotoxicity. Taken together, these data suggest that p38 MAPK signaling pathway plays a critical role in gp120-induced neurotoxicity and not LPS-induced neurotoxicity, and potential therapeutic approaches targeting neurodegeneration in HAND could focus on preventing activation of the neurotoxic p38 MAPK signaling pathway and its potential downstream targets, such as leukotriene biosynthesis.

4.2. INTRODUCTION

HIV encephalopathy (HIVE) generally occurs with direct viral infection of the central nervous system (CNS), but not via direct interaction with neurons, and is correlated with HIV-associated neurocognitive disorders. Macrophages, microglia and other monocytic cells are the principal target cells of HIV-1 in the CNS. Furthermore, infiltration of infected monocytes into the CNS establishing detectable viral load in the cerebral spinal fluid (CSF) and subsequent activation of resident monocytic cells appear to be critical for neuronal injury and the development of neurocognitive disorders (Garden et al., 2004; Gras G et al, 2010; Kaul et al, 2001), but how HIV-1 induces cellular monocytic activation in the CNS remains unknown.

Viral-host interactions occur through the HIV-1 envelope glycoprotein gp120 with host cell CD4 and G protein-coupled chemokine receptors, either CCR5 or CXCR4, with CCR5 being the main coreceptor for HIV infection of macrophages and microglia (He et al., 1997). In addition, most viruses isolated from brain or the CSF are CCR5 (R5)-preferring (Shieh et al., 1998). The normal function of CCR5 is to elicit G protein signaling in response to extracellular ligands, for instance by beta chemokines CCL4/MIP-1 β or CCL5/RANTES. However, the virus or HIV-1 gp120 are able to hijack this system and cause neurotoxicity in the brain (Gras et al., 2010). In addition, secretion of HIV-1 gp120 is thought to also stimulate uninfected microglia and macrophages to release neurotoxins (Gonzalez-Scarano et al., 2005; Kaul et al., 2001).

Past studies have shown that HIV-1 gp120-induced activation of macrophages elicited proinflammatory cytokines that are thought to be responsible for neurotoxic mechanisms (Cheung et al., 2008; Fantuzzi et al., 2008; Lee et al., 2005). We and others have previously shown that HIV-1 gp120 induces p38 MAPK activation in macrophages (Cheung et al., 2008; Lee et al., 2005; Medders et al., 2010) and this activation is required for the HIV-1 gp120-stimulated neurotoxic phenotype of macrophages (Medders et al., 2010). Gram-negative lipopolysaccharide (LPS) can also induce p38 MAPK activation and the production of proinflammatory cytokines in macrophages; and has also been implicated in neurotoxicity (Kim et al., 2000).

Our studies described here have focused on determining the potential neurotoxic mediators induced by HIV-1 gp120 after inhibition of p38 MAPK in monocytic cells and in comparison to LPS-induced neurotoxicity. We first established that depletion of microglia from neuronal cultures prevented LPS-induced neuronal death, which was shown by alternative approaches (Kim et al., 2000) and was similar to the requirement of monocytic cells for HIV-1 gp120-induced neuronal death (Garden et al., 2004; Kaul et al., 1999; Medders et al., 2010). We then used a model of human monocytic cells (THP-1 cells) which have been established for the use and investigations into HIV-1 gp120-induced neurotoxicity (Medders et al., 2010). Importantly, we found that p38 MAPK and downstream p38 MAPK target HSP27 were activated in monocytes after stimulation with R5-preferring HIV-1 gp120_{SF162} or LPS. In addition, pre-incubation of monocytic cells with the p38 MAPK inhibitor SB203580 prevented the activation of HSP27. Surprisingly, we determined that although LPS was able to stimulate neurotoxins from monocytic cells similarly to

HIV-1 gp120, inhibition of p38 MAPK in monocytic cells was only able to prevent HIV-1 gp120-induced neurotoxicity.

Using microarray and bead-based multiplex arrays, treatment of monocytes with LPS or SB230580 or SB203580 plus HIV-1 gp120 (SB+gp120) increased the expression and production of proinflammatory cytokines, growth factors and chemokines while HIV-1 gp120 did not. However, SB203580-stimulated release of proinflammatory cytokines was significantly lower than in LPS-treated cells. Our group and others have found that the CCR5 ligands CCL4 and CCL5 block neuronal death caused by HIV-1 gp120 *in vitro* (Kaul et al., 1999; Meucci et al., 1998). However, the concentrations of these chemokines after SB203580 were significantly lower than those seen as protective in those studies.

Interestingly, SB203580 and SB+gp120 treatments caused a significant reduction in the expression of cysteinyl leukotriene C₄ synthase (LTC₄S), which has been implicated in production of lipid inflammatory leukotrienes and potential neurotoxicity (Okubo et al., 2010). Furthermore, we were also able to show that pre-incubation of neuronal cultures with cysteinyl leukotriene receptor inhibitor, montelukast, prevented neuronal death caused by potential neurotoxins released from HIV-1 gp120 treated monocytes.

Our results presented here suggest that p38 MAPK signaling is responsible for the neurotoxic phenotype of monocytes exposed to HIV-1 gp120 and this signaling may not require the canonical inflammatory mediators, such as pro-inflammatory cytokines. Taken together, our study showed that inhibition of p38 MAPK activity may prevent the neurotoxic effects of HIV-1 gp120 by reducing the availability of the

leukotriene biosynthesis pathway and therefore implicated leukotrienes in HIV-1 gp120-induced neurotoxicity.

4.3. RESULTS

4.3.1. Presence of microglia is required for LPS-induced neurotoxicity, implying similarity to HIV-1 gp120 triggered toxicity

In our previous studies, depletion of microglia from cerebrocortical cultures was found to abrogate the neurotoxicity of gp120 (Kaul et al., 1999; Kaul et al., 2007; Medders et al., 2010). Therefore, we first tested whether LPS-induced neurotoxicity in our system was dependent on the presence of monocytic cells, as it was for gp120-induced neurotoxicity. Using the same experimental approach as in our previous neurotoxicity studies, we found that prior depletion of microglia before exposure to the bacterial endotoxin also reduced neuronal loss caused by LPS (Figure 4.1). In brief, 17 day old rat cerebrocortical cultures were depleted of microglia with 7.5 mM leucine methyl ester (LME) for 4 h prior to incubation with 1 µg/ml LPS for 24 h. After immunofluorescent staining with neuronal MAP-2 antibody and nuclear Hoechst, the number of MAP-2 positive cells was quantified and compared to total number of cells to determine whether neuronal cultures were insensitive to LPS-induced neurotoxicity in the absence of microglia. As shown in Figure 4.1, no significant loss of neurons was observed in cerebrocortical cultures without microglia

(with LME pre-treatment) and exposed to LPS for 24 h. Hence, the neurotoxicity in response to LPS exposure for 24 h is dependent on the presence of microglia.

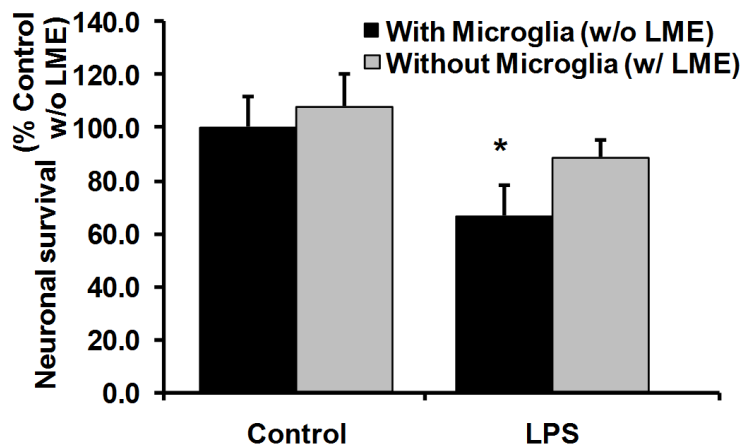


Figure 4.1 LPS requires presence of microglia in rat cerebrocortical cultures to reduce neuronal survival after 24 h. LPS (1 $\mu\text{g/ml}$) or 0.001% BSA-vehicle (Control) was added to rat cerebrocortical cultures either depleted of microglia (4 h pre-incubation with 7.5 mM LME (w/ LME)) or with microglia (w/o LME pre-treatment). Neuronal survival was assessed using fluorescence microscopy after fixation, permeabilization and immunolabeling of neurons for MAP-2 in combination with nuclear DNA staining by H33342. Vehicle-treated controls without LME (with microglia) were used to compare neuronal survival after other treatments, and set as baseline of 100%. Error bars represent the S.E.M. of three independent experiments. * = $p < 0.05$ compared to control values, with or without LME (ANOVA with Fisher's PLSD post hoc test).

4.3.2. HIV-1 gp120 and LPS increase p38 MAPK activation in THP-1 cells with different kinetics, while only LPS increases JNK activation

Previous studies have demonstrated that HIV-1 gp120 was able to increase the activation of p38 MAPK in macrophages and neuronal cells (Del Corno et al., 2001; Medders et al., 2010; Singh et al., 2005), either directly or indirectly. Stress-activated MAPK (p38 MAPK and JNK) pathways have been implicated in several inflammatory mechanisms, such as after exposure to LPS. Therefore, we next tested whether LPS increases activation of p38 MAPK similarly to HIV-1 gp120 and whether JNK

activation occurs in monocytes after HIV-1 gp120 exposure (Figure 4.2). Using immunocomplex kinase assays, we were able to determine that R5-preferring HIV-1 gp120_{SF162} and LPS both increased p38 MAPK activation in monocytes but with different kinetics (Figure 4.2A). Over a 24 h period, HIV-1 gp120 significantly increased p38 MAPK activity, while LPS significantly activated p38 MAPK within at least the first 30 min of exposure (Figure 4.2A and 4.2B). However, LPS-induced activation of p38 MAPK was reduced to basal levels at 24 h (Figure 4.2A). Using immunoblot analysis, we were able to determine that HIV-1 gp120 did not appear to increase activation of JNK, while LPS exposure increased JNK activation starting at around 15 min up to at least 1 h in monocytes (Figure 4.2C). Note that p38 MAPK activity was observed in basal control conditions, while activation of JNK was not (Figure 4.2B and 4.2C). Protein synthesis inhibitor Anisomycin was used as a positive control for activation of p38 MAPK and JNK (Hazzalin et al., 1998).

We next assessed the proteins associated with p38 MAPK after HIV-1 gp120 or LPS exposure in THP-1 cells. First we used co-immunoprecipitation approaches to isolate protein interactions with active p38 MAPK. Similar to the p38 MAPK kinase assay, we used an immobilized phospho-p38 monoclonal antibody to immunoprecipitate (IP) activated p38 MAPK from THP-1 cell lysates exposed to HIV-1 gp120 or LPS for 30 min. We then assayed the IP for proteins that could possibly be interacting with p38 MAPK via immunoblot. As described previously in Figure 4.2 and in Medders et al., 2010, HIV-1 gp120 increased the amount of active p38 MAPK in THP-1 cells, shown here after 30 min exposure (Figure 4.3A). Interestingly, upstream p38 MAPK activator TGF-beta-activated protein kinase 1-

binding protein 1 (TAB1) and downstream p38 MAPK substrate heat shock protein 27 (HSP27) were found to be in a complex with active p38 MAPK in all conditions after 30 min, including exposure to either 0.001% BSA (vehicle control), 1 nM HIV-1 gp120_{SF162} (Figure 4.3A), or 1 µg/ml LPS (data not shown). Activated p38 MAPK was not associated with its canonical upstream regulator mitogen-activated protein kinase kinase 3 (MKK3) at basal conditions or after HIV-1 gp120 exposure in THP-1 cells (data not shown).

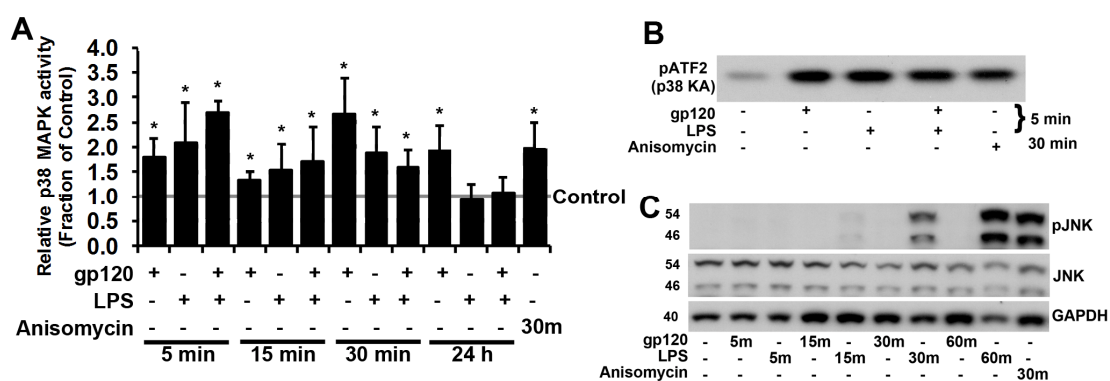


Figure 4.2 HIV-1 gp120 increase p38 MAPK activity, while LPS and Anisomycin increases p38 MAPK and SAPK/JNK activities in human monocytic THP-1 cells. HIV-1 gp120_{SF162} (1 nM), LPS (1 µg/ml), Anisomycin (10 µg/ml) or 0.001% BSA-vehicle (Control) were added to THP-1 cells for 5, 15, 30, 60 min, 24 h, or as indicated. Cell lysates were then collected and subjected to immunocomplex p38 MAPK assay with pATF2 as product (A and B) or immunoblot for active JNK, JNK, with GAPDH as loading control (C). HIV-1 gp120_{SF162} causes significant deviation of p38 MAPK activity from baseline control conditions at 5 min, 15 min, 30 min, and 24 h. LPS follows this similar trend, but with a return to basal levels at 24 h (A). Representative western blots of pATF2 (p38 MAPK kinase assay result) after exposure to gp120 or LPS at 5 min and Anisomycin at 30 min (B). In contrast, activity of JNK is only significantly elevated by LPS treatment at 15 min, 30 min and 60 min (C). The kinase assay results are shown in fold change from vehicle-treated controls defined as the baseline value (A). Equal amounts of cellular protein (40 µg per lane) were analyzed by SDS PAGE and immunoblotting. Anisomycin acts as positive control treatment for p38 MAPK or JNK activation. Error bars represent the S.E.M. of three to six independent experiments. * = $p < 0.05$; compared to control values (ANOVA with Fisher's PLSD post hoc test).

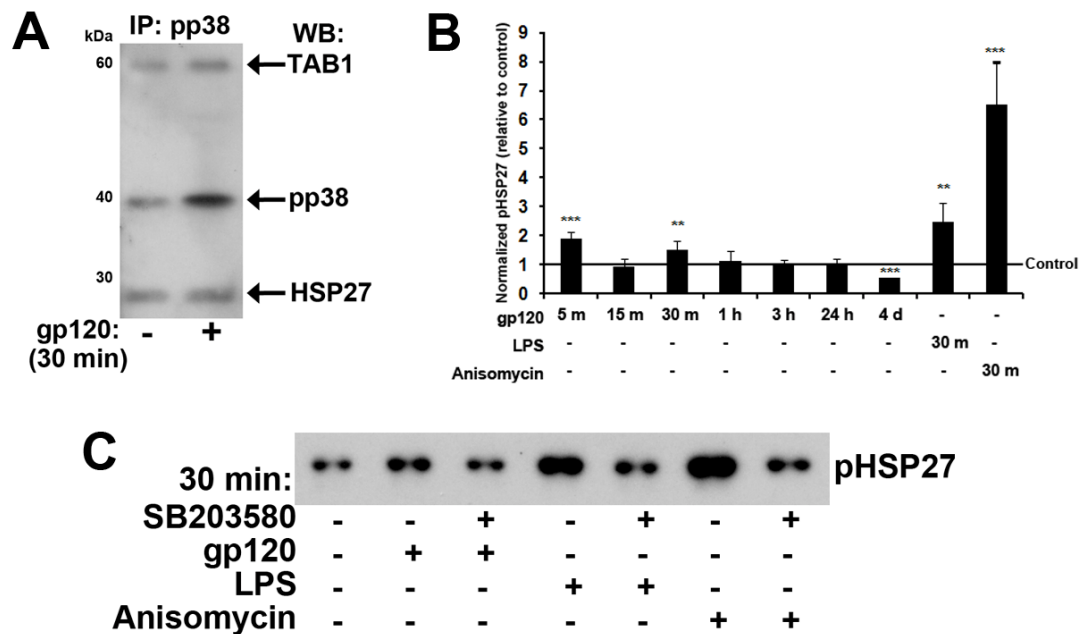


Figure 4.3 Inhibition of p38 MAPK reduces the phosphorylation of HSP27 by HIV-1 gp120, LPS and Anisomycin in human monocytic THP-1 cells. HIV-1 gp120_{SF162} (1 nM), LPS (1 µg/ml), Anisomycin (10 µg/ml) or 0.001% BSA-vehicle (Control) were added to THP-1 cells for 5, 15, 30 min, 1 h, 3 h, 24 h, or 4 d, or as indicated. Cell lysates were then collected and subjected to co-immunoprecipitation for phosphorylated p38 MAPK (pp38 IP) and immunoblot for TAB1 and HSP27 (WB) (A) or phosphorylated HSP27 (pHSP27), with GAPDH as loading control for normalization (B and C), respectively). HIV-1 gp120_{SF162} causes an increase in active p38 MAPK which is associated with TAB1 and HSP27 shown via co-IP after 30 min control or gp120-treatment (A). HIV-1 gp120 increases phosphorylation of HSP27 (pHSP27) at 5 and 30 min, and decreases at 4 d; while LPS and Anisomycin increases pHSP27 levels at 30 min (B). The immunoblot results (normalized against GAPDH), shown in fold change from vehicle-treated controls defined as the baseline value (B). Pre-treatment with 10 µM SB203580 reduces the pHSP27 levels seen after HIV-1 gp120, LPS or Anisomycin incubations, shown here at 30 min (C). Equal amounts of cellular protein (40 µg per lane) were analyzed by SDS PAGE and immunoblotting. Anisomycin acts as positive control treatment for p38 MAPK activation. Error bars represent the S.E.M. of three to six independent experiments. * = $p < 0.05$, ** = $p < 0.005$, *** = $p < 0.001$; compared to control values (ANOVA with Fisher's PLSD post hoc test).

Furthermore, HIV-1 gp120, LPS and Anisomycin (10µg/ml) increased the activation or phosphorylation of HSP27 (Figure 4.3B). HIV-1 gp120 significantly stimulated the phosphorylation of HSP27 at 5 and 30 min, but pHSP27 was reduced after 4 d incubation. LPS and Anisomycin both increased pHSP27 levels after 30 min exposure (Figure 4.3B). Inhibition of p38 MAPK activity via SB203580 (but not DMSO as vehicle) pretreatment was able to reduce the phosphorylation of HSP27

normally stimulated after HIV-1 gp120, LPS or Anisomycin treatments (Figure 4.3C). SB203580 returned pHSP27 levels to those observed at basal conditions in THP-1 cells, confirming that HSP27 is a downstream substrate of p38 MAPK.

4.3.3. Inhibition of p38 MAPK activity in THP-1 cells fails to rescue neurons from LPS-induced neurotoxicity

In our previous study, we were able to show that knockdown of p38 MAPK using siRNA reduced the loss in neuronal survival caused by HIV1- gp120 neurotoxicity from monocytic cells (Medders et al., 2010). Since LPS induces neurotoxicity in the presence of microglia (Figure 4.1), we then next explored whether LPS induces neurotoxicity from THP-1 cells. First, we used our microglia-depleted rat cerebrocortical cultures proven to be a robust and reproducible *in vitro* model of macrophage-mediated neurotoxicity (Kaul et al., 2007; Medders et al., 2010). These cells were incubated for 3 d with conditioned media collected from THP-1 cells incubated with HIV-1 gp120 (1 nM) or LPS (1 μ g/ml) and pretreated with SB203580 (10 μ M) (inset, Figure 4.4). Similarly to HIV-1 gp120, LPS (1 μ g/ml) significantly induced neurotoxicity with neuronal survival of $80\% \pm 5.2\%$ compared to control (Figure 4.4). LPS (1 μ g/ml) was also able to stimulate p38 MAPK activity in THP-1 cells similarly to HIV-1 gp120 (Figure 4.2 and 4.3). However, pharmacological p38 MAPK inhibition with 15 min 10 μ M SB203580 pretreatment (DMSO as vehicle) in THP-1 cells was unable to prevent LPS-induced neurotoxicity (Figure 4.4). HIV-1 gp120-induced neurotoxicity was reduced by p38 MAPK inhibition in THP-1 cells

(Figure 4.4), in accordance with our previous studies (Medders et al., 2010). Reduction of neurotoxin release from HIV-1 gp120 exposed THP-1 cells was not the result of decreased mononuclear cell viability after p38 MAPK inhibition, as the viability of both the control and treated samples had equal viability (data not shown). Conversely, increased neurotoxin production was not the result of decreased monocytic cell viability after LPS or HIV-1 gp120 exposure as these samples had similar viability compared to control (data not shown).

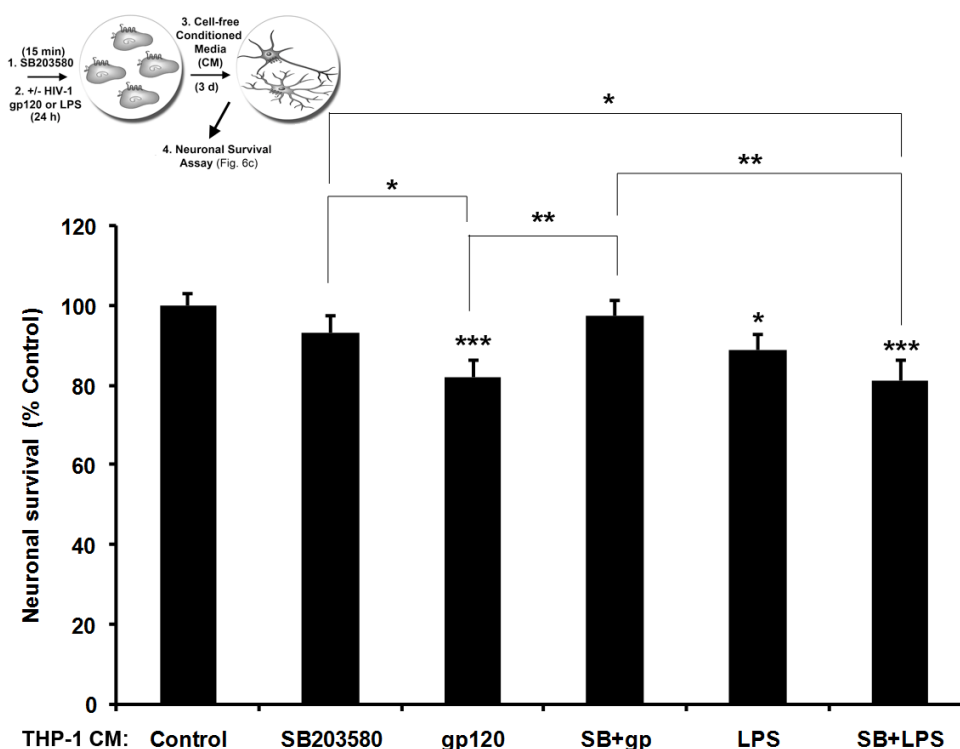


Figure 4.4 SB203580 increases neuronal survival after treatment with neurotoxic conditioned media from human monocytic THP-1 cells incubated with HIV-1 gp120, but not LPS. Conditioned media (CM) was collected from THP-1 cells treated with HIV-1 gp120_{SF162} (1 nM), LPS (1 µg/ml), or 0.001% BSA-vehicle (Control) for 4 d, with or without 15 min pretreatment of 10 µM SB203580. Microglia-depleted cerebrocortical cells were then incubated with THP-1 CM for 3 d and evaluated for survival. Neuronal survival was assessed using fluorescence microscopy after fixation, permeabilization and immunolabeling of neurons for MAP-2 in combination with nuclear DNA staining by H33342. Values obtained from THP-1 Control CM-treated cerebrocortical cells were used to compare neuronal survival by all other treatments, and set as baseline of 100%. Error bars represent the S.E.M. of three independent experiments. Lines connecting treatments were compared for statistical analysis. * = $p < 0.05$; ** = $p < 0.01$; *** = $p < 0.005$, compared to control values or those connected by lines (ANOVA with Fisher's PLSD post hoc test).

4.3.4. Cytokines, chemokines and growth factors are released from LPS- and SB203580-treated, but not from HIV-1 gp120 exposed THP-1 cells

Both the viral and bacterial products were able to induce neurotoxicity and stimulate p38 MAPK activity, however only HIV-1 gp120-induced neurotoxicity appeared to solely require p38 MAPK activation. Therefore, we next attempted to determine the identity of p38 MAPK-dependent soluble factors released from human monocytic THP-1 cells after HIV-1 gp120- or LPS-induced neurotoxin production. Using a combination of ELISA and bead-based multiplex assays, we were able to analyze roughly 13 analytes in the conditioned media from THP-1 cells. THP-1 cells were pretreated with 10 μ M SB203580 (or DMSO as vehicle) prior to exposure for 24 h or 4 d to vehicle control (0.001% BSA), HIV-1 gp120_{SF162} (1 nM), or LPS (1 μ g/ml). Conditioned media from the treated THP-1 cells were then collected and directly ran on an ELISA or bead-based multiplex array. Briefly, bead-based multiplex arrays capture ligands onto spherical beads in a suspension and use fluorescence as a reporter system (Luminex® xMAP). ELISAs use immobilized antibody to capture ligands and use enzyme amplification of a colorimetric substrate. Importantly, the two techniques provide similar experimental efficacy (Elshal et al., 2006).

SB203580 alone or SB203580 with HIV-1 gp120 (SB+gp120) was able to significantly increase the production of several cytokines, chemokines and growth factors compared to control or HIV-1 gp120 alone; including interleukin-1 beta (IL-1 β), Macrophage inflammatory protein-3 (MIP3 α)/chemokine (C-C motif) ligand 20

(CCL20), monocyte chemotactic protein-1 (MCP-1)/CCl₂, (MIP-1 α /CCL4, MIP-1 β /CCL4, interleukin 8 (IL8), vascular endothelial growth factor (VEGF), platelet-derived growth factor A/A (PDGF A/A) and Regulated upon Activation, Normal T-cell Expressed, and Secreted (RANTES)/CCL5 (Figure 4.5). HIV-1 gp120 alone did not significantly increase the production of any of the tested analytes compared to control (Figure 4.5), which was validated by ELISA (data not shown). These results suggest that neurotoxins stimulated by HIV-1 gp120 from THP-1 cells were not among these analytes. Note the different concentration scales on the three panels.

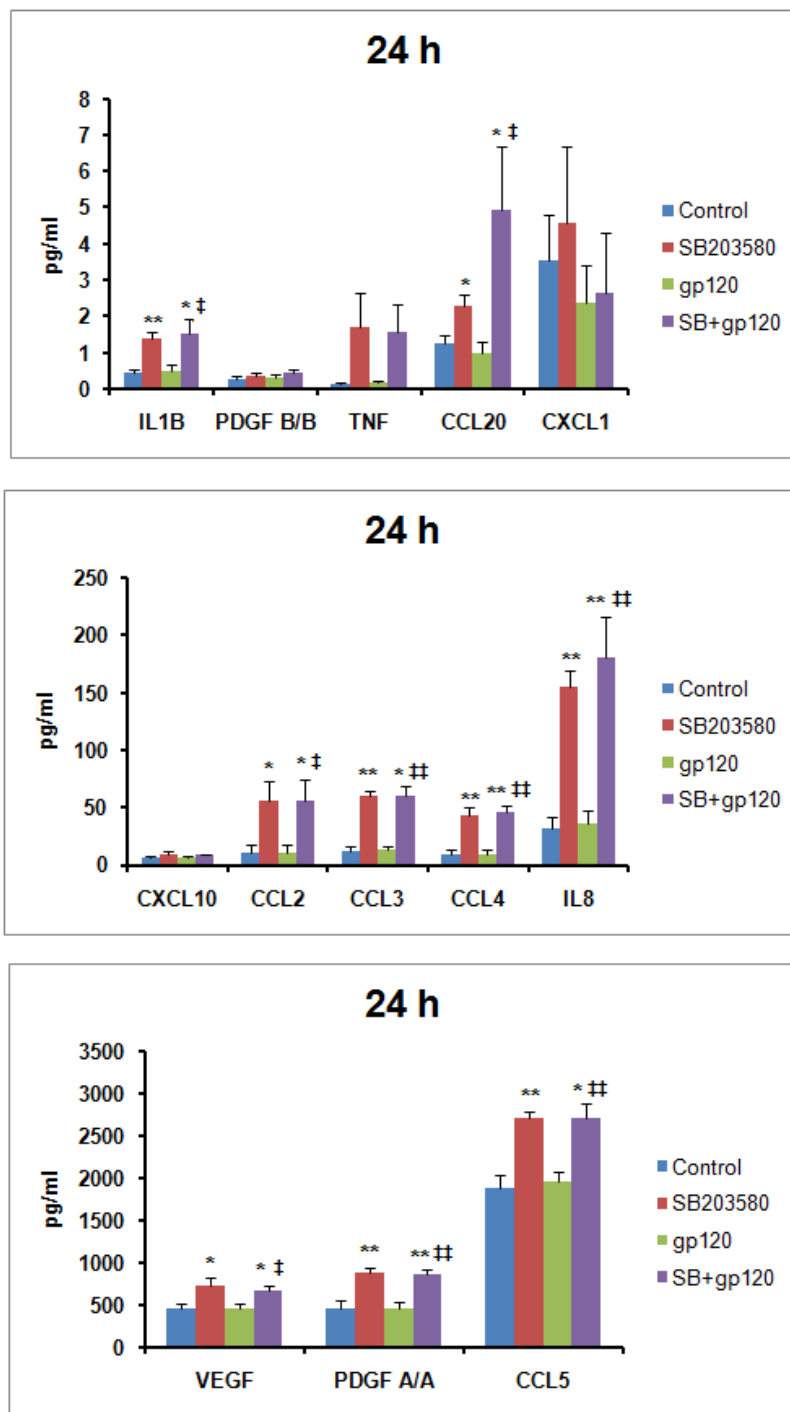


Figure 4.5 SB203580 alone increases release of several cytokines, chemokines and growth factors from human monocytic THP-1 cells after 24 h. Conditioned media (CM) was collected from THP-1 cells treated with HIV-1 gp120_{SF162} (1 nM) or 0.001% BSA-vehicle (Control) for 24 h, with or without 15 min pretreatment of 10 μ M SB203580 and assayed by bead-based multiplex array for cytokines, chemokines and growth factors. Note different scales for pg/ml protein on y-axis. Error bars represent the S.E.M. of three independent experiments. * = $p < 0.05$, ** = $p < 0.01$, compared to control values; ‡ = $p < 0.05$, ‡‡ = $p < 0.01$, compared to gp120 (ANOVA with Fisher's PLSD post hoc test).

We next assessed the production of the same 13 analytes after 24 h LPS (1 $\mu\text{g/ml}$) stimulation of THP-1 cells with or without SB203580 pretreatment. LPS or SB203580 and LPS (SB+LPS) significantly increased the production of PDGF B/B, IL-1 β , tumor necrosis factor (TNF), IL-8-related CXCL1, interferon gamma-induced protein 10 (IP-10)/CXCL10, VEGF, PDGF A/A, CCL4, IL8, CCL2 and CCL20 from control treatments (shown with asterisks (**)) in Figure 4.6). CCL3 and CCL5 were also increased after LPS incubation, but values could not be obtained as the amounts were above detection for both ELISA and multiplex array (data not shown). Several of these analytes were found to be significantly higher in SB203580-treated THP-1 cells compared to controls (Figure 4.5). However, the analytes were significantly higher in the LPS, or SB203580 and LPS (SB+LPS) treatments than with SB203580 alone (shown with \$\$ in Figure 4.6), except CCL20 and CCL2 for LPS or TNF for SB+LPS (although a trend exists for these to be higher as well). Only CXCL10 (red rectangle, Figure 4.6; and Appendix for microarray data) was found to be significantly reduced in LPS-treated THP-1 cells that were pretreated with SB203580 (SB+LPS) compared to LPS alone, although SB+LPS treatment still produced significantly higher amounts of CXCL10 than control or SB203580-treated samples. Note the different concentration scales on the three panels in Figure 4.6.

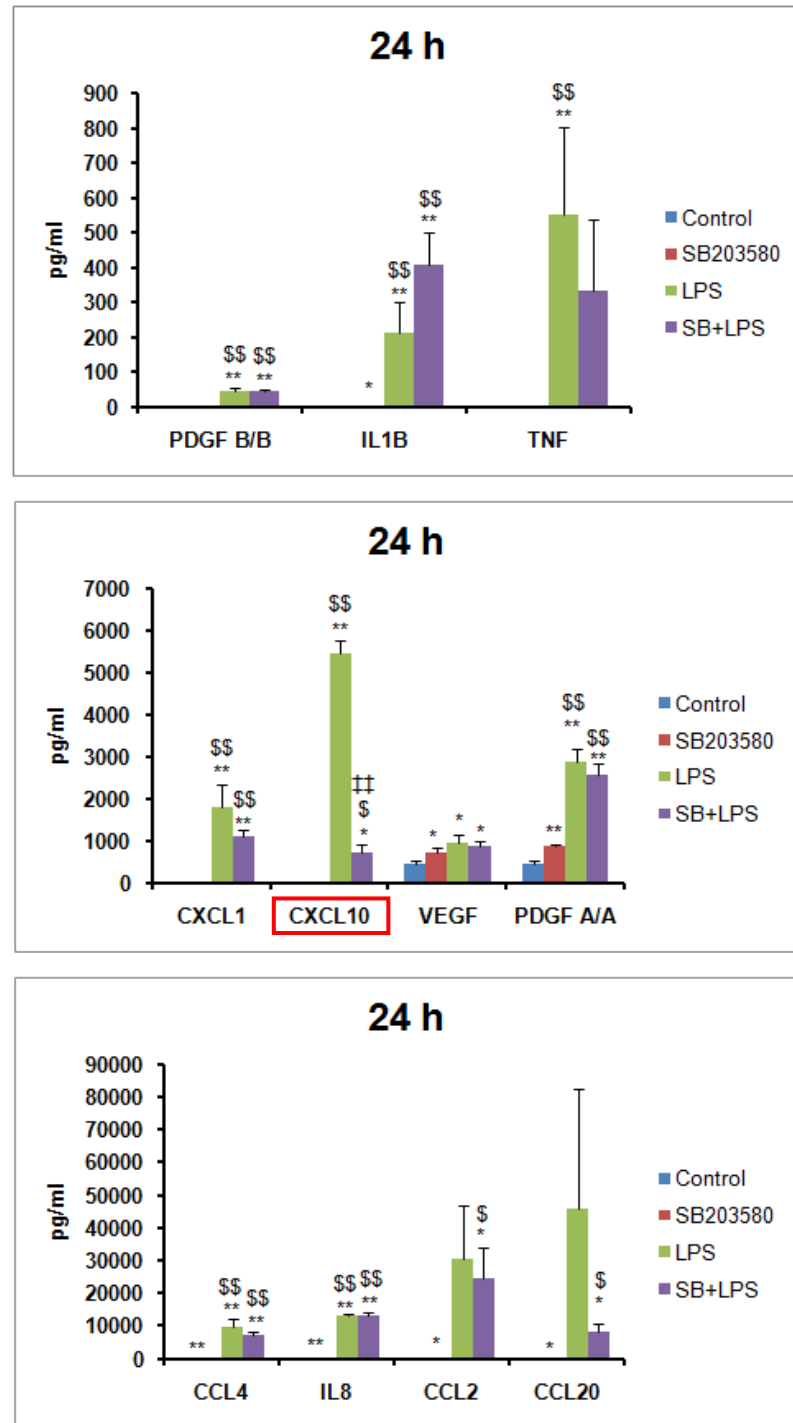


Figure 4.6 LPS-stimulated production of cytokines, chemokines and growth factors after 24 h in human monocytic THP-1 cells. Conditioned media (CM) was collected from THP-1 cells treated with LPS (1 $\mu\text{g/ml}$) or 0.001% BSA-vehicle (Control) for 24 h, after 15 min pretreatment of 10 μM SB203580 and assayed via bead-based multiplex arrays for cytokines, chemokines and growth factors. Note different scales for pg/ml protein on y-axis. Error bars represent the S.E.M. of three independent experiments. * = $p < 0.05$, ** = $p < 0.01$, compared to control values; \$ = $p < 0.05$, \$\$ = $p < 0.01$, compared to SB203580 alone; †† = $p < 0.01$ compared to LPS (ANOVA with Fisher's PLSD post hoc test).

Since we previously used media conditioned by THP-1 cells for 24 h and 4 d, we also assessed media collected from THP-1 cells treated after 4 d with HIV-1 gp120 or LPS, with or without p38 MAPK inhibitor (Figure 4.7). These experiments were only performed one time therefore no statistical analysis could be performed, however trends do exist for some of the analytes in specific treatments. SB203580 alone appeared to increase the production of IL-1 β , CCL20, IL8, PDGF A/A, and CCL5 from THP-1 cells (left panels, Figure 4.7); similar to that at 24 h. Interestingly, SB203580 alone increased the amount of PDGF A/A from control and possibly higher than LPS at 4 d (right middle panel, Figure 4.7). LPS appeared to increase all analytes measured (right panels, Figure 4.7). HIV-1 gp120 may increase the amount of VEGF compared to control as well (3700 pg/ml to 3100 pg/ml, respectively). Interestingly, LPS-stimulated CXCL10 production still appeared to be reduced with p38 MAPK inhibition (red rectangle, right panel, Figure 4.7). Moreover, SB+LPS may increase the production of CCL2 (838 to 1300 pg/ml), CCL3 (166 to 307 pg/ml), CCL20 (3227 to 5393 pg/ml) and IL-1 β (223 to 676) compared to LPS. Note the different concentration scales for the three separate panels on the left and on the right of Figure 4.7.

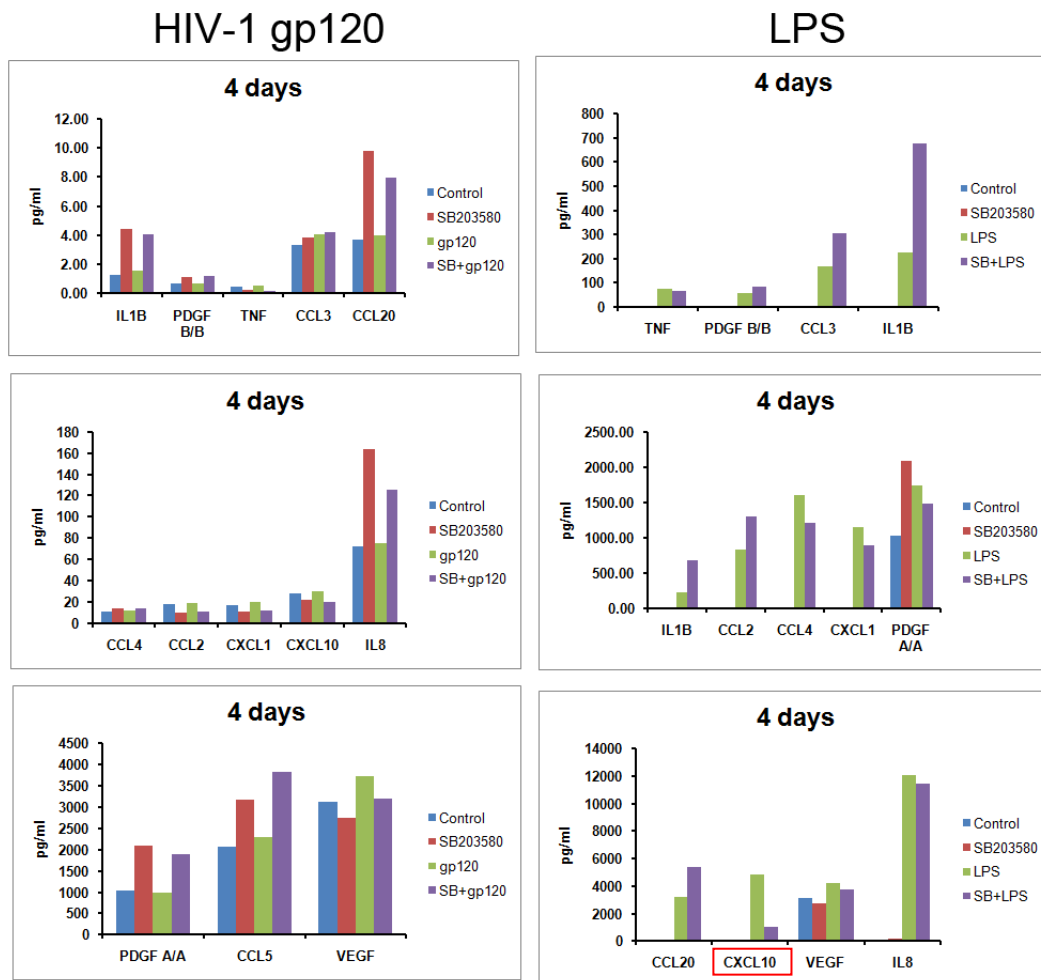


Figure 4.7 LPS or SB203580 alone, or combination of both (SB+LPS), may increase release of several cytokines, chemokines and growth factors from human monocytic THP-1 cells after 4 d. Conditioned media (CM) was collected from THP-1 cells treated with HIV-1 gp120_{SF162} (1 nM), LPS (1 μ g/ml) or 0.001% BSA-vehicle (Control) for 4 d, with or without 15 min pretreatment of 10 μ M SB203580 and assayed via bead-based multiplex arrays for cytokines, chemokines and growth factors. Note different scales for pg/ml protein on y-axis. Data represents one experiment.

4.3.5. p38 MAPK inhibitor, SB203580, alone causes more robust and significant changes in gene expression compared to HIV-1 gp120 in THP-1 cells

After determining that several proteins are increased by the p38 MAPK inhibitor SB203580 alone and that none of those analyzed were significantly different

after HIV-1 gp120 treatment compared to control, we concluded that performing a DNA microarray on the treated cells would provide valuable insight into how HIV-1 gp120 affects the phenotype of macrophages. Therefore, we ran RNA samples collected from THP-1 cells treated for 4 and 24 h with HIV-1 gp120 (1 nM), LPS (1 $\mu\text{g}/\text{ml}$), vehicle control (0.001% BSA), and/or SB203580 in a DNA microarray (Illumina HumanHT-12 v4 Expression BeadChip kit). Raw microarray data was analyzed via strict statistical cut-offs ($p < 0.05$ and fold change (FC) > 1.72) using modified t-tests and ANOVA (in collaboration with Sanford-Burnham Medical Research Institute Bioinformatics facility and Dr. Roy Williams). Many genes were differentially regulated after treatments with SB203580 (Table 4.2 and Appendix, Table 6.2 and 6.3) or LPS alone (see Appendix, Table 6.4). However, only after relaxing the stringency of the statistical analyses ($p < 0.1$ and fold change (FC) > 1.36) were we able to identify significant differences when comparing HIV-1 gp120 to control treatments (Table 4.1 and Appendix, Table 6.1). These genes listed in Table 4.1 are those that were significantly different when comparing HIV-1 gp120 to control and HIV-1 gp120 to SB203580 and gp120 (SB+gp120); and therefore considered genes regulated by p38 MAPK after HIV-1 gp120 treatment.

Table 4.1 p38 MAPK-dependent¹ genes possibly regulated by HIV-1 gp120 at 4 and 24 hours in human monocytic THP-1 cells^{**}

Incubation Time	Gene Product	GenBank Accession No.	Symbol	Fold Change ²	p value
4 Hours	NADH dehydrogenase (ubiquinone) 1 alpha subcomplex, 10	NM_004544	NDUFA10	1.50	0.077
	G protein-coupled receptor 1	NM_005279	GPR1	1.47	0.066
	Golgi-specific brefeldin A resistant guanine nucleotide exchange factor 1	NM_004193	GBF1	1.38	0.050
	Capping protein (actin filament) muscle Z-line, alpha 1	NM_006135	CAPZA1	-1.40	0.013
24 Hours	RAB1B, member RAS oncogene family	NP_112243	RAB1B	1.43	0.014
	ATP synthase, H ⁺ -transporting, mitochondrial F1 complex, delta subunit	NM_001687	ATP5D	1.38	0.081
	Vacuolar protein sorting 26	NM_004896	VPS26	-1.54	0.078
	Translin-associated factor X	NM_005999	TSNAX	-1.48	0.093
	RAP1A, member of RAS oncogene family	NM_001010935	RAP1A	-1.41	0.035
	RAB11A, member RAS oncogene family	NM_004663	RAB11A	-1.38	0.077
	Dihydropyrimidine dehydrogenase	NM_000110	DPYD	-1.38	0.087
	RRN3 RNA polymerase I transcription factor homolog	NM_018427	RRN3	-1.36	0.068
	24-dehydrocholesterol reductase	NM_014762	DHCR24	-1.36	0.025

¹p38 MAPK-dependent genes were determined by comparison of HIV-1 gp120 genes changed from control to gp120 v “SB203580 + gp120” raw data. ^{**}Results are considered significant at fold change of ≥ 1.5 or -1.5 , with a p value of < 0.05 ; therefore, none of the genes listed above are significantly different from control. ²Fold change was determined by comparing raw data from treatments against vehicle-control data.

The p38 MAPK inhibitor SB203580, on the other hand, caused significant changes in the expression of several genes (Figure 4.8 and Table 4.2). These genes were considered to be differentially expressed from control at either at 1.72 or -1.72 fold change (FC) and with a p value of less than 0.05. A full list of the genes modified by SB203580 alone after 4 and 24 h in THP-1 cells can be found in the Appendix

section. Of note, many genes are of the pro-inflammatory cytokine families (i.e. IL-1 β and TNF α), beta chemokines (i.e. CCL5), plasminogen family (i.e. PLAUR) and genes involved in arachidonic acid metabolism (i.e. LTC₄S).

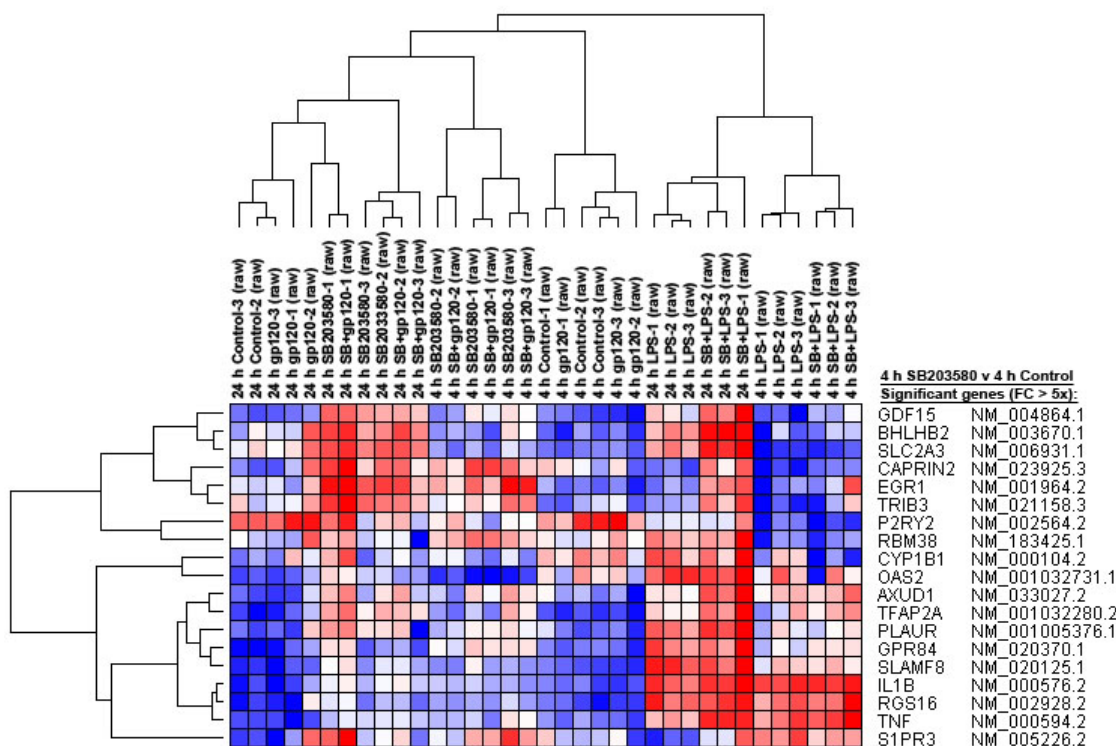


Figure 4.8 Heat map of genes differentially expressed by SB203580 versus control at 4 h in human monocytic THP-1 cells. RNA was collected from THP-1 cells after treatment with HIV-1 gp120_{SF162} (1 nM), LPS (1 μ g/ml), or 0.001% BSA-vehicle (Control) for 4 h or 24 h, with or without 15 min pretreatment of 10 μ M SB203580. RNA was reverse transcribed into cDNA and then assayed using Illumina HumanHT-12 v4 Expression BeadChip Kits. Data from microarray were further analyzed using GeneSpring platform for fold change between treatments and ANOVA was performed to test significance. Genes included here were those that are significantly different from control after 4 h SB203580 treatment ($p < 0.05$; Fold Change (FC) > 5x).

Table 4.2 Select genes differentially regulated by SB203580 alone at 24 hours in human monocytic THP-1 cells**

Gene Product	GenBank Accession No.	Symbol	Fold Change ¹	p value
Interleukin 1, beta	NM_000576	IL1B	5.51	0.004
Alpha-2-macroglobulin	NM_000014	A2M	4.82	0.001
Chemokine (C-C motif) ligand 3-like 3	NM_001001437	CCL3L3	3.40	0.027
Chemokine (C-C motif) ligand 5	NM_002985	CCL5	3.25	0.000
Chemokine (C-C motif) ligand 4-like 1	NM_001001435	CCL4L1	2.91	0.004

Table 4.2 continued:

Gene Product	GenBank Accession No.	Symbol	Fold Change ¹	p value
Chemokine (C-C motif) ligand 3	NM_002983	CCL3	2.56	0.007
TIMP metalloproteinase inhibitor 3	NM_000362	TIMP3	2.54	0.038
Serpin peptidase inhibitor, clade E (nexin, plasminogen activator inhibitor type 1), member 2	NM_006216	SERPINE2	2.51	0.001
Chemokine (C-C motif) ligand 5	NM_002985	CCL5	2.35	0.000
Plasminogen activator, urokinase receptor	NM_001005376	PLAUR	2.27	0.003
Chemokine (C-C motif) ligand 3-like 1	NM_021006	CCL3L1	2.20	0.011
Plasminogen activator, urokinase receptor	NM_002659	PLAUR	2.16	0.004
Tumor necrosis factor, alpha-induced protein 3	NM_006290	TNFAIP3	2.09	0.006
Dual specificity phosphatase 6	NM_022652	DUSP6	2.04	0.001
Chemokine (C-C motif) ligand 3-like 1	NM_021006	CCL3L1	2.04	0.005
Chemokine (C-C motif) ligand 3-like 1	NM_021006	CCL3L1	2.04	0.010
Tumor necrosis factor receptor superfamily, member 21	NM_014452	TNFRSF21	2.00	0.001
Chemokine (C-C motif) ligand 2	NM_002982	CCL2	1.99	0.006
Plasminogen activator, urokinase receptor	NM_001005376	PLAUR	1.97	0.000
Tripartite motif-containing 9	NM_015163	TRIM9	1.93	0.000
Interferon gamma receptor 1	NM_000416	IFNGR1	1.88	0.002
Colony stimulating factor 1 receptor	NM_005211	CSF1R	1.87	0.020
Fc fragment of IgE, high affinity I, receptor for; gamma polypeptide	NM_004106	FCER1G	1.85	0.003
Tripartite motif-containing 2	NM_015271	TRIM2	1.80	0.007
Serpin peptidase inhibitor, clade I (neuroserpin), member 1	NM_005025	SERPINI1	1.76	0.008
Prostaglandin-endoperoxide synthase 1 (prostaglandin G/H synthase and cyclooxygenase)	NM_080591	PTGS1	1.76	0.038
Chemokine (C-C motif) ligand 4-like 2	NM_207007	CCL4L2	1.75	0.000
Serpin peptidase inhibitor, clade B (ovalbumin), member 2	NM_002575	SERPINB2	-2.80	0.011
Serpin peptidase inhibitor, clade B (ovalbumin), member 2	NM_002575	SERPINB2	-2.72	0.002
Lysozyme (renal amyloidosis)	NM_000239	LYZ	-2.65	0.011
S100 calcium binding protein A8	NM_002964	S100A8	-2.24	0.023
TGFB1-induced anti-apoptotic factor 1	NM_004740	TIAF1	-2.05	0.003
Interferon regulatory factor 5	NM_002200	IRF5	-1.82	0.001
Mitogen-activated protein kinase kinase kinase kinase 1	NM_001042600	MAP4K1	-1.78	0.006
Leukotriene C4 synthase	NM_145867	LTC4S	-1.76	0.008

**Results are considered significant at fold change of ≥ 1.72 or -1.72 , with a p value of < 0.05 from control. ¹Fold change was determined by comparing raw data from SB203580 against control data.

Microarray results for a few of the genes were selected for validation using quantitative real time PCR (qRT-PCR). TNF α , PLAUR (Figure 4.9) and LTC $_4$ S mRNA (Figure 4.9 and 4.10) expression levels were analyzed after treatment with HIV-1 gp120 (1nM), LPS (1 μ g/ml) and/or SB203580 (10 μ M), or as indicated at 4 h. Using relative quantification analysis for qRT-PCR, we were able to confirm that the microarray results provided were accurate. The qRT-PCR results were similar in trend, if not exact, for all genes tested. Housekeeping gene human β -actin was used for quantification and calculations of relative amplification from control conditions, using the Δ CT method. TNF α mRNA expression was significantly increased from control (set at 1.0, see line in graphs) after 4 h incubation with SB203580 alone, LPS alone, or combination of SB+gp120 and SB+LPS (Figure 4.9A), similar to microarray results (inset, Figure 4.9A). Plasminogen activator urokinase receptor (PLAUR or uPAR) mRNA expression was significantly increased after 4 h treatment with SB203580 alone or combination of SB+gp120 (Figure 4.9C), similar to microarray data (inset, Figure 4.9C). We also investigated LTC $_4$ S mRNA expression, a gene that was unchanged at 4 h, but of interest at 24 h (Figure 4.10 and 4.11). The qRT-PCR data confirmed the microarray data (inset, Figure 4.9B), as LTC $_4$ S mRNA levels were not modified at 4 h (Figure 4.9B).

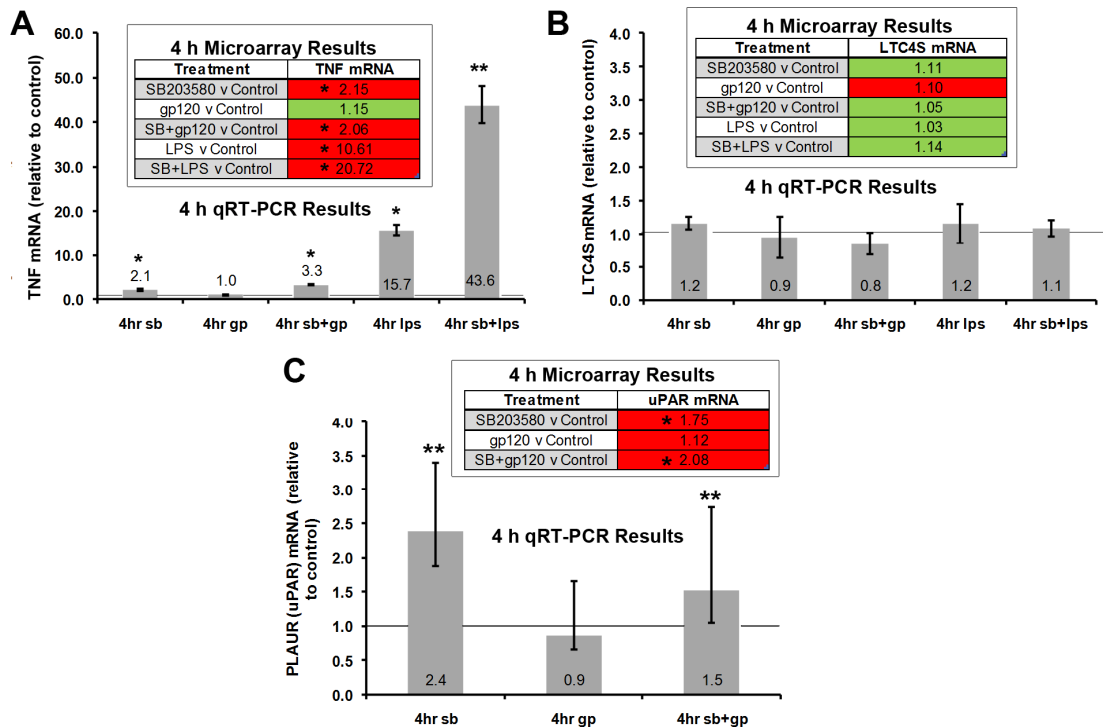


Figure 4.9 Validation of microarray results with qRT-PCR assay of TNF, LTC₄S and PLAUR at 4 h in human monocytic THP-1 cells. RNA was collected from THP-1 cells incubated with 1 nM HIV-1 gp120 or 1 µg/ml LPS for 24 h, with or without 15 min 10 µM SB203580 (SB) pretreatment. Expression of mRNA for TNF (A), LTC₄S (B) or PLAUR (C) were assessed via qRT-PCR to confirm selected results obtained from microarray data. Error bars represent the S.E.M. of three independent experiments for qRT-PCR results. Data was normalized against β-actin mRNA quantification. Microarray and qRT-PCR results for treated data versus untreated data were used for comparison and statistical analysis (modified Student's t-test). * = p < 0.05; ** = p < 0.01, compared to control values.

4.3.6. Cysteinyl leukotriene receptor antagonist, montelukast, protects neurons from gp120-induced neurotoxicity

Leukotrienes have been implicated in inflammation and neuronal injury. Cysteinyl leukotrienes are made by leukotriene C₄ synthase (LTC₄S) in most monocytic cells before being released into the extracellular space for further modification where they act upon their respective receptors, such as cysteinyl

leukotriene receptor 1 (CysLT1) for their function. One of the most interesting genes down-regulated by pretreatment p38 MAPK inhibitor SB203580 was part of the cysteinyl biosynthesis pathway, leukotriene C₄ synthase (LTC₄S). LTC₄S mRNA was reduced 1.76 fold by SB203580 alone after 24 h (bottom of Table 4.2). This gene is also significantly down-regulated by SB+gp120, LPS and SB+LPS as observed by microarray (Figure 4.10A). However, HIV-1 gp120 treatment did not affect the expression of the gene. We further tested whether the reduction in gene expression by p38 MAPK inhibition translated into reduction in protein levels. Using the p38 α MAPK siRNA techniques established in our previous studies (Medders et al., 2010), we were able to determine that as a consequence of the reduction in p38 MAPK expression there was a decrease in the protein levels of LTC₄S (Figure 4.10B). There also appeared to be a further reduction in LTC₄S protein after the addition of HIV-1 gp120 for 24 h with reduction in p38 MAPK (Figure 4.10B). The downstream substrate of p38 MAPK, HSP27, however was not affected by reduction in p38 MAPK (Figure 4.10B).

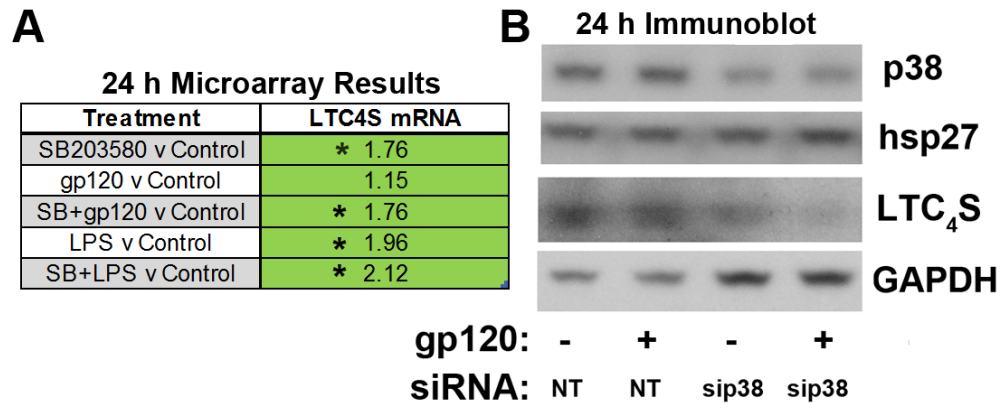


Figure 4.10 Inhibition of p38 MAPK activity reduces expression of LTC₄S in human monocytic THP-1 cells at 24 h. RNA was collected from THP-1 cells incubated with 1 nM HIV-1 gp120 or 1 μg/ml LPS for 24 h, with or without 15 min 10 μM SB203580 (SB) pretreatment. LTC₄S mRNA expression was significantly reduced from control by SB203580, LPS, or combination of SB and LPS (SB+LPS) or SB+gp120 (A). Alternatively, THP-1 cells were nucleofected with p38 MAPK siRNA and incubated with or without HIV-1 gp120 for 24 h. Immunoblot results showed that p38 MAPK siRNA reduced protein levels of p38 MAPK and LTC₄S (B). Microarray results for treated raw data versus untreated raw data were used for comparison and statistical analysis (modified Student's t-test). * = $p < 0.05$ compared to control values at 1.00.

Results from our previous experiment implicated the cysteinyl leukotriene biosynthesis pathway in a possible neurotoxic mechanism of HIV-1 gp120 (Figure 4.10). An increase in cysteinyl leukotriene receptor expression localized to neurons has also been reported to play a role in hypoxic brain injury (Ding et al., 2006; Zhang et al., 2006). Therefore, we next sought to determine if the addition of the cysteinyl leukotriene receptor antagonist might ameliorate the reduction in neuronal survival observed due to HIV-1 gp120 neurotoxicity. Montelukast (Singulair®), a specific cysteinyl leukotriene receptor 1 (CysLT1) antagonist (1 μM), was added to microglia-depleted cultures 30 min prior to incubation for 3 d with conditioned media from THP-1 cells treated with or without HIV-1 gp120 for 24 h, similar to schematic diagram shown in Figure 4.3. Pretreatment with montelukast was able to abrogate the

neuronal injury observed after treatment with neurotoxic THP-1 conditioned media (THP1 gp120 CM) (Figure 4.11).

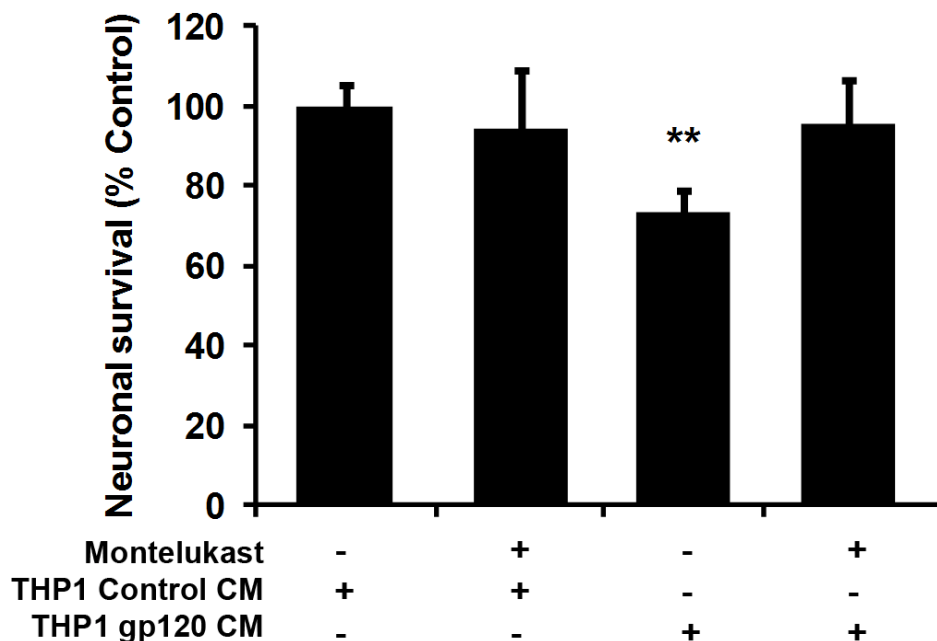


Figure 4.11 Montelukast prevents gp120-induced neurotoxicity from human monocytic THP-1 cells. Conditioned media (CM) was collected from THP-1 cells treated with HIV-1 gp120_{SF162} (1 nM) or 0.001% BSA-vehicle (Control) for 4 d. Microglia-depleted cerebrocortical cells were then pre-treated with 1 μ M montelukast for 30 min prior to incubation with THP-1 CM for 3 d and evaluated for survival. Neuronal survival was assessed using fluorescence microscopy after fixation, permeabilization and immunolabeling of neurons for MAP-2 in combination with nuclear DNA staining by H33342. Values obtained from THP-1 Control CM-treated cerebrocortical cells were used to compare neuronal survival by all other treatments, and set as baseline of 100%. Error bars represent the S.E.M. of three independent experiments. ** = $p < 0.01$ compared to control values (ANOVA with Fisher's PLSD post hoc test).

4.4. DISCUSSION

The present study provided evidence that HIV-1 gp120-induced neurotoxicity differs from LPS-induced neurotoxicity through dependence on p38 MAPK activity. Structural components of HIV-1 and Gram-negative bacteria, such as gp120 and

lipopolysaccharide (LPS), have been shown to be profoundly involved in the pathogenesis of inflammatory disorders and neurodegenerative diseases, such as HIV-associated neurocognitive disorders (HAND). This pathology has been linked primarily to the presence and activation of macrophages and other monocytic cells. HIV-1 gp120 interacts with CD4 and the viral coreceptors, CCR5 and/or CXCR4, found on the surface of monocytes/macrophages and has been shown to stimulate intracellular signaling and neurotoxicity (Cheung et al., 2008; Choi et al., 2007; Del Corno et al., 2001; Fantuzzi et al., 2008; Hesselgesser et al., 1998; Kaul et al., 1999; Kaul et al., 2007; Kitai et al., 2000; Medders et al., 2010; Meucci et al., 1998; O'Donnell et al., 2006; Ohagen et al., 1999; Porcheray et al., 2006; Singh et al., 2005; Zheng et al., 1999). The bacterial endotoxin LPS interacts with toll-like receptors, mostly TLR4, on the surface of many different cell types and has been shown to be responsible for overstimulation of the immune system (sepsis) and microglia-mediated neurotoxicity (Kim et al., 2000). In agreement with Kim et al., our current study supplies evidence that the presence of monocytic cells is required for LPS-induced neurotoxicity, similar to HIV-1 gp120 (this study and Kaul et al., 1999).

Previously, we and others showed that stress-activated p38 MAPK may play a central role in macrophage-mediated gp120-induced neurotoxicity (Kaul et al., 1999; Kaul et al., 2007; Medders et al., 2010; Perfettini et al., 2005). The present study provided further evidence that both HIV-1 gp120 and LPS were able to robustly activate p38 MAPK in monocytic cells over a 24 h time course. Furthermore, one of the downstream substrates of p38 MAPK, HSP27, and an upstream p38 MAPK regulator TAB1 were found in a complex with activated p38 MAPK at basal levels

and after treatment with HIV-1 gp120 or LPS. Many have reported that HSP27 is primarily a substrate of p38 MAPK activity. Our current study supported this, as HSP27 was associated with p38 MAPK. In addition, HSP27 was phosphorylated at 5 and 30 min by HIV-1 gp120 or 30 min by LPS; and this phosphorylation was significantly inhibited by the p38 MAPK inhibitor SB203580, a specific inhibitor of p38 α / β MAPK activity. TAB1 has been shown to be involved in the non-canonical activation of p38 MAPK, via autophosphorylation (Kang et al, 2006). Interestingly, Kang et al. showed that TAB1 only associates with the alpha isoform of p38 MAPK and not the beta isoform. Since activated p38 MAPK in our study interacted with TAB1, this suggested that the main isoform activated in monocytic cells by HIV-1 gp120 or LPS was p38 α MAPK, which further supported the usage of p38 α MAPK siRNA in our previous study (Medders et al., 2010) and in the current study as well.

Activation of p38 MAPK in microglia or macrophages has also been implicated in LPS-induced neurotoxicity (Culbert et al., 2006). In fact, Culbert et al. reported that microglia from MK2- (a downstream substrate of p38 MAPK) deficient mice protected neurons from LPS-induced neurotoxicity. However, the present study provides evidence that p38 MAPK and its activity are essential only for the neurotoxic phenotype of HIV-1 gp120-exposed macrophages and not for LPS-induced neurotoxicity. The disagreement between their study and ours could be due to the fact that Culbert et al. co-cultured MK2-deficient microglia with cortical neurons containing astrocytes. Our system isolated the monocytic cells or producers of neurotoxins from the cultures containing only astrocytes and neurons. A direct interaction between microglia and astrocytes may be required to prevent the release of

neurotoxins after inhibition of p38 MAPK activity, perhaps via a feedback mechanism. Alternatively, LPS also stimulated JNK activity in our monocytic cell model while HIV-1 gp120 did not. Inhibition of JNK activity alone or both kinases may be required to prevent LPS-induced neurotoxicity in our system, whereas HIV-1 gp120 only requires aberrant p38 MAPK activity. Dependence of LPS-neurotoxicity on both p38 MAPK and JNK has been supported by previous groups (Zeng et al., 2010). Further investigations are required to answer these queries. Although LPS and HIV-1 gp120 differed in their reliance on p38 MAPK for induction of neurotoxicity, we used LPS in the rest of our experiments as a comparative neuroinflammatory model.

Activation of p38 MAPK in macrophages by HIV-1 gp120 has been reported by several groups (Cheung et al., 2008; Fantuzzi et al., 2008; Lee et al., 2005; Yi et al., 2004). These same groups found that R5-preferring HIV-1 gp120 (JRFL) was able to induce the release of proinflammatory cytokines such as IL-1 β and TNF α from macrophages, which were reduced by p38 MAPK inhibition; and proposed that these cytokines may be potential mediators of neurotoxicity. However, our studies indicated that R5-preferring HIV-1 gp120_{SF162} did not significantly induce the expression of any cytokine or chemokine from the macrophages using bead-based multiplex assays. This difference is likely due to the fact that our group utilized 200 pM–1nM concentrations of R5 gp120 whereas the other studies used 10-100 times this dose (20 nM on average). Cheung et al. and Lee et al. performed dose-dependent studies on HIV-1 gp120-induced cytokine expression and only observed increased cytokine production when \geq 20 nM HIV-1 gp120 was used. This might be the case for our studies as well,

but important to note is that our more physiological, lower concentrations of HIV-1 gp120 are well established in causing significant neurotoxicity (Kaul et al., 1999; Kaul et al., 2007; Medders et al., 2010).

The induction of pro-inflammatory cytokine or chemokine production from macrophages has been linked to p38 α MAPK activation in previous studies (Kang et al., 2006). Activation of p38 MAPK was increased in HIV-1 gp120 treated monocytic cells, but did not increase cytokine or chemokine production. Paradoxically, the suppression of p38 MAPK activity in monocytic cells via pharmacological inhibitor SB203580, and SB203580 and HIV-1 gp120 (SB+gp120), were able to significantly increase the production of several cytokines, chemokines and growth factors shown in this study by microarray and bead-based multiplex arrays. Importantly, SB203580 pretreatment reduced HIV-1 gp120 neurotoxicity and SB203580 alone did not reduce neuronal survival, further supporting a role for p38 MAPK in HIV-1 gp120-induced neurotoxin production. This suggests that the inflammatory cytokine and chemokine production observed after p38 MAPK inhibition was not associated with neurotoxicity.

However, platelet-derived growth factor (PDGF-A/A) was found to be increased after SB203580 or SB+gp120 stimulation at 24 h and 4 d. PDGF has been implicated as a potential neuroprotective growth factor in HIV-1 associated neuronal injury and more specifically rescued neurons from HIV-1 gp120-mediated neurotoxicity (Peng et al., 2008). Further studies are required to validate the potential protective role PDGF may play after inhibition of p38 MAPK in HIV-1 gp120-induced neurotoxicity. Furthermore, increased beta chemokine release (CCL4, CCL3

and CCL5), the natural ligands for CCR5, by SB203580 alone may confer protection from HIV-1 gp120-induced neurotoxicity. However, the concentrations observed were well below previously shown protective levels (Kaul et al., 1999; Meucci et al., 1998). This does not rule out that a combination of protective factors such as PDGF and beta chemokines stimulated by p38 MAPK inhibition could be responsible for prevention of HIV-1 gp120-induced neurotoxicity.

Of note, the levels of cytokines or chemokines produced by SB203580 were significantly lower than levels produced by LPS alone or combination of SB+LPS in our study. Interestingly, other studies have shown that deletion of p38 α MAPK in macrophage cells failed to prevent the cells' reaction to LPS, except the induction of TNF α (Kang et al., 2008). Since p38 MAPK inhibition did not reduce LPS-induced neurotoxicity, we concluded that the significantly higher concentrations of pro-inflammatory cytokines and chemokines may play a neurotoxic role after LPS stimulation of monocytic cells.

Inhibition of p38 MAPK activity in monocytes sufficed to reduce HIV-1 gp120 neurotoxicity either by pharmacological inhibitor, p38 α siRNA knockdown (Medders et al., 2010) or heterologous overexpression of dominant negative p38 α MAPK mutant (Medders et al., 2010). Therefore, we inspected the differential gene expression for potential protective mechanisms induced by SB203580 alone or in combination with HIV-1 gp120. One gene, leukotriene C₄ synthase (LTC₄S), was significantly reduced in monocytes after treatment with SB203580 alone or combination of SB+gp120, and unchanged after HIV-1 gp120 alone, after 24 h. Leukotrienes are lipid mediators of inflammation and metabolites of arachidonic acid, a thoroughly investigated

neurotoxin, and have neurotoxic properties themselves which have been implicated in HIV-1 associated neurodegeneration (Basselin et al., 2010). Other groups have linked activation of p38 MAPK to leukotriene biosynthesis from monocytic cells with the potential for neuronal injury (Okubo et al., 2010; Werz et al., 2000). LTC₄S is involved in the conversion of LTA₄ into LTC₄ within monocytes, which is released from cells and can be further converted into LTCD₄ and LTE₄, collectively called cysteinyl leukotrienes (cysLT), all which have been implicated in mediating neuronal injury (Ding et al., 2006; Lecca et al. 2008; Zhang et al., 2006). Our study is the first to show that expression of LTC₄S, the key enzyme required for cysLT biosynthesis, is down-regulated by p38 MAPK inhibition, both at the mRNA and protein level. Importantly, an increase in cysLT receptor expression has been reported in injured neurons within the brain and addition of cysLT receptor antagonists (pranlukast and montelukast) protected neurons from injury (Ding et al., 2006; Yu et al., 2005; Zhang et al., 2006). In support of this research, our study showed that inhibition of cysLT receptor 1 (CysLT1) with the specific antagonist montelukast in neuronal cultures protected against HIV-1 gp120-induced neurotoxicity.

LPS also decreased (2X FC) the expression of LTC₄S mRNA in the monocytes after 24 h, which has been previously shown by other groups (Serio et al., 2003). However, this was accompanied by the highly increased expression of ALOX5 (> 5X FC) which is the upstream activator of LT biosynthesis (data not shown). ALOX5 up-regulation was not witnessed in SB203580-treated monocytic cells, further supporting the role of p38 MAPK activity in cysLT biosynthesis and HIV-1 gp120-induced neurotoxicity.

Taken together, this study revealed that despite dependence on monocytic cells for the neurotoxicity of both LPS and HIV-1 gp120, these neurotoxic mechanisms may be mediated by completely different pathways and downstream soluble factors. Release of proinflammatory cytokines and other inflammatory mediators remain good candidates for LPS-induced neurotoxicity, which may be upregulated by the activation of both p38 MAPK and JNK. HIV-1 gp120-induced neurotoxicity, on other hand, did not produce significant amounts of proinflammatory cytokines or chemokines, but required p38 MAPK activation. This may increase the production of inflammatory cysteinyl leukotrienes from monocytes and cause neurotoxicity, as the blockade of cysLT receptors in neuronal cultures prevented neurotoxicity implicating HIV-1 gp120 and inflammatory leukotrienes in the neuropathogenesis of HAND.

4.5. ACKNOWLEDGEMENTS

We thank Dr. Pedro Aza-Blanc (Sanford-Burnham Medical Research Institute) for advice on the selection of siRNAs. We also thank Dr. Roy Williams (Sanford-Burnham Medical Research Institute) for his hard work and timely help with the microarray analyses. We also thank Dr. Kang Liu (Sanford-Burnham Medical Research Institute) for her help with RNA work and completion of microarray experiments. We also thank Dr. Bas Baaten for advice on bead-based multiplex arrays. We also thank Irene Catalan, Cari Cox, Cyrus De Rozieres, Melanie Hoefler, Ricky Maung, Natalia Sejbuk and Rebecca Ruf for technical assistance in Western blotting, tissue culture, and image analysis.

Chapter 4, in full, is currently being prepared for submission for publication; Medders KE and Kaul M (2010) Inhibition of p38 MAPK activity in monocytic cells: potential protective regulators of gp120-induced neurotoxicity. The dissertation author was the primary investigator and author of this material. The work was supported by National Institutes of Health R01 Grants NS050621 and MH087332.

CHAPTER 5

CONCLUSIONS AND FUTURE DIRECTIONS

HIV-associated neurocognitive disorders (HAND) affect a large percentage of patients currently living with HIV. The most common feature is the progressive reduction in cognitive function associated with viral load in the central nervous system (CNS). The most severe form of HAND called HIV-associated dementia (HAD) is characterized by life-changing cognitive impairments, neuroinflammation, alterations in synaptic density and degeneration of neuronal populations throughout the brain.

More recent studies in HIV patients point to increasing prevalence of HAND despite success in the periphery with combination antiretroviral therapies (cART). This could be due to the lack of CNS-penetrating cART regimens and/or due to early infiltration of infected and activated monocytes in the CNS, where a viral reservoir may be maintained. Monocytic cell populations, such as microglia and macrophages, are thought to be the principal regulators of neuroinflammation. Targeting these cells and further understanding HIV neuropathology may be a critical step in reducing neurocognitive impairments in HIV patients. The role of HIV-1 envelope protein gp120 has been well established as a potential activator of macrophage-mediated neurotoxicity in both transgenic and *in vitro* models of HAD. Activation of stress signaling such as p38 MAPK is also well-established as a mediator of macrophage activation and involved in HIV-1 gp120-induced neuronal death. However, to better

understand the molecular mechanisms involved in HIV-associated neurodegeneration and identify potential future therapies, further research is required to determine the precise signaling pathways and neurotoxins responsible for neurocognitive defects.

For this reason, the main objectives of this dissertation were to 1) investigate the cellular mechanisms of neuronal injury in *in vitro* models of HAND; 2) examine the role of HIV-1 gp120 in neurotoxicity within different brain cell populations; and 3) analyze the activation of stress-activated kinase p38 MAPK and its downstream targets in the mechanisms of HIV-1 gp120-mediated neurotoxicity.

To address these aims, I first explored the p38 MAPK stress-activated signaling pathways potentially involved in HIV-1 gp120-induced neurotoxicity, in both the neuronal and monocyte cell type (Chapter 3). Previous studies showed that the stress-related p38 MAPK can mediate gp120-induced neuronal death (Kaul et al., 1999; Kaul et al., 2007; Singh et al., 2005). Furthermore, activation of p38 MAPK has been observed after HIV-1 gp120 treatment in macrophages and has been implicated in HIV pathogenesis and the development of AIDS (Del Corno et al., 2001; Lee et al., 2003). Chapter 3 supplies evidence that p38 MAPK activity is essential to not only the reduction of neuronal survival by HIV-1 gp120, but also the neurotoxic phenotype of HIV-1 gp120-exposed microglia and macrophages. In addition, the increased activation of p38 MAPK in neurons and subsequent neuronal death after HIV-1 gp120 exposure are dependent on the presence of microglia. Therefore, Chapter 3 (Medders et al., 2010) is the first study to show that p38 MAPK in two different cell types may be responsible and necessary for HIV-1 gp120-induced neurotoxicity in a mixed glial-neuronal environment.

Results in Chapter 3 show that HIV-1 gp120-induced p38 MAPK activity fluctuates over early time points with an overall increasing trend over a 24 h time course in mixed neuronal-glia cultures (Figure 3.1). Fluctuations in HIV-1 gp120-induced p38 MAPK may be due to tight regulation of its activity by phosphatases or the stimulation of neuronal p38 MAPK by release of neurotoxins over time. Interestingly, an early peak at 5 min in p38 MAPK activity does not correlate with neuronal death as it was not abolished by pre-treatment with CCL4 or by microglial depletion from mixed cultures (Figure 3.3 and 3.5), both factors which have been shown to inhibit HIV-1 gp120-induced neuronal loss (Kaul et al., 1999; Kaul et al., 2007). The question of why CCL4 was unable to block HIV-1 gp120-induced p38 MAPK at 5 min when incubated together also remains to be investigated, although that finding could be explained by direct competition at the receptor level or via heterologous desensitization (Kaul et al., 2007). Chapter 3 is also the first study to show the kinetics of CCL4-induced p38 MAPK activity in neuronal cultures over a 24 h time period and how it is different from HIV-1 gp120-induced p38 MAPK activity (Figure 3.3).

In addition, Chapter 3 provides evidence that phosphorylated p38 MAPK is localized in both neurons and microglia in mixed cerebrocortical cell cultures after HIV-1 gp120 treatments. Detection of active p38 MAPK via immunofluorescence in these cultures showed that microglia are activated by HIV-1 gp120 at early time points and may be sustained over 24 h, while activation in neurons occurred downstream of microglial activation perhaps after exposure to neurotoxins (Figure 3.4). Interestingly, the number of neurons positive for p38 MAPK did not differ with or without HIV-1

gp120, except at 24 h with a reduction in neuronal cell number indicating cell death. However, activation of p38 MAPK at 24 h in surviving neurons treated with HIV-1 gp120 or neurotoxic media from HIV-1 gp120-treated monocytes may be due to an adaptation of the remaining, surviving neurons to neurotoxic insult. Of note, a significant amount of neuronal loss occurred after addition of HIV-1 gp120-induced neurotoxins released from human monocytic THP-1 cells at 24 h as shown in Figure 3.6 and 3.8. Further studies are required to elucidate these potential mechanisms.

Other groups have shown that HIV-1 gp120 triggers p38 MAPK activation in macrophages and monocytes, which can enter in the brain soon after HIV infection and presumably contribute to the development of HAND (Del Corno et al., 2001; Lee et al., 2008). In concurrence with these previous studies, HIV-1 gp120 elicited p38 MAPK activation in rat microglia and in our model for microglia, THP-1 cells (Figure 3.6) and primary human monocyte-derived macrophages (MDM) (Figure 3.7). In addition, these monocytic cells produced significant neurotoxicity upon treatment with HIV-1 gp120 for 24 h to 4 d. Furthermore, suppressing p38 MAPK activity in the monocytic cells via the dominant-negative inactive p38 MAPK mutant or knockdown of p38 MAPK siRNA caused a significant reduction in neurotoxicity (Figure 3.6, 3.7 and 3.8). Therefore, Chapter 3 was able to show that p38 MAPK signaling plays a critical role in monocytes for HIV-1 gp120-induced neurotoxicity. Results from Chapter 3 also supports the notion that THP-1 cells are a suitable model for microglia or macrophages, based on similar signaling and neurotoxin production from primary human MDM and THP-1 cells.

As evidenced by addition of HIV-1 gp120 to microglia-depleted cultures directly and/or spiked in control monocyte media, direct neuronal interaction with HIV-1 gp120 did not cause significant neuronal death. Furthermore, chemokine receptor deficient mouse neuronal cultures which are resistant to HIV-1 gp120-induced toxicity (Kaul et al., 2007), were made sensitive to HIV-1 gp120 only upon the addition of THP-1 cells, which express the HIV coreceptors. Therefore, results in Chapter 3 support the theory that HIV-1 gp120 neurotoxicity is through indirect effects via release of neurotoxins from monocytes.

On the other hand, inhibition of p38 MAPK in cultures containing neurons and astrocytes prior to the addition of neurotoxic conditioned media from HIV-1 gp120-activated mononuclear cells prevented neuronal apoptosis as shown in Figure 3.9. Thus, inhibition of p38 MAPK signaling in neurons may provide a therapeutic target for prevention of further neuronal damage caused by HIV-1 gp120-induced neurotoxins.

Importantly, results in Chapter 3 determined that the blockade of p38 MAPK in monocytes, the cell type productively infected by HIV, prevented the indirect neurotoxicity of HIV-1 gp120. Therefore, further investigation into the mechanism of p38 MAPK-dependent, monocyte-mediated HIV-1 gp120 neurotoxicity was performed in Chapter 4.

Several other studies have linked the production of pro-inflammatory cytokines by monocytes and activation of p38 MAPK as likely mediators of HIV-1 gp120-induced neurotoxicity (Cheung et al., 2008; Fantuzzi et al., 2008; Lee et al., 2005). However, results from Chapter 4 show evidence that neurotoxic levels of HIV-1

gp120 do not elicit the expression or production of pro-inflammatory cytokines or chemokines from monocytes (Figure 4.5 and 4.7). These results differ most likely due to the fact that the other groups used 10-20 times the concentration of viral envelope protein used for the present studies. Importantly, the lower concentrations used in Chapter 3 and 4 produce neurotoxins from monocytes and activate p38 MAPK signaling required for neurotoxicity.

Results in Chapter 4 show that bacterial endotoxin lipopolysaccharide (LPS)-induced neurotoxicity also requires the presence of monocytes (microglia) (Figure 4.1) and also activates p38 MAPK signaling (Figure 4.2 and 4.3). However, different from HIV-1 gp120, LPS-induced neurotoxicity did not require p38 MAPK activity (Figure 4.4). In fact, LPS may require the activity of both p38 MAPK and JNK or JNK alone, as stress kinase JNK activation was induced by LPS, but not HIV-1 gp120 in monocytes. In addition, the robust production of pro-inflammatory cytokines after exposure to LPS (Figure 4.6 and 4.7) may play a role in neuronal injury.

Inhibition of p38 MAPK in monocytes also stimulated the release of many factors including pro-inflammatory cytokines, chemokines and growth factors. The concentrations of these proteins, however, were significantly lower than those stimulated by LPS. Thus, further analysis was performed to identify potential neurotoxic factors stimulated by HIV-1 gp120 that may be modulated by p38 MAPK inhibition.

Microarray analysis revealed a potential regulatory mechanism of basal p38 MAPK activity in monocytes. Upon inhibition of kinase activity, several genes were found to be differentially regulated (Figure 4.8 and Table 4.2). For example, LTC₄S

was reduced after treatment with the specific p38 MAPK inhibitor SB203580 or in combination with HIV-1 gp120 (Figure 4.10). The LTC₄S gene encodes for cysteinyl leukotriene C₄ synthase which participates in the biosynthesis of leukotrienes which are released from cells and are considered inflammatory mediators that can enhance neuronal damage. Furthermore, p38 MAPK knockdown with siRNA reduced the amount of LTC₄S protein with or without HIV-1 gp120 treatment (Figure 4.10).

To support a role for leukotrienes in HIV-1 gp120-induced neurotoxicity, neuronal cultures were treated with the cysteinyl leukotriene receptor-1 antagonist montelukast prior to addition of HIV-1 gp120-induced mononuclear neurotoxins. Blockade of the leukotriene receptor prevented neuronal loss (Figure 4.11). Thus, Chapter 4 provided evidence that inhibition of p38 MAPK in monocytes may prevent HIV-1 gp120 neurotoxicity either by decreasing the availability of specific enzymes required for neurotoxin production or by increasing the expression of potential protective factors, or by a combination of both effects.

Many other factors remain to be investigated that could participate in or ameliorate the neurotoxicity of HIV-1 gp120 (Figure 5.1). Further studies into the potential involvement of leukotrienes in HIV-1 gp120-induced neurotoxicity are warranted. For instance, measurement of leukotrienes in the HIV-1 gp120-induced neurotoxic supernatants could be performed, with or without p38 MAPK inhibition. Furthermore, up-regulation of cysteinyl leukotriene receptors in brain injury could also be studied. Since treatment with cysteinyl leukotriene receptor antagonist prevented HIV-1 gp120 neurotoxic insult, brains from the *in vivo* mouse model for HIV

neuropathology (gp120tg) could be analyzed for receptor expression, more specifically in neurons.

Additionally, an increase in the production of platelet derived growth factor (PDGF) after p38 MAPK inhibition in monocytes that was reported here in Chapter 4 results section may also contribute to the neuroprotective mechanism of SB203580 in HIV-1 gp120-induced neurotoxicity. Recent studies have shown that PDGF was able to prevent neuronal injury after HIV-1 gp120 treatment, and that HIV-1 gp120 reduced the expression of PDGF in neurons (Peng et al., 2008). Therefore, further studies could be performed to quantify PDGF expression in neurons exposed to HIV-1 gp120 neurotoxins and to determine if the amount of PDGF released from SB203580-treated monocytes and macrophages suffices to confer protection from HIV-1 gp120-induced neurotoxicity.

The matrix metalloproteinase (MMP) pathway has been implicated in HIV-1 gp120-induced neuronal death, particularly the activity of MMP9 (Misse et al., 2001). Misse et al. showed that p38 MAPK inhibition reduced MMP9 expression. Out of the several genes that were differentially regulated by p38 MAPK inhibition alone in monocytes (Table 4.2 and Appendix Table 6.2 and 6.3), tissue inhibitor of metalloproteinases (TIMP3) was upregulated by SB203580 alone (>2.5X FC) and in combination with HIV-1 gp120 (data not shown). TIMP3 is a known inhibitor of MMP2 and MMP9 activity (Murphy et al., 1999) and has been implicated in negative regulation of cytokines in response to LPS (Smookler et al., 2006). Interestingly, TIMP3 mRNA was reduced more than 4 fold in LPS-treated monocytes and more than 10 fold down with SB+LPS-treated monocytes. Taken together, my study validated

future experiments investigating the MMP pathway as a potential mediator of p38 MAPK-dependent HIV-1 gp120-induced neurotoxicity and p38 MAPK-independent LPS-induced neurotoxicity.

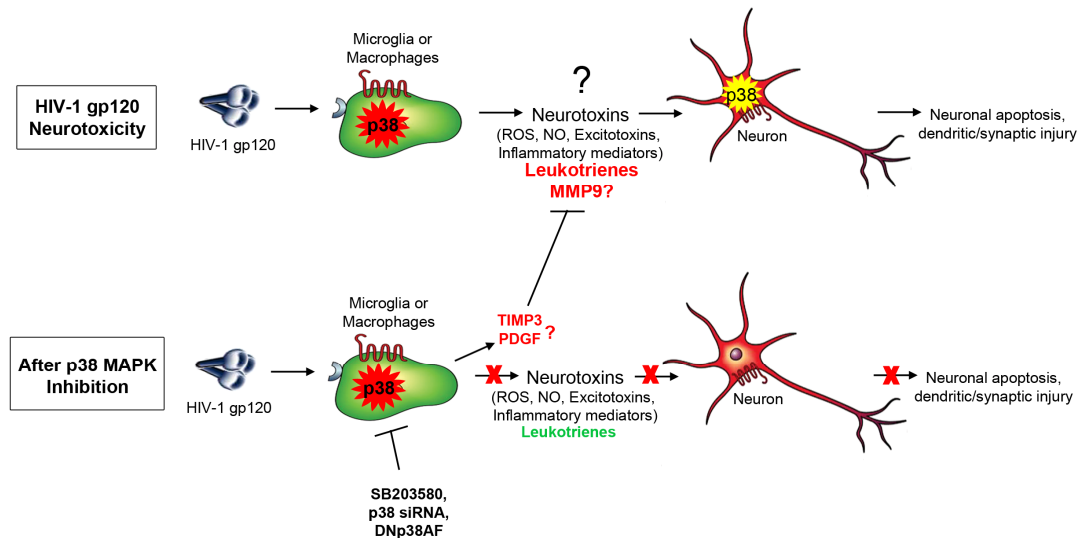


Figure 5.1 Schematic diagram of the potential mechanism of HIV-1 gp120-induced neurotoxicity and the potential mechanism of p38 MAPK inhibition of HIV-1 gp120-induced neurotoxicity. HIV-1 gp120 can activate p38 MAPK in monocytic cells (microglia/macrophages) and release neurotoxins, possibly leukotrienes, MMP9 and/or excitatory amino acids; which activate p38 MAPK in neurons and subsequent neuronal death. After p38 MAPK inhibition in monocytes, HIV-1 gp120 no longer produces sufficient amounts of neurotoxins, such as leukotrienes. Inhibition of p38 MAPK may also increase the release of tissue inhibitor of metalloproteinase-3 (TIMP3) and/or neurotrophic factor platelet derived growth factor (PDGF) further protecting neurons from HIV-1 gp120-induced neurotoxicity. Red-lettered words represent increased expression, while green-lettered words represent decreased expression.

CHAPTER 6

APPENDIX

Table 6.1 Full list of genes differentially regulated by HIV-1 gp120-treated versus vehicle-treated human monocytic THP-1 cells**

Incubation Time	Gene Product	GenBank Accession No.	Symbol	Fold Change ¹	p value
4 hours	NADH dehydrogenase (ubiquinone) 1 alpha subcomplex, 10	NM_004544	NDUFA10	1.50	0.077
	RER1 retention in endoplasmic reticulum 1 homolog	NM_00703	RER1	1.48	0.089
	G protein-coupled receptor 1	NM_005279	GPR1	1.47	0.0659
	FCF1 small subunit (SSU) processome component homolog	NM_015962	FCF1	1.46	0.089
	Amyloid beta (A4) precursor-like protein 2	NM_001642	APLP2	1.39	0.076
	Kelch-like ECH-associated protein 1	NM_012289	KEAP1	1.38	0.050
	TRM2 tRNA methyltransferase 2 homolog B	NM_024917	TRMT2B	1.38	0.088
	Golgi-specific brefeldin A resistant guanine nucleotide exchange factor 1	NM_004193	GBF1	1.38	0.050
	Upstream transcription factor 2, c-fos interacting	NM_207291	USF2	1.37	0.024
	RNA binding motif protein 38	NM_183425	RBM38	1.37	0.097
	TAO kinase 1	NM_020791	TAOK1	-1.67	0.014
	Zinc finger protein 121	NM_001008727	ZNF121	-1.59	0.057
	TAF15 RNA polymerase II, TATA box binding protein (TBP)-associated factor	NM_139215	TAF15	-1.56	0.066
	DNA fragmentation factor, 45kDa, alpha polypeptide	NM_004401	DFFA	-1.49	0.006
	Protein phosphatase 1, regulatory (inhibitor) subunit 12B	NM_032103	PPP1R12B	-1.48	0.048
	Iron-responsive element binding protein 2	NM_004136	IREB2	-1.48	0.053

Table 6.1 continued:

Incubation Time	Gene Product	GenBank Accession No.	Symbol	Fold Change ¹	p value	
4 hours	Small nuclear ribonucleoprotein D3 polypeptide 18kDa Predicted: Nudix (nucleoside diphosphate linked moiety X)-type motif 19	NM_004175	SNRPD3	-1.47	0.067	
	Zinc finger protein 765	NM_001040185	ZNF765	-1.45	0.010	
	TIP41, TOR signaling pathway regulator-like	NM_152902	TIPRL	-1.43	0.032	
	U2AF homology motif (UHM) kinase 1	NM_175866	UHMK1	-1.43	0.021	
	Striatin, calmodulin binding protein 3	NM_014574	STRN3	-1.42	0.047	
	TSC22 domain family, member 2	NM_014779	TSC22D2	-1.42	0.018	
	Kelch-like 28	NM_017658	KLHL28	-1.41	0.091	
	Capping protein (actin filament) muscle Z-line, alpha 1	NM_006135	CAPZA1	-1.40	0.013	
	B-cell CLL/lymphoma 10	NM_003921	BCL10	-1.40	0.065	
	Phosphoinositide-3-kinase, class 2, alpha polypeptide	NM_002645	PIK3C2A	-1.37	0.059	
	Homo sapiens CDC42 small effector 1	NM_001038707	CDC42SE1	-1.37	0.071	
	SATB homeobox 2	NM_015265	SATB2	-1.37	0.035	
	24 hours	CDKN2A interacting protein N-terminal like	NM_080656	CDKN2AIPNL	1.74	0.099
		DEAD (Asp-Glu-Ala-Asp) box polypeptide 51	NM_175066	DDX51	1.63	0.070
		RAB1B, member RAS oncogene family	NP_112243	RAB1B	1.43	0.014
Protein phosphatase 2, regulatory subunit B', beta isoform		NM_006244	PPP2R5B	1.42	0.027	
Pellino homolog 3		NM_145065	PELI3	1.40	0.081	
ATP synthase, H ⁺ transporting, mitochondrial F1 complex, delta subunit		NM_001687	ATP5D	1.38	0.081	
ST6 N-acetylgalactosaminide alpha-2,6-sialyltransferase 4		NM_175039	ST6GALNAC4	1.38	0.068	

Table 6.1 continued:

Incubation Time	Gene Product	GenBank Accession No.	Symbol	Fold Change ¹	p value
24 hours	Synaptojanin 2 binding protein	NM_018373	SYNJ2BP	1.37	0.088
	Nuclear factor of activated T-cells, cytoplasmic, calcineurin-dependent 3	NM_173163	NFATC3	1.36	0.084
	Histone deacetylase 5 (HDAC5), transcript variant 1	NM_005474	HDAC5	1.36	0.067
	Golgi phosphoprotein 4	NM_014498	GOLPH4	1.36	0.088
	Tumor protein p53 binding protein, 2	NM_005426	TP53BP2	-1.67	0.041
	Peptidylprolyl isomerase D	NM_005038	PPID	-1.61	0.074
	Vacuolar protein sorting 26	NM_004896	VPS26	-1.54	0.078
	N-myc (and STAT) interactor	NM_004688	NMI	-1.48	0.098
	Translin-associated factor X	NM_005999	TSNAX	-1.48	0.093
	RAP1A, member of RAS oncogene family	NM_001010935	RAP1A	-1.41	0.035
	Acidic (leucine-rich) nuclear phosphoprotein 32 family, member A	NM_006305	ANP32A	-1.40	0.080
	Ribosomal protein SA	NM_001012321	RPSA	-1.39	0.080
	RAB11A, member RAS oncogene family	NM_004663	RAB11A	-1.38	0.077
	Dihydropyrimidine dehydrogenase	NM_000110	DPYD	-1.38	0.087
	Zinc finger protein 92	NM_007139	ZNF92	-1.36	0.073
	RRN3 RNA polymerase I transcription factor homolog	NM_018427	RRN3	-1.36	0.068
	Zinc finger protein 680	NM_178558	ZNF680	-1.36	0.070
	24-dehydrocholesterol reductase	NM_014762	DHCR24	-1.36	0.025

**Results are considered significant at fold change of ≥ 1.35 or -1.35 , with a p value of < 0.1 from control. ¹Fold change was determined by comparing raw data from HIV-1 gp120-treated against vehicle-control data.

Table 6.2 Genes differentially regulated by SB203580 alone at 4 hours in human monocytic THP-1 cells**

Gene Product	GenBank Accession No.	Symbol	Fold Change ¹	p value
Early growth response 1	NM_001964	EGR1	6.57	0.002
Interleukin 1, beta	NM_000576	IL1B	3.05	0.024
Tribbles homolog 3	NM_021158	TRIB3	2.60	0.008
G protein-coupled receptor 84	NM_020370	GPR84	2.48	0.002
Tumor necrosis factor (TNF superfamily, member 2)	NM_000594	TNF	2.15	0.009
Caprin family member 2	NM_001002259	CAPRIN2	2.15	0.021
Transcription factor AP-2 alpha (activating enhancer binding protein 2 alpha)	NM_001042425	TFAP2A	2.10	0.003
Plasminogen activator, urokinase receptor	NM_001005376	PLAUR	2.01	0.039
Growth differentiation factor 15	NM_004864	GDF15	2.01	0.027
RNA binding motif protein 38	NM_183425	RBM38	2.00	0.018
Transcription factor AP-2 alpha (activating enhancer binding protein 2 alpha)	NM_001032280	TFAP2A	1.98	0.022
Regulator of G-protein signalling 16	NM_002928	RGS16	1.92	0.007
Solute carrier family 2 (facilitated glucose transporter)	NM_006931	SLC2A3	1.85	0.000
Plasminogen activator, urokinase receptor	NM_002659	PLAUR	1.82	0.027
SLAM family member 8	NM_020125	SLAMF8	1.74	0.046
Sphingosine-1-phosphate receptor 3	NM_005226	S1PR3	1.74	0.034
Basic helix-loop-helix domain containing, class B, 2	NM_003670	BHLHB2	1.73	0.022
AXIN1 up-regulated 1	NM_033027	AXUD1	1.72	0.032
Cytochrome P450, family 1, subfamily B, polypeptide 1	NM_000104	CYP1B1	-2.06	0.040
2'-5'-oligoadenylate synthetase 2, 69/71kDa	NM_001032731	OAS2	-1.85	0.007
Purinergic receptor P2Y, G-protein coupled, 2	NM_002564	P2RY2	-1.83	0.038

**Results are considered significant at fold change of ≥ 1.72 or -1.72 , with a p value of < 0.05 from control. ¹Fold change was determined by comparing raw data from SB203580 against vehicle-control data.

Table 6.3 Full list of genes differentially regulated by SB203580 alone at 24 hours in human monocytic THP-1 cells**

Gene Product	GenBank Accession No.	Symbol	Fold Change ¹	p value
Epithelial membrane protein 1	NM_001423	EMP1	6.83	0.003
Interleukin 1, beta	NM_000576	IL1B	5.51	0.004
Alpha-2-macroglobulin	NM_000014	A2M	4.82	0.001

Table 6.3 continued:

Gene Product	GenBank Accession No.	Symbol	Fold Change ¹	p value
Pleckstrin homology-like domain, family A, member 1	NM_007350	PHLDA1	4.69	0.001
Growth differentiation factor 15	NM_004864	GDF15	4.20	0.000
Secreted phosphoprotein 1	NM_000582	SPP1	4.12	0.040
Early growth response 1	NM_001964	EGR1	3.75	0.013
CD209 molecule	NM_021155	CD209	3.56	0.000
v-maf musculoaponeurotic fibrosarcoma oncogene homolog B	NM_005461	MAFB	3.56	0.005
Chemokine (C-C motif) ligand 3-like 3	NM_001001437	CCL3L3	3.40	0.027
Neuropilin 1	NM_003873	NRP1	3.38	0.007
Ras and Rab interactor 2	NM_018993	RIN2	3.27	0.001
Chemokine (C-C motif) ligand 5	NM_002985	CCL5	3.25	0.000
Vasohibin 1	NM_014909	VASH1	3.17	0.000
CD83 molecule	NM_004233	CD83	3.16	0.003
Secreted phosphoprotein 1	NM_001040058	SPP1	3.12	0.048
Family with sequence similarity 129, member B	NM_022833	FAM129B	3.02	0.002
Interleukin 7 receptor	NM_002185	IL7R	3.00	0.002
Chemokine (C-C motif) ligand 4-like 1	NM_001001435	CCL4L1	2.91	0.004
Early growth response 2	NM_000399	EGR2	2.90	0.001
DNA-damage-inducible transcript 4-like	NM_145244	DDIT4L	2.86	0.007
PREDICTED: Interleukin 7 receptor	XM_937367	IL7R	2.84	0.009
Dickkopf homolog 2	NM_014421	DKK2	2.82	0.001
Solute carrier family 2 (facilitated glucose transporter), member 3	NM_006931	SLC2A3	2.72	0.011
Early growth response 3	NM_004430	EGR3	2.71	0.000
Transcription factor AP-2 alpha (activating enhancer binding protein 2 alpha)	NM_001042425	TFAP2A	2.68	0.003
Transcription factor AP-2 alpha (activating enhancer binding protein 2 alpha)	NM_001032280	TFAP2A	2.68	0.001
Collagen, type XXII, alpha 1	NM_152888	COL22A1	2.67	0.004
CD9 molecule	NM_001769	CD9	2.65	0.010
Serum/glucocorticoid regulated kinase	NM_005627	SGK	2.65	0.020
CD83 molecule	NM_001040280	CD83	2.63	0.007
Formin-like 2	NM_052905	FMNL2	2.59	0.001
Gardner-Rasheed feline sarcoma viral (v-fgr) oncogene homolog	NM_001042729	FGR	2.59	0.001
Chemokine (C-C motif) ligand 3	NM_002983	CCL3	2.56	0.007
TIMP metalloproteinase inhibitor 3	NM_000362	TIMP3	2.54	0.038
Serpin peptidase inhibitor, clade E (nexin, plasminogen activator inhibitor type 1), member 2	NM_006216	SERPINE2	2.51	0.001
CD44 molecule	NM_001001392	CD44	2.50	0.005
Protein tyrosine phosphatase, receptor type, E	NM_130435	PTPRE	2.48	0.004

Table 6.3 continued:

Gene Product	GenBank Accession No.	Symbol	Fold Change ¹	p value
PREDICTED: Meteorin, glial cell differentiation regulator-like	XM_941466	METRNL	2.48	0.000
SH3 domain and tetratricopeptide repeats 1	NM_018986	SH3TC1	2.45	0.003
PREDICTED: Similar to meteorin, glial cell differentiation regulator-like	XM_927769	LOC653506	2.45	0.002
CD44 molecule	NM_001001391	CD44	2.43	0.007
Anthrax toxin receptor 2	NM_058172	ANTXR2	2.42	0.000
Growth arrest-specific 7	NM_201433	GAS7	2.40	0.003
Serum/glucocorticoid regulated kinase 1	NM_005627	SGK1	2.39	0.030
Integrin, alpha X (complement component 3 receptor 4 subunit)	NM_000887	ITGAX	2.38	0.001
Cytochrome P450, family 19, subfamily A, polypeptide 1	NM_000103	CYP19A1	2.38	0.001
Chemokine (C-C motif) ligand 5	NM_002985	CCL5	2.35	0.000
Fc fragment of IgE, low affinity II, receptor for (CD23)	NM_002002	FCER2	2.35	0.022
Metastasis suppressor 1	NM_014751	MTSS1	2.32	0.003
Gardner-Rasheed feline sarcoma viral (v-fgr) oncogene homolog	NM_005248	FGR	2.32	0.000
Hepatitis A virus cellular receptor 2	NM_032782	HAVCR2	2.31	0.008
SH2B adaptor protein 3	NM_005475	SH2B3	2.30	0.001
Plasminogen activator, urokinase receptor	NM_001005376	PLAUR	2.27	0.003
Serum/glucocorticoid regulated kinase 1	NM_005627	SGK1	2.27	0.016
Egf-like module containing, mucin-like, hormone receptor-like 2	NM_152916	EMR2	2.27	0.008
Cytochrome P450, family 19, subfamily A, polypeptide 1	NM_031226	CYP19A1	2.24	0.000
Transmembrane protein 158	NM_015444	TMEM158	2.24	0.023
Dickkopf homolog 2	NM_014421	DKK2	2.24	0.000
Uridine phosphorylase 1	NM_003364	UPP1	2.21	0.001
GTP binding protein overexpressed in skeletal muscle	NM_181702	GEM	2.20	0.001
Transmembrane 4 L six family member 19	NM_138461	TM4SF19	2.20	0.027
Chemokine (C-C motif) ligand 3-like 1	NM_021006	CCL3L1	2.20	0.011
Cyclin-dependent kinase inhibitor 1A (p21, Cip1)	NM_000389	CDKN1A	2.19	0.000
Tyrosine phosphatase, receptor type, E	NM_130435	PTPRE	2.17	0.012
Meteorin, glial cell differentiation regulator-like	NM_001004431	METRNL	2.16	0.001
Plasminogen activator, urokinase receptor	NM_002659	PLAUR	2.16	0.004
Rho family GTPase 3	NM_005168	RND3	2.15	0.000
Ferritin, heavy polypeptide 1	NM_002032	FTH1	2.13	0.018
CD52 molecule	NM_001803	CD52	2.13	0.008
Solute carrier family 20 (phosphate transporter), member 1	NM_005415	SLC20A1	2.12	0.000

Table 6.3 continued:

Gene Product	GenBank Accession No.	Symbol	Fold Change ¹	p value
3'-phosphoadenosine 5'-phosphosulfate synthase 1	NM_005443	PAPSS1	2.11	0.029
Tumor necrosis factor, alpha-induced protein 3	NM_006290	TNFAIP3	2.09	0.006
Dual specificity phosphatase 6	NM_022652	DUSP6	2.04	0.001
HEG homolog 1	NM_020733	HEG1	2.04	0.011
Cyclin D1	NM_053056	CCND1	2.04	0.004
ST6 (alpha-N-acetyl-neuraminy-2,3-beta-galactosyl-1, 3)-N-acetylgalactosaminide alpha-2,6-sialyltransferase 3	NM_152996	ST6GALNA C3	2.04	0.013
Chemokine (C-C motif) ligand 3-like 1	NM_021006	CCL3L1	2.04	0.005
Chemokine (C-C motif) ligand 3-like 1	NM_021006	CCL3L1	2.04	0.010
Caprin family member 2	NM_001002259	CAPRIN2	2.03	0.001
Small cell adhesion glycoprotein	NM_001033873	SMAGP	2.01	0.000
Zinc finger and BTB domain containing 46	NM_025224	ZBTB46	2.00	0.007
PTK2 protein tyrosine kinase 2	NM_005607	PTK2	2.00	0.007
RAS p21 protein activator (GTPase activating protein) 1	NM_002890	RASA1	2.00	0.002
Netrin 1	NM_004822	NTN1	2.00	0.003
Tumor necrosis factor receptor superfamily, member 21	NM_014452	TNFRSF21	2.00	0.001
Chemokine (C-C motif) ligand 2	NM_002982	CCL2	1.99	0.006
Tribbles homolog 3	NM_021158	TRIB3	1.98	0.028
SLAM family member 8	NM_020125	SLAMF8	1.97	0.001
Neural precursor cell expressed, developmentally down-regulated 9	NM_006403	NEDD9	1.97	0.000
Phosphoprotein associated with glycosphingolipid microdomains 1	NM_018440	PAG1	1.97	0.000
Plasminogen activator, urokinase receptor	NM_001005376	PLAUR	1.97	0.000
ST8 alpha-N-acetyl-neuraminide alpha-2,8-sialyltransferase 4	NM_005668	ST8SIA4	1.94	0.003
Guanylate binding protein 2, interferon-inducible	NM_004120	GBP2	1.94	0.008
B-cell CLL/lymphoma 6 (zinc finger protein 51)	NM_001706	BCL6	1.94	0.004
Versican	NM_004385	VCAN	1.93	0.045
Tripartite motif-containing 9	NM_015163	TRIM9	1.93	0.000
SH3 domain binding glutamic acid-rich protein like 3	NM_031286	SH3BGRL3	1.93	0.010
Phosphoprotein associated with glycosphingolipid microdomains 1	NM_018440	PAG1	1.93	0.003
UL16 binding protein 2	NM_025217	ULBP2	1.92	0.006
PREDICTED: Similar to cytokine	XM_001133190	LOC728835	1.92	0.010
Potassium intermediate/small conductance calcium-activated channel, subfamily N, member 4	NM_002250	KCNN4	1.91	0.021

Table 6.3 continued:

Gene Product	GenBank Accession No.	Symbol	Fold Change ¹	p value
Purinergic receptor P2Y, G-protein coupled, 5	NM_005767	P2RY5	1.90	0.000
Transmembrane and tetratricopeptide repeat containing 1	NM_175861	TMTC1	1.89	0.000
Solute carrier family 35, member F2	NM_017515	SLC35F2	1.88	0.007
ATPase, Na ⁺ /K ⁺ transporting, beta 1 polypeptide	NM_001677	ATP1B1	1.88	0.002
Cat eye syndrome chromosome region, candidate 6	NM_031890	CECR6	1.88	0.001
Interferon gamma receptor 1	NM_000416	IFNGR1	1.88	0.002
Colony stimulating factor 1 receptor, formerly McDonough feline sarcoma viral (v-fms) oncogene homolog	NM_005211	CSF1R	1.87	0.020
Fc fragment of IgE, high affinity I, receptor for; gamma polypeptide	NM_004106	FCER1G	1.85	0.003
Proline rich 16	NM_016644	PRR16	1.85	0.003
3'-phosphoadenosine 5'-phosphosulfate synthase 1	NM_005443	PAPSS1	1.85	0.006
Aldo-keto reductase family 1, member C3 (3-alpha hydroxysteroid dehydrogenase, type II)	NM_003739	AKR1C3	1.85	0.003
Epstein-Barr virus induced 3	NM_005755	EBI3	1.83	0.020
PREDICTED: Meteorin, glial cell differentiation regulator-like	XM_941466	METRNL	1.83	0.001
Calcium channel, voltage-dependent, alpha 2/delta subunit 4	NM_172364	CACNA2D4	1.83	0.007
Aldo-keto reductase family 1, member C4 (chlordecone reductase; 3-alpha hydroxysteroid dehydrogenase, type I; dihydrodiol dehydrogenase 4)	NM_001818	AKR1C4	1.83	0.040
Pleckstrin homology-like domain, family A, member 1	NM_007350	PHLDA1	1.82	0.023
Family with sequence similarity 129, member B	NM_001035534	FAM129B	1.82	0.008
Kruppel-like factor 4 (gut)	NM_004235	KLF4	1.81	0.004
Protein phosphatase 1M (PP2C domain containing)	NM_144641	PPM1M	1.81	0.016
Rho guanine nucleotide exchange factor (GEF) 3	NM_019555	ARHGEF3	1.81	0.002
ATPase, Na ⁺ /K ⁺ transporting, beta 1 polypeptide	NM_001001787	ATP1B1	1.80	0.000
Integrin, alpha 6	NM_000210	ITGA6	1.80	0.006
Tripartite motif-containing 2	NM_015271	TRIM2	1.80	0.007
Adenosine A2b receptor	NM_000676	ADORA2B	1.79	0.020
Ankyrin repeat domain 28	NM_015199	ANKRD28	1.79	0.013
Copine II	NM_152727	CPNE2	1.78	0.002
Kruppel-like factor 6	NM_001008490	KLF6	1.78	0.002

Table 6.3 continued:

Gene Product	GenBank Accession No.	Symbol	Fold Change ¹	p value
Integrin, beta 5	NM_002213	ITGB5	1.78	0.035
Neuronal guanine nucleotide exchange factor	NM_019850	NGEF	1.77	0.017
ArfGAP with SH3 domain, ankyrin repeat and PH domain 1	NM_018482	ASAP1	1.77	0.006
Calponin 3, acidic	NM_001839	CNN3	1.77	0.008
Homer homolog 1	NM_004272	HOMER1	1.77	0.009
Sprouty homolog 4	NM_030964	SPRY4	1.77	0.001
GTP binding protein overexpressed in skeletal muscle	NM_181702	GEM	1.76	0.005
Serpin peptidase inhibitor, clade I (neuroserpin), member 1	NM_005025	SERPINI1	1.76	0.008
Integrin, beta 5	NM_002213	ITGB5	1.76	0.016
1-acylglycerol-3-phosphate O-acyltransferase 9	NM_032717	AGPAT9	1.76	0.039
Prostaglandin-endoperoxide synthase 1 (prostaglandin G/H synthase and cyclooxygenase)	NM_080591	PTGS1	1.76	0.038
Metastasis suppressor 1	NM_014751	MTSS1	1.76	0.006
CAP, adenylate cyclase-associated protein, 2	NM_006366	CAP2	1.76	0.003
Sprouty homolog 2	NM_005842	SPRY2	1.76	0.001
Triggering receptor expressed on myeloid cells 2	NM_018965	TREM2	1.76	0.000
Bridging integrator 2	NM_016293	BIN2	1.75	0.004
Basic helix-loop-helix domain containing, class B, 2	NM_003670	BHLHB2	1.75	0.041
RNA binding motif protein 47	NM_019027	RBM47	1.75	0.013
Chemokine (C-C motif) ligand 4-like 2	NM_207007	CCL4L2	1.75	0.000
Rho-related BTB domain containing 3	NM_014899	RHOBTB3	1.74	0.010
Tryptophanyl-tRNA synthetase	NM_173701	WARS	1.74	0.043
CD276 molecule	NM_001024736	CD276	1.74	0.012
Major facilitator superfamily domain containing 2	NM_032793	MFS2	1.73	0.005
Myelin basic protein	NM_001025090	MBP	1.73	0.018
Neurotensin receptor 1 (high affinity)	NM_002531	NTSR1	1.72	0.034
Signal sequence receptor, gamma (translocon-associated protein gamma)	NM_007107	SSR3	1.72	0.024
Membrane-spanning 4-domains, subfamily A, member 3 (hematopoietic cell-specific)	NM_006138	MS4A3	-3.07	0.001
Serpin peptidase inhibitor, clade B (ovalbumin), member 2	NM_002575	SERPINB2	-2.80	0.011
Serpin peptidase inhibitor, clade B (ovalbumin), member 2	NM_002575	SERPINB2	-2.72	0.002
Lysozyme (renal amyloidosis)	NM_000239	LYZ	-2.65	0.011
Napsin B aspartic peptidase pseudogene	NR_002798	NAPSB	-2.64	0.000
Proteinase 3	NM_002777	PRTN3	-2.60	0.004
Neurocalcin delta	NM_032041	NCALD	-2.51	0.012

Table 6.3 continued:

Gene Product	GenBank Accession No.	Symbol	Fold Change ¹	p value
Purinergic receptor P2Y, G-protein coupled, 2	NM_002564	P2RY2	-2.44	0.004
Neurocalcin delta	NM_001040626	NCALD	-2.42	0.009
DEP domain containing 6	NM_022783	DEPDC6	-2.30	0.016
S100 calcium binding protein A8	NM_002964	S100A8	-2.24	0.023
Myosin IG	NM_033054	MYO1G	-2.21	0.037
Coagulation factor XIII, A1 polypeptide	NM_000129	F13A1	-2.18	0.029
Arylformamidase	NM_001010982	AFMID	-2.18	0.009
Membrane-spanning 4-domains, subfamily A, member 6A	NM_022349	MS4A6A	-2.18	0.016
BCL2-interacting killer (apoptosis-inducing)	NM_001197	BIK	-2.17	0.002
Membrane-spanning 4-domains, subfamily A, member 3 (hematopoietic cell-specific)	NM_006138	MS4A3	-2.14	0.010
Iroquois homeobox 3	NM_024336	IRX3	-2.12	0.003
Tudor domain containing 7	NM_014290	TDRD7	-2.10	0.006
Monoxygenase, DBH-like 1	NM_015529	MOXD1	-2.06	0.035
TGFB1-induced anti-apoptotic factor 1	NM_004740	TIAF1	-2.05	0.003
B-cell CLL/lymphoma 11A (zinc finger protein)	NM_022893	BCL11A	-1.88	0.004
Membrane-spanning 4-domains, subfamily A, member 6A	NM_152851	MS4A6A	-1.86	0.028
DEP domain containing 6	NM_022783	DEPDC6	-1.84	0.003
MAX dimerization protein 4	NM_006454	MXD4	-1.83	0.002
Interferon regulatory factor 5	NM_002200	IRF5	-1.82	0.001
Telomerase reverse transcriptase	NM_003219	TERT	-1.81	0.023
Purinergic receptor P2Y, G-protein coupled, 2	NM_176071	P2RY2	-1.80	0.011
Endothelial PAS domain protein 1	NM_001430	EPAS1	-1.79	0.038
Zinc finger protein 296	NM_145288	ZNF296	-1.79	0.000
Ret proto-oncogene	NM_020975	RET	-1.78	0.010
Mitogen-activated protein kinase kinase kinase 1	NM_001042600	MAP4K1	-1.78	0.006
Ret proto-oncogene	NM_020630	RET	-1.78	0.000
Tropomodulin 1	NM_003275	TMOD1	-1.77	0.009
Napsin A aspartic peptidase	NM_004851	NAPSA	-1.77	0.009
Androgen-induced 1	NM_016108	AIG1	-1.77	0.000
Neural cell adhesion molecule 2	NM_004540	NCAM2	-1.76	0.001
Cytochrome P450, family 26, subfamily B, polypeptide 1	NM_019885	CYP26B1	-1.76	0.002
Leukotriene C4 synthase	NM_145867	LTC4S	-1.76	0.008
G protein-coupled receptor 160	NM_014373	GPR160	-1.74	0.000
Aldehyde dehydrogenase 2 family (mitochondrial)	NM_000690	ALDH2	-1.74	0.007

**Results are considered significant at fold change of ≥ 1.72 or -1.72 , with a p value of < 0.05 from control. ¹Fold change was determined by comparing raw data from SB203580 against vehicle-control data.

Table 6.4 Full list of genes differentially regulated by LPS versus SB+LPS at 4 and 24 hours in human monocytic THP-1 cells**

Incubation Time	Gene Product	GenBank Accession No.	Symbol	Fold Change ¹	p value
4 hours	Thrombospondin 1	NM_003246	THBS1	6.07	0.005
	Oxidized low density lipoprotein (lectin-like) receptor 1	NM_002543	OLR1	4.31	0.009
	EP300 interacting inhibitor of differentiation 3	NM_001008394	EID3	3.46	0.011
	Heme oxygenase (decycling) 1	NM_002133	HMOX1	3.29	0.037
	Cytochrome P450, family 1, subfamily B, polypeptide 1	NM_000104	CYP1B1	3.14	0.029
	Tumor necrosis factor (ligand) superfamily, member 10	NM_003810	TNFSF10	2.96	0.014
	Membrane-spanning 4-domains, subfamily A, member 7	NM_206938	MS4A7	2.72	0.010
	Oxidative stress induced growth inhibitor 1	NM_182980	OSGIN1	2.60	0.012
	Nicotinamide phosphoribosyltransferase	NM_005746	NAMPT	2.59	0.036
	Pleckstrin homology, Sec7 and coiled-coil domains, binding protein	NM_004288	PSCDBP	2.47	0.010
	Histone cluster 2, H2aa3	NM_003516	HIST2H2AA3	2.45	1E-04
	Fasciculation and elongation protein zeta 1 (zygin I)	NM_022549	FEZ1	2.40	0.046
	ER lipid raft associated 1	NM_006459	ERLIN1	2.32	0.013
	Zinc finger protein 366	NM_152625	ZNF366	2.32	0.027
	Snail homolog 2 (Drosophila)	NM_003068	SNAI2	2.23	0.034
	PR domain containing 1, with ZNF domain	NM_001198	PRDM1	2.20	0.002
	E1A binding protein p300	NM_001429	EP300	2.19	0.043
	PR domain containing 1, with ZNF domain	NM_001198	PRDM1	2.13	0.010
	Sialidase 4	NM_080741	NEU4	2.13	0.022
	Chemokine (C-C motif) ligand 24	NM_002991	CCL24	2.09	0.046
	KIAA1199	NM_018689	KIAA1199	2.09	0.023
	BCL2-like 11	NM_006538	BCL2L11	2.09	0.012
	R-spondin 3 homolog (Xenopus laevis)	NM_032784	RSPO3	2.05	0.038
	Chemokine ligand 10	NM_001565	CXCL10	2.04	0.028

Table 6.4 continued:

Incubation Time	Gene Product	GenBank Accession No.	Symbol	Fold Change ¹	p value
4 hours	Fasciculation and elongation protein zeta 1 (zygin I)	NM_022549	FEZ1	2.03	0.019
	H2.0-like homeobox	NM_021958	HLX	2.02	0.014
	Insulin-like growth factor binding protein 3	NM_001013398	IGFBP3	2.01	0.012
	Zinc fingers and homeoboxes 2	NM_014943	ZHX2	2.01	0.024
	Unkempt homolog (Drosophila)-like	NM_023076	UNKL	2.00	0.032
	Zinc fingers and homeoboxes 2	NM_014943	ZHX2	2.00	0.016
	Sterile alpha motif domain containing 4B	NM_018028	SAMD4B	1.99	0.025
	Ras-like without CAAX 1	NM_006912	RIT1	1.97	0.006
	SLAM family member 7	NM_021181	SLAMF7	1.94	0.037
	Chemokine (C-C motif) receptor 7	NM_001838	CCR7	1.92	0.001
	Solute carrier family 7, (cationic amino acid transporter, y+ system) member 11	NM_014331	SLC7A11	1.90	0.005
	Family with sequence similarity 70, member A	NM_017938	FAM70A	1.89	0.016
	Fasciculation and elongation protein zeta 1 (zygin I)	NM_022549	FEZ1	1.89	0.025
	MAF1 homolog (S. cerevisiae)	NM_032272	MAF1	1.88	0.044
	Dihydropyrimidinase-like 3	NM_001387	DPYSL3	1.88	0.021
	Thioredoxin reductase 1	NM_001093771	TXNRD1	1.87	0.041
	Bromodomain adjacent to zinc finger domain, 1A	NM_013448	BAZ1A	1.86	0.017
	PREDICTED: Sphingosine-1-phosphate phosphatase 2	XM_938742	SGPP2	1.85	0.046
	PREDICTED: Similar to histone H2A.o (H2A/o) (H2A.2) (H2a-615)	XM_928387	LOC653610	1.85	0.019
	Tubulin tyrosine ligase-like family, member 4	NM_014640	TTLL4	1.84	6E-05
	Rumor protein p53 inducible nuclear protein 2.	NM_021202	TP53INP2	1.84	0.034
	BAI1-associated protein 2-like 1	NM_018842	BAIAP2L1	1.83	0.033

Table 6.4 continued:

Incubation Time	Gene Product	GenBank Accession No.	Symbol	Fold Change ¹	p value
4 hours	Tight junction protein 2 (zona occludens 2)	NM_004817	TJP2	1.83	0.019
	BCL2-like 11 (apoptosis facilitator)	NM_207002	BCL2L11	1.81	0.020
	Quaking homolog, KH domain RNA binding (mouse)	NM_006775	QKI	1.80	0.046
	Interleukin enhancer binding factor 3, 90kDa	NM_012218	ILF3	1.80	0.031
	Paraspeckle component 1	NR_003272	PSPC1	1.80	0.028
	Transportin 1	NM_153188	TNPO1	1.79	0.020
	Human immunodeficiency virus type I enhancer binding protein 1	NM_002114	HIVEP1	1.78	0.030
	Kynureninase (L-kynurenine hydrolase)	NM_001032998	KYNU	1.78	0.023
	ATP-binding cassette, sub-family A (ABC1)	NM_080284	ABCA6	1.77	0.040
	LY6/PLAUR domain containing 1	NM_144586	LYPD1	1.76	0.045
	Interferon regulatory factor 2 binding protein 2	NM_182972	IRF2BP2	1.75	0.014
	Ornithine decarboxylase antizyme 2	NM_002537	OAZ2	1.74	0.034
	Insulin-like growth factor binding protein 3	NM_000598	IGFBP3	1.74	0.032
	Signal transducer and activator of transcription 1, 91kDa	NM_007315	STAT1	1.74	0.035
	Hydroxysteroid (11-beta) dehydrogenase 1	NM_181755	HSD11B1	1.73	0.036
	Nucleoporin 98kDa	NM_016320	NUP98	1.72	0.015
	LFNG O-fucosylpeptide 3-beta-N-acetylglucosaminyltransferase	NM_001040167	LFNG	-3.45	0.005
	Early growth response 1	NM_001964	EGR1	-3.41	0.024
	Pleckstrin homology, Sec7 and coiled-coil domains 4	NM_013385	PSCD4	-2.66	0.030
	Inositol 1,4,5-trisphosphate 3-kinase A	NM_002220	ITPKA	-2.38	0.006
Tribbles homolog 3 (Drosophila)	NM_021158	TRIB3	-2.33	0.033	
Cytohesin 4	NM_013385	CYTH4	-2.31	0.030	

Table 6.4 continued:

Incubation Time	Gene Product	GenBank Accession No.	Symbol	Fold Change ¹	p value
4 hours	Pleckstrin homology-like domain, family A, member 2	NM_003311	PHLDA2	-2.23	0.010
	Platelet-derived growth factor beta polypeptide (simian sarcoma viral (v-sis) oncogene homolog)	NM_002608	PDGFB	-2.19	0.029
	Solute carrier family 2 (facilitated glucose transporter), member 10	NM_030777	SLC2A10	-2.15	0.003
	Nninein (GSK3B interacting protein)	NM_020921	NIN	-2.08	0.043
	Transcription factor AP-2 alpha (activating enhancer binding protein 2 alpha)	NM_001032280	TFAP2A	-2.08	0.033
	LysM, putative peptidoglycan-binding, domain containing 2	NM_153374	LYSMD2	-2.05	0.019
	Family with sequence similarity 134, member B	NM_001034850	FAM134B	-2.04	0.032
	Neurotensin receptor 1 (high affinity)	NM_002531	NTSR1	-2.03	0.013
	Growth arrest and DNA-damage-inducible, alpha	NM_001924	GADD45A	-2.01	0.024
	Chemokine (C-C motif) ligand 2	NM_002982	CCL2	-1.99	0.042
	Tumor necrosis factor (TNF superfamily, member 2)	NM_000594.2	TNF	-1.95	0.014
	Rho guanine nucleotide exchange factor (GEF) 10	NM_014629	ARHGEF10	-1.93	0.033
	Myeloid-associated differentiation marker	NM_138373	MYADM	-1.93	1E-04
	Uridine phosphorylase 1	NM_003364	UPP1	-1.90	0.027
	Transforming growth factor, beta receptor II	NM_001024847	TGFBR2	-1.90	0.001
	Sorting nexin 10	NM_013322	SNX10	-1.85	0.012
	Interleukin 27 receptor, alpha	NM_004843	IL27RA	-1.85	0.042
	Prostaglandin-endoperoxide synthase 1 (prostaglandin G/H synthase and cyclooxygenase)	NM_080591	PTGS1	-1.83	0.034

Table 6.4 continued:

Incubation Time	Gene Product	GenBank Accession No.	Symbol	Fold Change ¹	p value
4 hours	Tryptophan rich basic protein	NM_004627	WRB	-1.82	0.009
	3'-phosphoadenosine 5'-phosphosulfate synthase 1	NM_005443	PAPSS1	-1.81	0.026
	Serum/glucocorticoid regulated kinase	NM_005627	SGK	-1.80	0.005
	Chemokine (C-X-C motif) receptor 7	NM_020311	CXCR7	-1.79	0.016
	Carbonic anhydrase II	NM_000067	CA2	-1.77	0.032
	Sema domain, immunoglobulin domain (Ig), transmembrane domain (TM) and short cytoplasmic domain, (semaphorin) 4D	NM_006378	SEMA4D	-1.76	0.033
	Basic helix-loop-helix domain containing, class B, 2	NM_003670	BHLHB2	-1.75	0.034
	tRNA splicing endonuclease 15 homolog (S. cerevisiae)	NM_001127394	TSEN15	-1.75	0.008
	Mitochondrial ribosomal protein L3	NM_007208	MRPL3	-1.74	0.010
	Family with sequence similarity 134, member B	NM_001034850	FAM134B	-1.74	0.031
	Histone deacetylase 4	NM_006037	HDAC4	-1.73	0.004
	Rhomboid 5 homolog 1 (Drosophila)	NM_022450	RHBDF1	-1.73	0.018
	KDEL (Lys-Asp-Glu-Leu) endoplasmic reticulum protein retention receptor 3	NM_006855	KDELR3	-1.72	0.021
24 hours	Interferon-induced protein 44-like	NM_006820	IFI44L	3.95	0.001
	Tryptophan 2,3-dioxygenase	NM_005651	TDO2	3.88	0.038
	Chemokine (C-X-C motif) ligand 13 (B-cell chemoattractant)	NM_006419	CXCL13	3.84	0.005
	ADAM-like, decysin 1	NM_014479	ADAMDEC1	3.76	0.002
	Chemokine (C-X-C motif) ligand 10	NM_001565	CXCL10	3.53	2E-04
	GTPase, IMAP family member 8	NM_175571	GIMAP8	3.50	0.045
	Interferon, alpha-inducible protein 27	NM_005532	IFI27	3.44	0.005

Table 6.4 continued:

Incubation Time	Gene Product	GenBank Accession No.	Symbol	Fold Change ¹	p value
24 hours	Interferon, gamma-inducible protein 30	NM_006332	IFI30	3.22	0.021
	Insulin-like growth factor binding protein 3	NM_000598	IGFBP3	3.01	0.049
	Aldehyde dehydrogenase 2 family (mitochondrial)	NM_000690	ALDH2	2.94	5E-05
	Interferon-induced protein with tetratricopeptide repeats 1	NM_001548	IFIT1	2.91	0.004
	S100 calcium binding protein A8	NM_002964	S100A8	2.87	0.007
	ADAM-like, decysin 1	NM_014479	ADAMDEC1	2.84	0.001
	Anthrax toxin receptor 1	NM_032208	ANTXR1	2.82	0.004
	Interferon induced transmembrane protein 1 (9-27)	NM_003641	IFITM1	2.80	0.005
	Sema domain, immunoglobulin domain (Ig), transmembrane domain (TM) and short cytoplasmic domain, (semaphorin) 4A	NM_022367	SEMA4A	2.73	0.002
	Insulin-like growth factor binding protein 3	NM_001013398	IGFBP3	2.72	0.046
	Interferon-induced protein 44	NM_006417	IFI44	2.71	0.002
	Myxovirus (influenza virus) resistance 2 (mouse)	NM_002463	MX2	2.64	0.001
	PREDICTED: Similar to Complement C3 precursor	XM_936226	LOC653879	2.54	0.024
	SLAM family member 7	NM_021181	SLAMF7	2.50	0.047
	Lysozyme (renal amyloidosis)	NM_000239	LYZ	2.49	0.038
	Interferon, alpha-inducible protein 6	NM_022872	IFI6	2.47	0.009
	Oxidized low density lipoprotein (lectin-like) receptor 1	NM_002543	OLR1	2.43	0.003
	ISG15 ubiquitin-like modifier	NM_005101	ISG15	2.30	0.022
	Interferon induced transmembrane protein 2 (1-8D)	NM_006435	IFITM2	2.29	0.008
	S100 calcium binding protein A9 (calgranulin B)	NM_002965	S100A9	2.28	0.001

Table 6.4 continued:

Incubation Time	Gene Product	GenBank Accession No.	Symbol	Fold Change ¹	p value
24 hours	2',5'-oligoadenylate synthetase 1, 40/46kDa	NM_001032409	OAS1	2.27	0.002
	S100 calcium binding protein A12	NM_005621	S100A12	2.27	0.049
	Interferon-induced protein with tetratricopeptide repeats 3	NM_001031683	IFIT3	2.26	0.001
	Epithelial stromal interaction 1 (breast)	NM_033255	EPSTI1	2.24	0.010
	Interferon-induced protein with tetratricopeptide repeats 2	NM_001547	IFIT2	2.22	0.004
	Interferon induced transmembrane protein 3 (1-8U)	NM_021034	IFITM3	2.22	0.007
	Endothelial cell growth factor 1 (platelet-derived)	NM_001953	ECGF1	2.17	0.003
	Toll-like receptor 8	NM_138636	TLR8	2.17	0.004
	Mannosyl (alpha-1,3)-glycoprotein beta-1,4-N-acetylglucosaminyltransferase, isozyme A	NM_012214	MGAT4A	2.16	0.010
	Major histocompatibility complex, class II, DR alpha	NM_019111	HLA-DRA	2.16	0.010
	Plexin domain containing 2	NM_032812	PLXDC2	2.15	0.023
	Interferon stimulated exonuclease gene 20kDa	NM_002201	ISG20	2.13	0.002
	Guanylate binding protein 1, interferon-inducible, 67kDa	NM_002053	GBP1	2.12	0.007
	Fibrinogen-like 2	NM_006682	FGL2	2.11	0.009
	Toll-like receptor 8	NM_016610	TLR8	2.11	0.002
	2',5'-oligoadenylate synthetase 1, 40/46kDa	NM_002534	OAS1	2.09	0.010
	2',5'-oligoadenylate synthetase 1, 40/46kDa	NM_001032409	OAS1	2.09	0.013
	Lysozyme	NM_000239	LYZ	2.09	0.042
	Potassium inwardly-rectifying channel, subfamily J, member 2	NM_000891	KCNJ2	2.07	0.022
	Complement component 3	NM_000064	C3	2.04	0.043
	Decorin	NM_133505	DCN	2.04	0.010
	Radical S-adenosyl methionine domain containing 2	NM_080657	RSAD2	2.03	0.011

Table 6.4 continued:

Incubation Time	Gene Product	GenBank Accession No.	Symbol	Fold Change ¹	p value
24 hours	Platelet-activating factor receptor	NM_000952	PTAFR	2.02	0.030
	Solute carrier family 43, member 2	NM_152346	SLC43A2	2.02	0.039
	Thromboxane A synthase 1 (platelet, cytochrome P450, family 5, subfamily A)	NM_001061	TBXAS1	2.02	0.022
	Hect domain and RLD 5	NM_016323	HERC5	1.99	0.014
	Superoxide dismutase 2, mitochondrial	NM_001024466	SOD2	1.99	0.033
	Signal transducer and activator of transcription 1, 91kDa	NM_007315	STAT1	1.98	0.002
	Mediterranean fever	NM_000243	MEFV	1.97	0.001
	Adhesion molecule, interacts with CXADR antigen 1	NM_153206	AMICA1	1.97	0.010
	Legumain	NM_001008530	LGMN	1.97	0.024
	Podoplanin	NM_001006625	PDPN	1.96	0.002
	Chemokine (C-C motif) receptor 2	NM_000647	CCR2	1.96	0.026
	Collagen, type XXIII, alpha 1	NM_173465	COL23A1	1.95	0.005
	Interferon, alpha-inducible protein 6	NM_022873	IFI6	1.94	2E-04
	Natural killer cell group 7 sequence	NM_005601	NKG7	1.91	0.027
	2'-5'-oligoadenylate synthetase-like	NM_198213	OASL	1.90	0.018
	Chemokine (C-C motif) receptor 2	NM_000648	CCR2	1.90	0.012
	Arylformamidase	NM_001010982	AFMID	1.90	0.002
	Neutrophil cytosolic factor 1	NM_000265	NCF1	1.89	0.023
	Phosphodiesterase 4B, cAMP-specific (phosphodiesterase E4 dunce homolog, Drosophila)	NM_002600	PDE4B	1.89	0.024
	MARCKS-like 1	NM_023009	MARCKSL1	1.89	0.019
	Apolipoprotein C-II	NM_000483	APOC2	1.88	0.017
	Chemokine (C-C motif) receptor 2	NM_000647	CCR2	1.88	0.025
	N-sulfoglucosamine sulfohydrolase (sulfamidase)	NM_000199	SGSH	1.87	0.024
	Interferon-induced protein with tetratricopeptide repeats 3	NM_001549	IFIT3	1.86	0.008

Table 6.4 continued:

Incubation Time	Gene Product	GenBank Accession No.	Symbol	Fold Change ¹	p value
24 hours	Bcl2 modifying factor	NM_033503	BMF	1.85	0.028
	Tumor necrosis factor (ligand) superfamily, member 13b	NM_006573	TNFSF13B	1.85	0.003
	2'-5'-oligoadenylate synthetase 3, 100kDa	NM_006187	OAS3	1.85	0.003
	2'-5'-oligoadenylate synthetase 2, 69/71kDa	NM_016817	OAS2	1.84	0.024
	Ubiquitin-conjugating enzyme E2L 6	NM_004223	UBE2L6	1.83	0.004
	Guanylate binding protein 1, interferon-inducible,	NM_002053	GBP1	1.81	0.014
	2'-5'-oligoadenylate synthetase 3, 100kDa	NM_006187	OAS3	1.81	0.003
	CD86 molecule	NM_006889	CD86	1.81	0.004
	Proline-serine-threonine phosphatase interacting protein 2	NM_024430	PSTPIP2	1.80	0.016
	Signal transducer and activator of transcription 1, 91kDa	NM_007315	STAT1	1.80	0.001
	Ectonucleoside triphosphate diphosphohydrolase 1	NM_001098175	ENTPD1	1.80	0.003
	Mucin 1, cell surface associated	NM_001044391	MUC1	1.80	0.039
	GTPase, IMAP family member 4	NM_018326	GIMAP4	1.79	0.003
	Poly (ADP-ribose) polymerase family, member 9	NM_031458	PARP9	1.79	0.001
	Neutrophil cytosolic factor 4, 40kDa	NM_000631	NCF4	1.78	0.017
	Tripartite motif-containing 16-like	NM_001037330	TRIM16L	1.78	0.026
	Poly (ADP-ribose) polymerase family, member 10	NM_032789	PARP10	1.78	0.005
	Signal transducer and activator of transcription 1, 91kDa	NM_139266	STAT1	1.77	0.008
	Neutrophil cytosolic factor 4, 40kDa	NM_000631	NCF4	1.77	0.044
	Poly (ADP-ribose) polymerase family, member 14	NM_017554	PARP14	1.76	0.016
	Histone cluster 2, H2aa4	NM_001040874	HIST2H2AA4	1.76	0.032
	Sterile alpha motif domain containing 9-like	NM_152703	SAMD9L	1.76	0.013

Table 6.4 continued:

Incubation Time	Gene Product	GenBank Accession No.	Symbol	Fold Change ¹	p value
24 hours	Amyloid beta (A4) precursor protein-binding, family B, member 3	NM_133172	APBB3	1.75	0.039
	Ferritin, heavy polypeptide-like 11	NR_002204	FTHL11	1.75	0.007
	Ferritin, heavy polypeptide-like 11	NR_002204	FTHL11	1.73	0.022
	2'-5'-oligoadenylate synthetase 2, 69/71kDa	NM_002535	OAS2	1.73	0.028
	Tumor necrosis factor (ligand) superfamily, member 13b	NM_006573	TNFSF13B	1.72	0.003
	Interferon induced with helicase C domain 1	NM_022168	IFIH1	1.72	0.008
	Epithelial membrane protein 1	NM_001423	EMP1	-3.85	0.006
DNA-damage-inducible transcript 4-like	NM_145244	DDIT4L	-2.75	0.024	
Early growth response 1	NM_001964	EGR1	-2.71	0.004	
Growth differentiation factor 15	NM_004864	GDF15	-2.38	0.033	
Transmembrane protein 158	NM_015444	TMEM158	-2.27	0.002	
Pleckstrin homology-like domain, family A, member 1	NM_007350	PHLDA1	-2.16	0.009	
Uridine phosphorylase 1	NM_003364	UPP1	-2.15	0.003	
Acyl-Coenzyme A oxidase 2, branched chain	NM_003500	ACOX2	-2.02	0.003	
SERTA domain containing 2	NM_014755	SERTAD2	-1.95	0.002	
Tumor necrosis factor (TNF superfamily, member 2)	NM_000594	TNF	-1.95	0.025	
Peroxisome proliferator-activated receptor gamma	NM_138712	PPARG	-1.93	0.015	
Neural precursor cell expressed, developmentally down-regulated 9	NM_006403	NEDD9	-1.93	1E-04	
Palladin, cytoskeletal associated protein	NM_016081	PALLD	-1.93	0.041	
Dehydrogenase/reductase member 3	NM_004753	DHRS3	-1.92	0.013	
Solute carrier family 2 (facilitated glucose transporter), member 3	NM_006931	SLC2A3	-1.92	0.019	

Table 6.4 continued:

Incubation Time	Gene Product	GenBank Accession No.	Symbol	Fold Change ¹	p value
24 hours	ST6 (alpha-N-acetylneuraminyl-2,3-beta-galactosyl-1, 3)-N-acetylgalactosaminide alpha-2,6-sialyltransferase 3	NM_152996	ST6GALNAC3	-1.89	0.013
	Ras and Rab interactor 2	NM_018993	RIN2	-1.88	0.024
	Cbl-interacting protein Sts-1	NM_032873	STS-1	-1.88	0.006
	Early growth response 3	NM_004430	EGR3	-1.88	0.006
	Tribbles homolog 1 (Drosophila)	NM_025195	TRIB1	-1.87	0.015
	Formin-like 2	NM_052905	FMNL2	-1.83	0.014
	Integrin, alpha M (complement component 3 receptor 3 subunit)	NM_000632	ITGAM	-1.82	0.015
	Cytochrome P450, family 19, subfamily A, polypeptide 1	NM_000103	CYP19A1	-1.81	0.006
	GTP binding protein overexpressed in skeletal muscle	NM_181702	GEM	-1.81	0.030
	Transmembrane and tetratricopeptide repeat containing 1	NM_175861	TMTC1	-1.81	0.016
	Aldo-keto reductase family 1, member C4 (chlordecone reductase; 3-alpha hydroxysteroid dehydrogenase, type I; dihydrodiol dehydrogenase 4)	NM_001818	AKR1C4	-1.81	0.028
	Dystrobrevin, alpha	NM_001392	DTNA	-1.81	5E-04
	Neural precursor cell expressed, developmentally down-regulated 9	NM_006403	NEDD9	-1.80	0.010
	Tribbles homolog 3 (Drosophila)	NM_021158	TRIB3	-1.80	0.003
	ATPase, Na ⁺ /K ⁺ transporting, beta 1 polypeptide	NM_001677	ATP1B1	-1.78	0.016
	Megakaryocyte-associated tyrosine kinase	NM_139354	MATK	-1.76	0.006
	Fc fragment of IgE, low affinity II, receptor for (CD23)	NM_002002	FCER2	-1.76	0.017

Table 6.4 continued:

Incubation Time	Gene Product	GenBank Accession No.	Symbol	Fold Change ¹	p value
24 hours	Discs, large (Drosophila) homolog-associated protein 4	NM_001042486	DLGAP4	-1.74	1E-04
	Tripartite motif-containing 9	NM_015163.4	TRIM9	-1.73	0.032

**Results are considered significant at fold change of ≥ 2.0 or -2.0 , with a p value of < 0.05 from control. ¹Fold change was determined by comparing raw data from LPS-treated THP-1 mRNA against SB+LPS-treated data.

CHAPTER 7

REFERENCES

Adle-Biassette H., J.E. Bell, A. Creange, V. Sazdovitch, F.J. Authier, F. Gray, J.J. Hauw, R. Gherardi. 1998. DNA breaks detected by in situ end-labelling in dorsal root ganglia of patients with AIDS. *Neuropathol. Appl. Neurobiol.* 24: 373-380.

Adle-Biassette, H., F. Chretien, L. Wingertsman, C. Hery, T. Ereau, F. Scaravilli, M. Tardieu, and F. Gray. 1999. Neuronal apoptosis does not correlate with dementia in HIV infection but is related to microglial activation and axonal damage. *Neuropathol. Appl. Neurobiol.* 25: 123-133.

Ahn, Y.M., S.W. Oh, U.G. Kang, J. Park, and Y.S. Kim. 2000. An N-methyl-D-aspartate antagonist, MK-801, preferentially reduces electroconvulsive shock-induced phosphorylation of p38 mitogen-activated protein kinase in the rat hippocampus. *Neurosci Lett.* 296: 101-4.

Anthony I.C. and J.E. Bell. 2008. The neuropathology of HIV/AIDS. *Int. Rev. Psychiatry.* 20: 15-24.

Antinori, A., G. Arendt, J. T. Becker, B. J. Brew, D. A. Byrd, M. Cherner, D. B. Clifford, P. Cinque, L. G. Epstein, K. Goodkin, M. Gisslen, I. Grant, R. K. Heaton, J. Joseph, K. Marder, C. M. Marra, J. C. McArthur, M. Nunn, R. W. Price, L. Pulliam, K. R. Robertson, N. Sacktor, V. Valcour, and V. E. Wojna. 2007. Updated research nosology for HIV-associated neurocognitive disorders. *Neurology.* 69: 1789-1799.

Barber, S. A., J. L. Uhrlaub, J. B. DeWitt, P. M. Tarwater, and M. C. Zink. 2004. Dysregulation of mitogen-activated protein kinase signaling pathways in simian immunodeficiency virus encephalitis. *Am. J Pathol.* 164: 355-362.

Barone, F. C., E. A. Irving, A. M. Ray, J. C. Lee, S. Kassis, S. Kumar, A. M. Badger, J. J. Legos, J. A. Erhardt, E. H. Ohlstein, A. J. Hunter, D. C. Harrison, K. Philpott, B. R. Smith, J. L. Adams, and A. A. Parsons. 2001. Inhibition of p38 mitogen-activated protein kinase provides neuroprotection in cerebral focal ischemia. *Med Res. Rev.* 21: 129-145.

Basselin, M., E. Ramadan, M. Igarashi, L. Chang, M. Chen, A.D. Kraft, G.I. Harry, and S.I. Rapoport. 2010. Imaging upregulated brain arachidonic acid metabolism in HIV-1 transgenic rats. [Epub ahead of print]

Buffo, M. Cimino, and M.P. Abbracchio. 2008. The recently identified P2Y-like receptor GPR17 is a sensor of brain damage and a new target for brain repair. *PLoS One*. 3: e3579.

Chaparro-Huerta, V., M. Flores-Soto, G. Gudiño-Cabrera, M. Rivera-Cervantes, O. Bitzer-Quintero, and C. Beas-Zárate. 2008. Role of p38 MAPK and pro-inflammatory cytokines expression in glutamate-induced neuronal death of neonatal rats. *Int J Dev Neurosci*. 26: 487-495.

Cheung, R., V. Ravyn, L. Wang, A. Ptasznik, and R. G. Collman. 2008. Signaling mechanism of HIV-1 gp120 and virion-induced IL-1beta release in primary human macrophages. *J Immunol*. 180: 6675-6684.

Choi, W. T., M. Kaul, S. Kumar, J. Wang, I. M. Kumar, C. Z. Dong, J. An, S. A. Lipton, and Z. Huang. 2007. Neuronal apoptotic signaling pathways probed and intervened by synthetically and modularly modified (SMM) chemokines. *J Biol. Chem*. 282: 7154-7163.

Cocchi, F., A. L. Devico, A. Garzino-Demo, S. K. Arya, R. C. Gallo, and P. Lusso. 1995. Identification of RANTES, MIP-1 alpha, and MIP-1 beta as the major HIV-suppressive factors produced by CD8+ T cells. *Science*. 270: 1811-1815.

Culbert A.A., S.D. Skaper, D.R. Howlett, N.A. Evans, L. Facci, P.E. Soden, Z.M. Seymour, F. Guillot, M. Gaestel, J.C. Richardson. 2006. MAPK-activated protein kinase 2 deficiency in microglia inhibits pro-inflammatory mediator release and resultant neurotoxicity. Relevance to neuroinflammation in a transgenic mouse model of Alzheimer disease. *J Biol Chem*. 281: 23658-67.

Davies, S. P., H. Reddy, M. Caivano, and P. Cohen. 2000. Specificity and mechanism of action of some commonly used protein kinase inhibitors. *Biochem. J*. 351: 95-105.

Dean, J.L., M. Brook, A.R. Clark, and J. Saklatvala. 1999. p38 mitogen-activated protein kinase regulates cyclooxygenase-2 mRNA stability and transcription in lipopolysaccharide-treated human monocytes. *J Biol Chem*. 274: 264-9.

Del Corno, M., Q. H. Liu, D. Schols, E. De Clercq, S. Gessani, B. D. Freedman, and R. G. Collman. 2001. HIV-1 gp120 and chemokine activation of Pyk2 and mitogen-activated protein kinases in primary macrophages mediated by calcium-dependent, pertussis toxin-insensitive chemokine receptor signaling. *Blood*. 98: 2909-2916.

Delgado, M., N. Varela, and E. Gonzalez-Rey. 2008. Vasoactive intestinal peptide protects against beta-amyloid-induced neurodegeneration by inhibiting microglia activation at multiple levels. *Glia*. 56: 1091-1103.

- Ding, Q., E.Q. Wei, Y.J. Zhang, W.P. Zhang, and Z. Chen. 2006. Cysteinyl leukotriene receptor 1 is involved in N-methyl-D-aspartate-mediated neuronal injury in mice. *Acta Pharma. Sinica*. 27: 1526–1536.
- D'hooge, R., F. Franck, L. Mucke and P.P. De Deyn. 1999. Age-related behavioural deficits in transgenic mice expressing the HIV-1 coat protein gp120. *Eur J Neurosci*. 11: 4398–4402.
- Dreyer, E.B., P.K. Kaiser, J.T. Offermann, and S.A. Lipton. 1990. HIV-1 coat protein neurotoxicity prevented by calcium channel antagonists. *Science*. 248: 364-367.
- Ellis, R.J., D. Langford, and E. Masliah. 2007. HIV and antiretroviral therapy in the brain: neuronal injury and repair. *Nat. Rev. Neurosci*. 8: 33-44.
- Elshal, M.F., and J.P. McCoy. 2006. Multiplex bead array assays: performance evaluation and comparison of sensitivity to ELISA. *Methods*. 38: 317–323.
- Everall, I.P., C. Bell, M. Mallory, D. Langford, A. Adame, E. Rockenstein, and E. Masliah. 2002. Lithium ameliorates HIV-gp120-mediated neurotoxicity. *Mol Cell Neurosci*. 21: 493-501.
- Fantuzzi, L., F. Spadaro, C. Purificato, S. Cecchetti, F. Podo, F. Belardelli, S. Gessani, and C. Ramoni. 2008. Phosphatidylcholine-specific phospholipase C activation is required for CCR5-dependent, NF- κ B-driven CCL2 secretion elicited in response to HIV-1 gp120 in human primary macrophages. *Blood*. 111: 3355-3363.
- Garden, G. A., W. Guo, S. Jayadev, C. Tun, S. Balcaitis, J. Choi, T. J. Montine, T. Moller, and R. S. Morrison. 2004. HIV associated neurodegeneration requires p53 in neurons and microglia. *FASEB J*. 18: 1141-1143.
- Giulian, D., E. Wendt, K. Vaca, and C. A. Noonan. 1993. The envelope glycoprotein of human immunodeficiency virus type 1 stimulates release of neurotoxins from monocytes. *Proc Natl Acad Sci U S A*. 90: 2769-2773.
- Giulian, D., K. Vaca, and C. A. Noonan. 1990. Secretion of neurotoxins by mononuclear phagocytes infected with HIV-1. *Science*. 250: 1593-1596.
- Glass, J. D., H. Fedor, S. L. Wesselingh, and J. C. McArthur. 1995. Immunocytochemical quantitation of human immunodeficiency virus in the brain: correlations with dementia. *Ann. Neurol*. 38: 755-762.
- Gonzalez-Scarano, F., and J. Martin-Garcia. 2005. The neuropathogenesis of AIDS. *Nat. Rev. Immunol*. 5: 69-81.

- Gras G. and M. Kaul. 2010. Molecular mechanisms of neuroinvasion by monocytes-macrophages in HIV-1 infection. *Retrovirology*. 7: 30.
- Hazzalin, C.A., P.R. Le, E. Cano, and L.C. Mahadevan. 1998. Anisomycin selectively desensitizes signaling components involved in stress kinase activation and fos and jun induction. *Mol Cell Biol*. 18:1844-54.
- He, J., Y. Chen, M. Farzan, H. Choe, A. Ohagen, S. Gartner, J. Busciglio, X. Yang, W. Hofmann, W. Newman, C. R. Mackay, J. Sodroski, and D. Gabuzda. 1997. CCR3 and CCR5 are co-receptors for HIV-1 infection of microglia. *Nature*. 385: 645-649.
- Hesselgesser, J., D. Taub, P. Baskar, M. Greenberg, J. Hoxie, D. L. Kolson, and R. Horuk. 1998. Neuronal apoptosis induced by HIV-1 gp120 and the chemokine SDF-1 alpha is mediated by the chemokine receptor CXCR4. *Curr. Biol*. 8: 595-598.
- Hesselgesser, J., M. Halks-Miller, V. DelVecchio, S. C. Peiper, J. Hoxie, D. L. Kolson, D. Taub, and R. Horuk. 1997. CD4-independent association between HIV-1 gp120 and CXCR4: functional chemokine receptors are expressed in human neurons. *Curr Biol*. 7: 112-121.
- Hui, W., G.J. Litherland, M. Jefferson, M.J. Barter, M.S. Elias, T.E. Cawston, A.D. Rowan, and D.A. Young. 2010. Lithium protects cartilage from cytokine-mediated degradation by reducing collagen-degrading MMP production via inhibition of the P38 mitogen-activated protein kinase pathway. *Rheumatology*. [Epub ahead of print]
- James, A.J., J.F. Penrose, A.M. Cazaly, S.T. Holgate, and A.P. Sampson. 2006. Human bronchial fibroblasts express the 5-lipoxygenase pathway. *Respir Res*. 7: 102.
- Johnson, G. V., and C. D. Bailey. 2003. The p38 MAP kinase signaling pathway in Alzheimer's disease. *Exp Neurol*. 183: 263-268.
- Kaminska, B., A. Gozdz, M. Zawadzka, A. Ellert-Miklaszewska, and M. Lipko. 2009. MAPK signal transduction underlying brain inflammation and gliosis as therapeutic target. *Anat Rec*. 292: 1902-13.
- Kang, Y.J., A. Seit-Nebi, R.J. Davis, and J. Han. 2006. Multiple activation mechanisms of p38alpha mitogen-activated protein kinase. *J Biol Chem*. 281: 26225-34.
- Kang, Y. J., J. Chen, M. Otsuka, J. Mols, S. Ren, Y. Wang, and J. Han. 2008. Macrophage deletion of p38alpha partially impairs lipopolysaccharide-induced cellular activation. *J Immunol*. 180: 5075-5082.
- Kaplan, G., and G. Gaudernack. 1982. In vitro differentiation of human monocytes Differences in monocyte phenotypes induced by cultivation on glass or on collagen. *J. Exp. Med*. 156: 1101-1114.

Kaul, M., and M. Loos. 1995. Collagen-like complement component C1q is a membrane protein of human monocyte-derived macrophages that mediates endocytosis. *J Immunol.* 155: 5795-5802.

Kaul, M., and S. A. Lipton. 1999. Chemokines and activated macrophages in HIV gp120-induced neuronal apoptosis. *Proc Natl Acad Sci U S A.* 96: 8212-8216.

Kaul, M., G. A. Garden, and S. A. Lipton. 2001. Pathways to neuronal injury and apoptosis in HIV-associated dementia. *Nature.* 410: 988-994.

Kaul, M., Q. Ma, K. E. Medders, M. K. Desai, and S. A. Lipton. 2007. HIV-1 coreceptors CCR5 and CXCR4 both mediate neuronal cell death but CCR5 paradoxically can also contribute to protection. *Cell Death. Differ.* 14: 296-305.

Kerr, S. J., P. J. Armati, L. A. Pemberton, G. Smythe, B. Tattam, and B. J. Brew. 1997. Kynurenine pathway inhibition reduces neurotoxicity of HIV-1- infected macrophages. *Neurology.* 49: 1671-1681.

Kim, C., Y. Sano, K. Todorova, B. A. Carlson, L. Arpa, A. Celada, T. Lawrence, K. Otsu, J. L. Brissette, J. S. Arthur, and J. M. Park. 2008. The kinase p38 alpha serves cell type-specific inflammatory functions in skin injury and coordinates pro- and anti-inflammatory gene expression. *Nat Immunol.* 9: 1019-1027.

Kim, W.G., R.P. Mohny, B. Wilson, G.H. Jeohn, B. Liu, and J.S. Hong. 2000. Regional difference in susceptibility to lipopolysaccharide-induced neurotoxicity in the rat brain: role of microglia. *J Neurosci.* 20: 6309-6316.

Kitai, R., M. L. Zhao, N. Zhang, L. L. Hua, and S. C. Lee. 2000. Role of MIP-1beta and RANTES in HIV-1 infection of microglia: inhibition of infection and induction by IFNbeta. *J Neuroimmunol.* 110: 230-239.

Koenig, S., H. E. Gendelman, J. M. Orenstein, M. C. Dal Canto, G. H. Pezeshkpour, M. Yungbluth, F. Janotta, A. Aksamit, M. A. Martin, and A. S. Fauci. 1986. Detection of AIDS virus in macrophages in brain tissue from AIDS patients with encephalopathy. *Science.* 233: 1089-1093.

Kraft-Terry, S.D., J.S. Buch, H.S. Fox, and H.E. Gendelman. 2009. A coat of many colors: neuroimmune crosstalk in human immunodeficiency virus infection. *Neuron.* 64: 133-145.

Lecca, D., M.L. Trincavelli, P. Gelosa, L. Sironi, P. Ciana, M. Fumagalli, G. Villa, C. Verderio, C. Grumelli, U. Guerrini, E. Tremoli, P. Rosa, S. Cuboni, C. Martini, A.

- Lee, Y.B., J.W. Schrader, and S.U. Kim. 2000. p38 MAP kinase regulates TNF- α production in human astrocytes and microglia by multiple mechanisms. *Cytokine*. 12: 874–880.
- Lee, C., Q. H. Liu, B. Tomkowicz, Y. Yi, B. D. Freedman, and R. G. Collman. 2003. Macrophage activation through CCR5- and CXCR4-mediated gp120-elicited signaling pathways. *J Leukoc. Biol.* 74: 676-682.
- Lee, C., B. Tomkowicz, B.D. Freedman, and R.G. Collman. 2005. HIV-1 gp120-induced TNF- α production by primary human macrophages is mediated by phosphatidylinositol-3 (PI-3) kinase and mitogen-activated protein (MAP) kinase pathways. *J Leukoc Biol.* 78: 1016-23.
- Lee, J. C., S. Kassis, S. Kumar, A. Badger, and J. L. Adams. 1999. p38 mitogen-activated protein kinase inhibitors--mechanisms and therapeutic potentials. *Pharmacol. Ther.* 82: 389-397.
- Letendre S.L., R.J. Ellis, B.M. Ances, and J.A. McCutchan. 2010. Neurologic complications of HIV disease and their treatment. *Top. HIV Med.* 18: 45-55.
- Masliah E., R.K. Heaton, T.D. Marcotte, R.J. Ellis, C.A. Wiley, M. Mallory, C.L. Achim, J.A. McCutchan, J.A. Nelson, J.H. Atkinson, and I. Grant. HNRC Group. 1997. Dendritic injury is a pathological substrate for human immunodeficiency virus-related cognitive disorders. *Ann. Neurol.* 42: 963-972.
- Masliah, E., N. Ge, C. L. Achim, L. A. Hansen, and C. A. Wiley. 1992. Selective neuronal vulnerability in HIV encephalitis. *J Neuropathol Exp Neurol.* 51: 585-593.
- Mayer, R.J., and J.F. Callahan. 2006. p38 MAP kinase inhibitors: A future therapy for inflammatory diseases. *Drug Discovery Today: Therap Strat.* 3: 49-54.
- McArthur J.C., J. Steiner, N. Sacktor, and A. Nath. 2010. Human immunodeficiency virus-associated neurocognitive disorders: Mind the gap. *Ann. Neurol.* 67: 699-714.
- Medders, K.E., N. Sejbuk, R. Maung, M.K. Desai, and M. Kaul. 2010. Activation of p38 MAPK is required in monocytic and neuronal cells for HIV gp120-induced neurotoxicity. *J Immunol.* 185. In press.
- Meucci, O., A. Fatatis, A. A. Simen, T. J. Bushell, P. W. Gray, and R. J. Miller. 1998. Chemokines regulate hippocampal neuronal signaling and gp120 neurotoxicity. *Proc Natl Acad Sci U S A.* 95: 14500-14505.
- Misse, D., P. O. Esteve, B. Renneboog, M. Vidal, M. Cerutti, Y. St Pierre, H. Yssel, M. Parmentier, and F. Veas. 2001. HIV-1 glycoprotein 120 induces the MMP-9

cytopathogenic factor production that is abolished by inhibition of the p38 mitogen-activated protein kinase signaling pathway. *Blood*. 98: 541-547.

Mueller, A., N. G. Mahmoud, M. C. Goedecke, J. A. McKeating, and P. G. Strange. 2002. Pharmacological characterization of the chemokine receptor, CCR5. *Br. J Pharmacol*. 135: 1033-1043.

Murphy, G., V. Knäuper, S. Cowell, R. Hembry, H. Stanton, G. Butler, J. Freije, A.M. Pendás, and C. López-Otín. 1999. Evaluation of some newer matrix metalloproteinases. *Ann N Y Acad Sci*. 878: 25-39.

Munoz, L., H. R. Ranaivo, S. M. Roy, W. Hu, J. M. Craft, L. K. McNamara, L. W. Chico, L. J. Van Eldik, and D. M. Watterson. 2007. A novel p38 alpha MAPK inhibitor suppresses brain proinflammatory cytokine up-regulation and attenuates synaptic dysfunction and behavioral deficits in an Alzheimer's disease mouse model. *J Neuroinflammation*. 4: 21.

Naggie, S. and C. Hicks. 2010. Protease inhibitor-based antiretroviral therapy in treatment-naive HIV-1-infected patients: the evidence behind the options. *J. Antimicrob. Chemother*. 65: 1094-9.

Nguyen, T.B., G.R. Lucero, G. Chana, B.J. Hult, E.T. Tatro, E. Masliah, I. Grant, C.L. Achim, and I.P. Everall; HIV Neurobehavioral Research Group. 2009. Glycogen synthase kinase-3beta (GSK-3beta) inhibitors AR-A014418 and B6B3O prevent human immunodeficiency virus-mediated neurotoxicity in primary human neurons. *J Neurovirol*. 15: 434-8.

Nosheny, R.L., F. Ahmed, A. Yakovlev, E.M. Meyer, K. Ren, L. Tessarollo, and I. Moccchetti. 2007. Brain-derived neurotrophic factor prevents the nigrostriatal degeneration induced by human immunodeficiency virus-1 glycoprotein 120 in vivo. *Eur J Neurosci*. 25: 2275-84.

O'Donnell, L. A., A. Agrawal, K. L. Jordan-Sciutto, M. A. Dichter, D. R. Lynch, and D. L. Kolson. 2006. Human immunodeficiency virus (HIV)-induced neurotoxicity: roles for the NMDA receptor subtypes. *J Neurosci*. 26: 981-990.

Ohagen, A., S. Ghosh, J. He, K. Huang, Y. Chen, M. Yuan, R. Osathanondh, S. Gartner, B. Shi, G. Shaw, and D. Gabuzda. 1999. Apoptosis induced by infection of primary brain cultures with diverse human immunodeficiency virus type 1 isolates: evidence for a role of the envelope. *J Virol*. 73: 897-906.

Okubo, M., H. Yamanaka, K. Kobayashi, and K. Noguchi. 2010. Leukotriene synthases and the receptors induced by peripheral nerve injury in the spinal cord contribute to the generation of neuropathic pain. 58: 599-610.

- Ono, K., and J. Han. 2000. The p38 signal transduction pathway: activation and function. *Cell Signal*. 12: 1-13.
- Oppermann, M. 2004. Chemokine receptor CCR5: insights into structure, function, and regulation. *Cell Signal*. 16: 1201-1210.
- Peng, F., N. Dhillon, S. Callen, H. Yao, S. Bokhari, X. Zhu, H.H. Baydoun, and S. Buch. 2008. Platelet-derived growth factor protects neurons against gp120-mediated toxicity. *J Neurovirol*. 14: 62-72.
- Perfettini, J. L., M. Castedo, R. Nardacci, F. Ciccocanti, P. Boya, T. Roumier, N. Larochette, M. Piacentini, and G. Kroemer. 2005. Essential role of p53 phosphorylation by p38 MAPK in apoptosis induction by the HIV-1 envelope. *J Exp. Med*. 201: 279-289.
- Petito C.K., E.S. Cho, W. Lemann, B.A. Navia, and R.W. Price. 1986. Neuropathology of acquired immunodeficiency syndrome (AIDS): an autopsy review. *J. Neuropathol. Exp. Neurol*. 45: 635-646.
- Porcheray, F., B. Samah, C. Leone, N. Dereuddre-Bosquet, and G. Gras. 2006. Macrophage activation and human immunodeficiency virus infection: HIV replication directs macrophages towards a pro-inflammatory phenotype while previous activation modulates macrophage susceptibility to infection and viral production. *Virology*. 349: 112-120.
- Ronaldson, P.T., and R. Bendayan. 2009. HIV-1 viral envelope glycoprotein gp120 triggers an inflammatory response in cultured rat astrocytes and regulates the functional expression of P-glycoprotein. *Mol Pharmacol*. 70: 1087-98.
- Serio, K.J., S.C. Johns, L. Luo, C.R. Hodulik, and T.D. Bigby. 2003. Lipopolysaccharide down-regulates the leukotriene C4 synthase gene in the monocyte-like cell line, THP-1. *J Immunol*. 170: 2121-8.
- Shi, B., G. U. De, J. He, S. Wang, A. Lorenzo, J. Busciglio, and D. Gabuzda. 1996. Apoptosis induced by HIV-1 infection of the central nervous system. *J Clin Invest*. 98: 1979-1990.
- Shieh, J.T., A.V. Albright, M. Sharron, S. Gartner, J. Strizki, R.W. Doms, and F. González-Scarano. 1998. Chemokine receptor utilization by human immunodeficiency virus type 1 isolates that replicate in microglia. *J Virol*. 72: 4243-9.
- Singh, I. N., N. El-Hage, M. E. Campbell, S. E. Lutz, P. E. Knapp, A. Nath, and K. F. Hauser. 2005. Differential involvement of p38 and JNK MAP kinases in HIV-1 Tat and gp120-induced apoptosis and neurite degeneration in striatal neurons. *Neuroscience*. 135: 781-790.

- Smookler, D.S., F.F. Mohammed, Z. Kassiri, G.S. Duncan, T.W. Mak, and R. Khokha. 2006. Tissue inhibitor of metalloproteinase 3 regulates TNF-dependent systemic inflammation. *J Immunol.* 176: 721-5.
- Terheyden, P., M. Loos, S. Storkel, and M. Kaul. 2005. Human macrophages simultaneously express membrane-C1q and Fc-receptors for IgG. *Immunol Lett.* 101: 202-209.
- Thornton, T.M., G. Pedraza-Alva, B. Deng, C.D. Wood, A. Aronshtam, J.L. Clements, G. Sabio, R.J. Davis, D.E. Matthews, B. Doble, and M. Rincon. 2008. Phosphorylation by p38 MAPK as an alternative pathway for GSK3beta inactivation. *Science.* 320: 667-70.
- Toggas, S. M., E. Masliah, E. M. Rockenstein, G. F. Rall, C. R. Abraham, and L. Mucke. 1994. Central nervous system damage produced by expression of the HIV-1 coat protein gp120 in transgenic mice. *Nature.* 367: 188-193.
- Toggas, S.M., E. Masliah, L. Mucke. 1996. Prevention of HIV-1 gp120-induced neuronal damage in the central nervous system of transgenic mice by the NMDA receptor antagonist memantine. *Brain Research.* 706: 303-307.
- Werz, O., J. Klemm, B. Samuelsson, O. Rådmark. 2000. 5-lipoxygenase is phosphorylated by p38 kinase-dependent MAPKAP kinases. *Proc Natl Acad Sci U S A.* 97: 5261-6.
- Woods, S.P., D.J. Moore, E. Weber, and I. Grant. 2009. Cognitive neuropsychology of HIV-associated neurocognitive disorders. *Neuropsychol. Rev.* 19: 152–168.
- Xie, Z., C.J. Smith, and L.J. Van Eldik. 2004. Activated glia induce neuron death via MAP kinase signaling pathways involving JNK and p38. *Glia.* 45: 170–179.
- Xing, B., T. Xin, R. Hunter and G. Bing. 2008. Pioglitazone inhibition of lipopolysaccharide-induced nitric oxide synthase is associated with altered activity of p38 MAP kinase and PI3K/Akt. *J Neuroinflamm.* 5: 4.
- Yi, Y., C.H. Lee, Q.H. Liu, B.D. Freedman, and R.G. Collman. 2004. Chemokine receptor utilization and macrophage signaling by human immunodeficiency virus type 1 gp120: Implications for neuropathogenesis. *J Neurovir.* 10(supp.1): 91.96.
- Yu, G.L., E.Q. Wei, M.L. Wang, W.P. Zhang, S.H. Zhang, J.Q. Weng, L.S. Chu, S.H. Fang, Y. Zhou, Z. Chen, Q. Zhang, and L.H. Zhang. 2005. Pranlukast, a cysteinyl leukotriene receptor-1 antagonist, protects against chronic ischemic brain injury and inhibits the glial scar formation in mice. *Brain Res.* 1053: 116-25.

Zeng K.W., H. Fu, G.X. Liu, and X.M. Wang. 2010. Icariin attenuates lipopolysaccharide-induced microglial activation and resultant death of neurons by inhibiting TAK1/IKK/NF-kappaB and JNK/p38 MAPK pathways. *Int Immunopharmacol.* 10: 668-78.

Zhang, Y.J., L. Zhang, Y.L. Ye, S.H. Fang, Y. Zhou, W.P. Zhang, Y.B. Lu. and E.Q. Wei. 2006. Cysteinyl leukotriene receptors CysLT1 and CysLT2 are upregulated in acute neuronal injury after focal cerebral ischemia in mice. *Acta Pharma. Sinica.* 27: 1553–1560.

Zhao, M., L. New, V. V. Kravchenko, Y. Kato, H. Gram, F. Di Padova, E. N. Olson, R. J. Ulevitch, and J. Han. 1999. Regulation of the MEF2 family of transcription factors by p38. *Mol. Cell Biol.* 19: 21-30.

Zheng, J., A. Ghorpade, D. Niemann, R. L. Cotter, M. R. Thylin, L. Epstein, J. M. Swartz, R. B. Shepard, X. Liu, A. Nukuna, and H. E. Gendelman. 1999. Lymphotropic virions affect chemokine receptor-mediated neural signaling and apoptosis: implications for human immunodeficiency virus type 1-associated dementia. *J Virol.* 73: 8256-8267.